UNIVERSIDAD COMPLUTENSE DE MADRID
FACULTAD DE MEDICINA

TESIS DOCTORAL

Perfil metabolómico de los tumores neuroendocrinos de origen gastrointestinal y pulmonar: papel pronóstico y relevancia biológica

Metabolomic profile of neuroendocrine tumors of gastrointestinal and pulmonary origin : prognostic role and biological relevance

MEMORIA PARA OPTAR AL GRADO DE DOCTOR

PRESENTADA POR

Anna La Salvia

Directoras

Rocío García Carbonero
Beatriz Soldevilla Navarro

Madrid

UNIVERSIDAD COMPLUTENSE DE MADRID

FACULTAD DE MEDICINA

TESIS DOCTORAL

PERFIL METABOLÓMICO DE LOS TUMORES NEUROENDOCRINOS DE ORIGEN GASTROINTESTINAL Y PULMONAR. PAPEL PRONÓSTICO Y RELEVANCIA BIOLÓGICA.

-

METABOLOMIC PROFILE OF NEUROENDOCRINE TUMORS OF GASTROINTESTINAL AND PULMONARY ORIGIN. PROGNOSTIC ROLE AND BIOLOGICAL RELEVANCE.

MEMORIA PARA OPTAR AL GRADO DE DOCTOR

PRESENTADA POR:
Anna La Salvia

DIRECTORAS:
Rocío García Carbonero
Beatriz Soldevilla Navarro

ACKNOWLEDGEMETS

First and foremost, I am extremely grateful to my supervisors, Prof. Rocio Garcia Carbonero and Dr. Beatriz Soldevilla Navarro for their invaluable advice, continuous support, and patience during my PhD study. Their immense knowledge and plentiful experience have encouraged me in all the time of my academic research and daily life. I would like to thank both of them for their treasured support which was really influential in shaping my experimental methods and critical judgement, providing me the opportunity to improve my knowledge and skills as a young researcher.

I would like to express my sincere gratitude to Prof. Antongiulio Faggiano, the responsible of my abroad fellowship at the Experimental Medicine Department, Sapienza University of Rome, Italy, for his insightful suggestions and for his unwavering support and belief in me.

My gratitude extends to the Institute Carlos III of Madrid for the funding opportunity to undertake my studies thanks to a Rio Hortega contract (code CM19/00132).

I would also like to thank the Clinical and Translational Oncology Laboratory, Gastrointestinal Unit, i+12 at the Research Institute Hospital 12 De Octubre (Imas12-CNIO) for their continuous collaboration and technical support on my study. I would like to thank all my clinical colleagues at the Gastrointestinal Tumor Unit of 12 de Octubre University Hospital of Madrid. It is their kind help and support that have made my study and life in Spain a wonderful time and experience.

Additionally, I would like to express my gratitude to my parents, my husband and my brother. My appreciation also goes out to my friends for their encouragement and support all through my studies. Without their tremendous understanding and encouragement in the past few years, it would be impossible for me to complete my study.

Finally, I would like to express my sincere gratitude to all the patients included in this study for the samples'< donation and to all AXINET investigators for their fundamental contribution to this work.

RESUMEN/SUMMARY

RESUMEN

La reprogramación del metabolismo permite a las células para responder o adaptar su regulación metabólica para permitir la supervivencia celular en condiciones desfavorables u hostiles. Esta capacidad aumenta en las células cancerosas para mejorar su fenotipo adaptativo y mantener tanto la viabilidad como la proliferación incontrolada. Así, la flexibilidad metabólica es una de las características distintivas del cáncer, aunque todavía quedan por dilucidar las vías implicadas en la plasticidad metabólica de cada tipo de tumor. Los metabolitos son los productos finales de esta adaptación, que en último término reflejan los cambios aberrantes que sufren los tumores reflejando la variabilidad genómica, transcriptómica y proteómica de los mismos y, por lo tanto, proporcionando información relevante sobre la biología del cáncer. Además, el estudio de los perfiles de metabolitos (metabolómica) puede realizarse fácilmente en muestras biológicas de fácil acceso (plasma, orina), constituyendo así una herramienta prometedora para caracterizar el fenotipo tumoral e identificar nuevos biomarcadores de potencial utilidad clínica.

Las neoplasias neuroendocrinas son una familia heterogénea de tumores de incidencia creciente y manejo clínico complejo. Se originan en el sistema neuroendocrino difuso y, por tanto, pueden surgir de prácticamente cualquier órgano. Los tumores neuroendocrinos bien diferenciados (TNE) tienen la peculiar capacidad de secretar aminas u hormonas peptídicas que producen síndromes clínicos característicos que pueden afectar seriamente la calidad de vida y el pronóstico de los pacientes. Hasta la fecha, su baja incidencia, amplia distribución anatómica y comportamiento biológico heterogéneo han dificultado los esfuerzos por descifrar los mecanismos moleculares implicados en el desarrollo y progresión tumoral. El reciente desarrollo y la mayor accesibilidad a las tecnologías "ómicas" han mejorado nuestra comprensión de los eventos genómicos y epigenómicos implicados en la patogénesis de las neoplasias neuroendocrinas. Sin embargo, su perfil metabolómico no ha sido estudiado en profundidad.

La hipótesis en la que se basa este trabajo es que los TNEs presentan una huella metabolómica particular, y que su perfil de metabolitos permitirá una mejor caracterización del fenotipo tumoral, así como la identificación de nuevos biomarcadores pronósticos y de las vías desreguladas más relevantes implicadas en la biología tumoral y asociadas con la supervivencia de los pacientes.

Así, el propósito de nuestro estudio fue caracterizar de manera integral el perfil metabolómico de los pacientes con TNE para comprender mejor la desregulación metabólica en estos tumores e identificar nuevos biomarcadores pronósticos de utilidad clínica, así como caracterizar funcionalmente las vías moleculares con un impacto significativo en la supervivencia del paciente. Con este objetivo y mediante múltiples plataformas (electroforesis capilar, cromatografía líquida y cromatografía de gases acoplada a espectrometría de masas) se realizó un estudio no dirigido del perfil metabolómico en el plasma de 77 pacientes con TNE extra-pancreáticos G1-2 avanzados (cohorte de estudio) y de 68 individuos sin cáncer (cohorte de control), pareados por edad, sexo e índice de masa corporal (IMC). La población del estudio incluyó a pacientes con TNEs reclutados en el ensayo AXINET de fase II/III, prospectivo, multicéntrico, aleatorizado (1: 1) y doble ciego (ClinicalTrials.gov Identificador: NCT01744249). Los pacientes de este estudio fueron aleatorizados a recibir Axitinib y Octeotride LAR versus Placebo y Octreotide LAR hasta la progresión de la enfermedad o toxicidad inaceptable, y otorgaron su consentimiento para la realización de estudios traslacionales en muestras plasmáticas. Los objetivos específicos de nuestro estudio fueron los siguientes: i) identificar metabolitos plasmáticos con disponibilidad diferencial en pacientes con TNEs avanzados (cohorte de estudio) en comparación con individuos sin cáncer (controles); ii) identificar metabolitos diferenciales significativamente asociados con la supervivencia libre de progresión (SLP) y/o la supervivencia global (SG) del paciente (biomarcadores pronósticos) mediante análisis univariante y multivariante ajustado por otros factores pronósticos conocidos o variables de confusión; y iii) analizar la relevancia biológica de los metabolitos identificados y las vías moleculares desreguladas involucradas para proporcionar una mayor comprensión de los mecanismos moleculares subyacentes a la patogénesis y el comportamiento clínico de los TNEs.

La integración de los datos metabólicos adquiridos por diferentes plataformas analíticas dio como resultado la identificación de 155 metabolitos con una disponibilidad diferencial en pacientes con TNEs en comparación con individuos sin cáncer ($p < 0,05$). De estos 155 metabolitos, 34 se asociaron significativamente con la SLP (N = 16) y/o la SG (N = 27). Trece de estos metabolitos demostraron ser factores pronósticos independientes en el análisis multivariante tras el ajuste con otros factores pronósticos conocidos y/o variables de confusión: 5 se asociaron significativamente con la SLP y 11 se asociaron significativamente con la SG. Tres de ellos, Glu-Hyp, Glu-Lys / Ɛ-Glu-Lys

2 y 3-hidroxi-5-octenoilcarnitina, mostraron un impacto significativo tanto en la SLP como en la SG. El análisis de agrupamiento no supervisado de estos 3 metabolitos estratificó a los pacientes en 3 grupos pronósticos: 1) Un grupo de buen pronóstico (*cluster* 3), con tasas de SLP a 1 año del 71.1% y de SG a 5 años del 69.7%; 2) Un grupo de pronóstico intermedio (*cluster* 1), con tasas de SLP a 1 año del 47.4% y de SG a 5 años del 32.5%, y 3) Un grupo de mal pronóstico (*cluster* 2) tasas de SLP a 1 año del 15.4% y de SG a 5 años del 27.7%) (p=0.003 para SLP y SG). El análisis multivariante confirmó que esta firma metabólica se asoció de manera independiente con la SLP (p=0.012) y la SG (p=0.007). El análisis de enriquecimiento de conjuntos de metabolitos (MSEA) y el análisis de las vías metabólicas (MPA) de la firma de 13 metabolitos identificaron el metabolismo de la metionina, la porfirina y el triptófano como las tres vías desreguladas más relevantes asociadas con el pronóstico de los pacientes con TNEs.

Este es el estudio metabolómico más completo realizado hasta la fecha en TNEs. Los resultados de nuestro estudio demuestran que los pacientes con TNEs tienen un perfil metabolómico específico que proporciona información nueva y relevante sobre la biología de la enfermedad con una posible aplicación clínica. De hecho, hemos identificado una firma metabolómica que mejora la estratificación pronóstica de los pacientes, más allá de los factores pronósticos clásicos conocidos, que puede ayudar a la toma de decisiones clínicas. Además, las vías metabólicas desreguladas que hemos descrito identifican nuevas vulnerabilidades tumorales que pueden fomentar el desarrollo de nuevas estrategias terapéuticas para estos pacientes. No obstante, se necesitan más estudios prospectivos para confirmar nuestros hallazgos y validar estos resultados alentadores.

SUMMARY

Reprogrammed metabolism encompasses the capacity of cells to respond or adapt their metabolic signalling to support and enable cell survival in unfavourable or hostile conditions. This ability is enhanced in cancer cells to improve their adaptive phenotype and maintain both viability and uncontrolled proliferation. Metabolic flexibility is therefore one of the key hallmarks of cancer, although pathways involved in the metabolic plasticity of each cancer type remain to be elucidated. Metabolites are the final products of this adaptation, reflecting the aberrant changes in the genomic, transcriptomic and proteomic variability of tumors, and therefore provide useful biological and clinical information on cancer biology. This, together with the fact that metabolomics can be easily performed in readily accessible biological samples (i.e. plasma, urine), makes metabolic profiling of cancer patients a promising tool to characterize the tumor phenotype and identify novel biomarkers of potential clinical use.

Neuroendocrine neoplasms are a heterogenous family of tumors of increasing incidence and challenging clinical management. They originate from the diffuse neuroendocrine system and can thus arise from virtually any organ. Well differentiated neuroendocrine tumors (NETs) have the unique ability to secrete amines or peptide hormones that produce characteristic clinical syndromes that may seriously impair patient´s quality of life and prognosis. Their low incidence, wide anatomic distribution and heterogeneous biological behaviour have hindered the efforts to decipher the molecular mechanisms involved in tumor development and progression. The recent development and increased accessibility to "omic" technologies has improved our understanding of the genomic and epigenomic events driving NEN pathogenesis. However, metabolomics remains largely unexplored in these tumors.

The hypothesis of this study was that NETs present a distinct metabolomic fingerprint, and its profiling will enable an improved characterization of the tumor phenotype, and the identification of novel biomarkers associated with clinical outcome (prognostic biomarkers) and of most relevant dysregulated pathways associated with tumor biology and patient's survival.

On this basis, the purpose of our study was to comprehensively characterize the metabolomic profile of NET patients to better understand metabolic dysregulation in these tumors, and identify novel prognostic biomarkers of clinical use, as well as to functionally characterize molecular pathways with a significant impact on patient's survival. To this aim, multiplatform untargeted metabolomic profiling (capillary electrophoresis, liquid chromatography and gas chromatography coupled to mass spectrometry) was performed in plasma of 77 patients with advanced G1-2 extra-pancreatic NETs (study cohort), and of 68 non-cancer individuals (control cohort), matched per age, gender and BMI. The study population included NET patients enrolled in the phase II/III, prospective, multicenter, randomized (1:1), double-blind AXINET trial (ClinicalTrials.gov

Identifier: NCT01744249). Patients in this study were randomized to receive Axitinib and Octeotride LAR versus Placebo and Octreotide LAR until disease progression or unacceptable toxicity, and provided consent to use baseline plasma samples for translational studies. The specific objectives of our study were: i) to identify plasma metabolites with a differential availability in NET patients (study cohort) as compared to non-cancer individuals (controls); ii) to identify differential metabolites significantly associated with patient's progression-free or overall survival (prognostic biomarkers) by univariate and multivariate analysis adjusted for other known prognostic factors or potentially confounding variables; and iii) to analyze the biological relevance of identified metabolites and dysregulated molecular pathways involved to provide further insight into the molecular mechanisms underlying NET pathogenesis and clinical behaviour.

The integration of metabolic data acquired by different analytical platforms resulted in 155 identified metabolites with a differential availability in NET patients as compared to non-cancer individuals ($p<0.05$). Among these 155 metabolites, 34 metabolites were significantly associated with PFS (N=16) and/or OS (N=27). Thirteen of these metabolites remained significant independent prognostic factors after adjustment for other potential confounding factors in the mutivariable model, 5 were significantly associated with PFS and 11 were significantly associated with OS. Three of them, Glu-Hyp, Glu-Lys/Ɛ-Glu-Lys 2 and 3-hydroxy-5-octenoylcarnitine, showed a significant impact on both PFS and OS. Unsupervised clustering analysis of these 3 metabolites stratified patients in 3 distinct prognostic groups: 1) A good prognosis group (cluster 3), with a PFS rate at 1 year of 71.1% and an OS rate at 5 years of 69.7%; 2) An intermediate prognosis group (cluster 1), with a PFS rate at 1 year of 47.4% and an OS rate at 5 years of 32.5%, and 3) A poor prognosis group (cluster 2), with a PFS rate at 1 year of 15.4% and an OS rate at 5 years of 27.7% (p=0.003 for PFS and OS). Multivariate analysis confirmed metabolic clusters were independently associated with both PFS (p=0.012) and OS (p=0.007). Metabolite Set Enrichment Analysis (MSEA) and Metabolite Pathway Analysis (MPA) of the 13-metabolite signature identified methionine, porphyrin and tryptophan metabolism as the three most relevant dysregulated pathways associated with the prognosis of NET patients.

This is to our knowledge the most comprehensive metabolic profiling study performed to date in NETs. The results of our study demonstrate that NET patients have a distinct metabolomic profile that provides new relevant information on disease biology of potential clinical application. Indeed, we have identified a metabolomic signature that improves the prognostic stratification of patients beyond classical prognostic factors for clinical decisions. In addition, new enriched metabolic pathways described identified novel tumor vulnerabilities that may foster the

development of new therapeutic strategies for these patients. Further prospective studies are nevertheless needed to confirm our results and validate these encouraging data.

INDEX

INDEX OF TABLES

SUPPLEMENTARY TABLES

INDEX OF FIGURES

ABBREVIATIONS

Abbreviations

AC: atypical carcinoids

ACTH: adrenocorticotropic hormone

ALP: Alkaline phosphatase

AUC: area under the curve

BGE: background electrolyte

BMI: body mass index

BVR-A: biliverdin reductase-A

CAPTEM: capecitabine and temozolomide

CgA: chromogranin A

CE-MS: capillary electrophoresis-mass spectrometry

CDDP: cisplatin

CDKN1B: cyclin-dependent kinase inhibitor 1B gene

CHD: carcinoid heart disease

CI: confidence interval

CID: collision-induced dissociation

CKI: cyclin-dependent kinase inhibitor

CMM: CEU Mass Mediator

CRC: colorectal cancer

CS: Carcinoid syndrome

CT: computed tomography

DECT: dual energy CT

DIA: data independent analysis

Drip1: Dynamin-related protein 1

Defcr2: cryptdin-2

ECM: extra-cellular matrix

ELST: endolymphatic sac tumors

EMA: European Medicines Agency

EMR: endoscopic mucosal resection

EP: extrapulmonary

ESD: endoscopic submucosal dissection

FDA: food and drug administration

FH: fumarate hydratase

FMTC: familial medullary thyroid carcinoma

FSH: follicle stimulating hormone

F-pNETs: functioning pancreatic tumors

GC-MS: gas chromatography-mass spectrometry

GI: gastrointestinal

GEP: gastroenteropancreatic

GH: growth hormone

GOT: aspartate transaminase

GCK: glucokinase

GLUT1: glucose transporter 1

GLUT2: glucose transporter 2

G6PC2: glucose 6-phosphatase

FbI: Find by Ion

FOXJ1: Forkhead Box J1

HETE: arachidonic acid

HG-NEC: high-grade neuroendocrine carcinomas

HIF: hypoxia-inducible factor

HPF: high-power field

HR: hazard ratio

HRMAS: High-Resolution Magic Angle Spinning

H2Ras: histamine 2 receptor antagonists

IDH: isocitrate dehydrogenase

IGF-1: insulin growth factor-1

IS-CID: in-source collision-induced dissociation

INF: interferon

IS: internal standard

KDR: kinase insert domain receptor

LAR: long-acting repeatable

LCAT: lecithin:cholesterol acyltransferase

LC-MS: liquid chromatography-mass spectrometry

LCNEC: large cell neuroendocrine lung carcinoma

LDH: lactate dehydrogenase A

LH: luteinizing hormone

LN: lymph-nodes

LPL: lysophospholipids

LPL-R: lysophospholipid receptors

MANEC: mixed adeno-neuroendocrine carcinoma

MAPK: mitogen-activated protein kinase

MDH2: malate dehydrogenase

Me1: cytoplasmic malic enzyme 1

MEN1: multiple endocrine neoplasia type 1

MEN2: multiple endocrine neoplasia type 2

MEN4: multiple endocrine neoplasia type 4

MFE: Molecular Feature Extraction

MG: Methylglyoxal

ML: machine-learning

MLP: metastasis-like primary

MOFA: multi-omics factor analyses

MPA: Metabolite Pathway Analysis

MSEA: Metabolite SetEnrichment Analysis

MsrA: methionine sulfoxide reductase A

MSI: microsatellite instability

MTC: medullary thyroid carcinoma

MiNEN: mixed neuroendocrine-no-neuroendocrine Neoplasms

MRI: Magnetic Resonance Imaging

NANA: N-acetylneuraminic acid

NECs: neuroendocrine carcinomas

NENs: neuroendocrine neoplasms

NETs: neuroendocrine tumors

NF-NETs: no functioning-NETs

NF1: neurofibromatosis type 1

NIST: National Institute of Standards and Technology

NMR: Nuclear Magnetic Resonance

NSE: Neuron-specific enolase

ORR: Overall response rate

OS: overall survival

OxLPCs: oxidized lysoglycerophospholipids

OXPHOS: oxidative phosphorylation

PET: positron emission tomography

PHEO: pheochromocytoma

PIK3CA: phosphatidylinositol-4,5-bisphosphate 3-kinase

pNENs: pancreatic NENs

PD: poorly differentiated

PDK1: pyruvate dehydrogenase kinase isozyme 1

PGL: paraganglioma

PN: plexiform neurofibromas

PNETs: pancreatic NETs

PDGF: platelet-derived growth factor

PDGFR: platelet-derived growth factor receptor

PFS: progression-free survival

PPIs: proton pump inhibitors

PRRT: Peptide receptor radionuclide therapy

PTEN: chromosome ten protein

PTH: parathyroid hormone

PKM2: pyruvate kinase M2

PUD: peptic ulcer disease

RET: REarranged during Transfection

RFA: radiofrequency ablation

RFE: Recursive Feature Extraction

RT: retention time

SCLC: small cell lung carcinomas

SDH: succinate dehydrogenase

SDHB: succinate dehydrogenase subunit B

SI: small bowel

SIRT: selective internal radiotherapy

SNVs: single-nucleotide variants

SSA: somatostatin analogues

SSTR: somatostatin receptors

SSTR2: somatostatin receptors subtype 2

SUV: standardized uptake value

RCC: renal clear-cell carcinomas

TCA cycle: tricarboxylic acid cycle

TIC: total ion chromatograms

TKI: tyrosine kinase inhibitor

TG2: transglutaminase 2

TSH: thyroid stimulating hormone

TC: typical carcinoids

VEGF: vascular endothelial growth factor

VEGFR: vascular endothelial growth factor receptor

VHL: Von-Hippel Lindau

VIP: vasoactive intestinal peptide

WD: Well-Differentiated

WHO: World Health Organization

ZES: Zollinger-Ellison syndrome

M1A: 1-Methyladenosine

2HG: 2-hydroxyglutarate

5-HIAA: 5-hydroxyindoleacetic acid

5-HT: 5-hydroxytryptamine

18-FDG: 18-fluorodeoxyglucose

1. INTRODUCTION

INTRODUCTION

1.1 EPIDEMIOLOGY, ORIGIN AND CLASSIFICATION OF NEUROENDOCRINE NEOPLASMS

1.1.1 Epidemiology

Neuroendocrine neoplasms (NENs) have traditionally been considered as rare tumors, but their incidence has substantially increased over the last decades reaching 6.98 new cases/100.000 inh/year in the latest 2012 update of the United States of America (USA) Surveillance Epidemiology and End Results (SEER) population registry (1–3) (Figure 1, A). This is about a 6.4-fold increase from 1973 through 2012 and has been observed across all sites, stages and grades. The great majority of NENs originate in the gastro-entero-pancreatic (GEP) tract (60%) and in the lung (30%), although they may develop in any organ. Possible contributing factors for this constantly rising incidence include the increased use of endoscopy and of imaging modalities of improved sensitivity, leading to increased detection of early-stage, asymptomatic disease (1). NENs are overall considered indolent tumors, although their prognosis widely varies by tumor differentiation and proliferation rate, primary tumor site and tumor stage. The median overall survival (OS) for all NEN patients was reported to be 9.3 years according to SEER data (1), ranging from a median OS >30 years for patients with localized disease, to 10.2 years or 12 months for those with regional or distant metastasis. Additionally, patients' outcome is highly different by tumor grade, with a median OS of 16.2 years for low-grade G1 well-differentiated tumors (NETs), 8.3 years for G2 NETs and 10 months for G3 NENs. Primary tumor site has also a relevant impact on patients' survival, with rectal and appendiceal NENs associated with the best outcomes (24.6 years and >30.0 years, respectively) and, on the other side, pancreatic (3.6 years) and bronchopulmonary (5.5 years) NENs carrying the worse prognosis (Figure 1, B).

A)

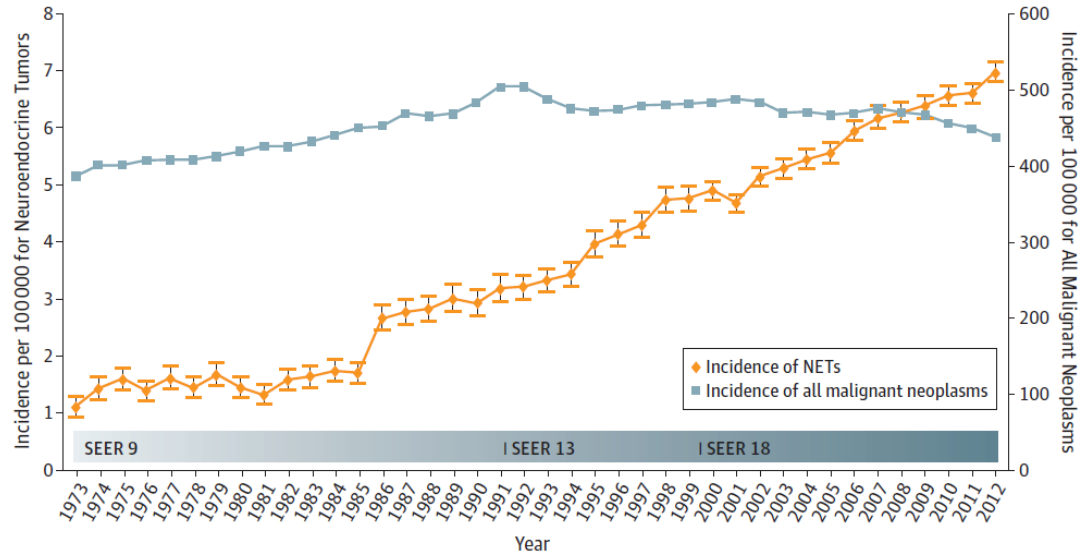

B)

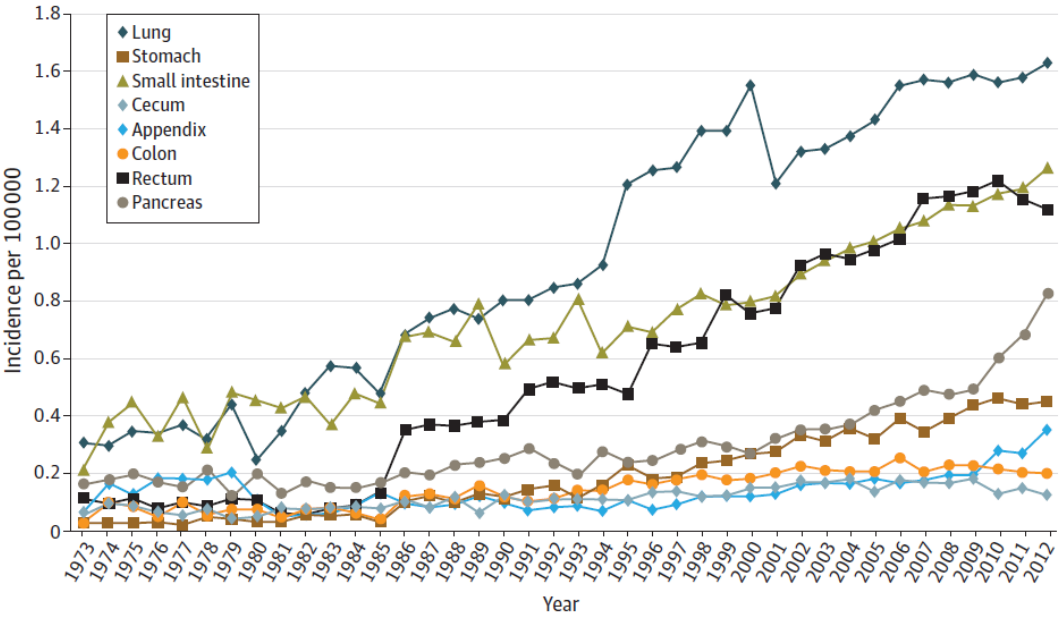

Figure 1. A) Incidence of NETs from 1973 to 2012 according to SEER registry; B) Incidence of NETs by site of origin. Figure adapted from "*Dasari A, Shen C, Halperin D, Zhao B, Zhou S, Xu Y, Shih T, Yao JC. Trends in the Incidence, Prevalence, and Survival Outcomes in Patients With Neuroendocrine Tumors in the United States. JAMA Oncol. 2017 Oct 1;3(10):1335-1342.*".

1.1.2 Origin

Neuroendocrine neoplasms (NENs) comprise a heterogeneous family of tumours originating from neuroendocrine cells widely distributed throughout the body. Neuroendocrine cells are located in nearly every organ, either diffusely scattered in mucosal membranes constituting the diffuse neuroendocrine system (4,5), particularly in the digestive tract but also in the lungs, thyroid (C-cells) or other organs, or forming glands or organized cell clusters with endocrine function such as the pituitary, parathyroids, pancreatic islets, adrenal medulla or paraganglia.

Several types of neuroendocrine cells have been identified with the peculiar ability to produce and secrete into the bloodstream hormones (i.e. insulin, glucagon, gastrin, vasoactive intestinal peptide (VIP) or somatostatin), peptides and neurotransmitters. All these vasoactive substances play a role in the control of many physiological functions. Besides this cell type-specific peptide hormones and/or biogenic amines, which are stored in electron-dense membrane-bound granules, neuroendocrine cells are characterized by the presence of general neuroendocrine cell markers. These include the secretory granule proteins which reside in intracytoplasmic small presynaptic-like vesicles (synaptophysin) or large dense granules (chromogranin A (CgA)), and the cytosolic enzyme neurone specific enolase (NSE) (6). NENs constitute a spectrum of variably differentiated neoplasms, ranging from well-differentiated tumors with a protracted clinical course over many years to poorly differentiated carcinomas that have a very aggressive behaviour.

1.1.3 Classification

NENs are commonly classified according to their embryological and anatomical site of origin, morphology, proliferation rate (mitotic count or Ki-67 index by immunohistochemistry) and their ability to secrete bioactive peptides (functional versus non-functional). The most recent World Health Organization (WHO) 2019 pathological classification of digestive tumors categorize these neoplasms, based on tumor differentiation and proliferation index, as well-differentiated neuroendocrine tumours (NETs) grades 1–3 or poorly differentiated neuroendocrine carcinomas (NECs) that are always grade 3 (7). G3 NENs can

therefore be well differentiated tumors (G3 NETs) or poorly differentiated carcinomas (G3 NECs or simply NECs). NETs are subclassified by proliferation rate in G1, tumors with <2/10 mitosis per 10 high-power field (HPF) and Ki-67 index ≤2%, G2, tumors with 2-20 mitosis/10 HPF and a Ki-67 index of 3–20%, and G3, tumors with >20 mitosis/10 HPF and/or a Ki-67 index >20%. Poorly differentiated neuroendocrine carcinomas (NEC) may be subclassified based on cellular size in large and small cell NECs. The WHO 2019 also includes a mixed category of neuroendocrine/non-neuroendocrine neoplasms (MiNEN), when both neoplastic components comprise at least 30% of the tumor tissue (8). Despite the heterogeneity of this entity, MINENs are usually highly aggressive, generally poorly differentiated neoplasms with high Ki67 index and poor prognosis (9) .Besides morphological features, the assessment of genetic alterations is increasingly used in standard practice to help discriminate G3 NETs from NECs, the latest commonly characterized by p53 mutations and Rb loss (10). These and other molecular markers shall be incorporated in future classifications to further characterize and stratify the prognosis and guide therapy of patients with NENs. The most recent 2015 WHO classification of lung NENs defines four subtypes: well-differentiated, low-grade typical carcinoids (TCs); well-differentiated, intermediate-grade atypical carcinoids (ACs); poorly differentiated, high-grade large cell neuroendocrine carcinomas (LCNECs); and poorly differentiated, high-grade small cell neuroendocrine carcinomas (SCLCs) (11). Well-differentiated lung NETs are classified based on the mitotic count and the absence or presence of necrosis (TC are characterized by a mitotic count <2 per 10 HPF and absence of necrosis, and AC are characterized by a mitotic count of 2 to 10 per 10 HPF and the presence of necrosis). On the other hand, poorly differentiated tumors are sub-classified based on cellular size as small (SCNEC or SCLC) or large cell NECs (LCNEC). Poorly differentiated lung NENs are characterized by high mitotic counts (> 10 per 10 HPF), the presence of necrosis and are associated with an aggressive biological behaviour and a dismal prognosis. The WHO classification refers to well differentiated NETs as carcinoid tumors, which differs from the WHO classification terminology proposed for NETs arising in the other anatomic sites, where the term carcinoid has been replaced by well-differentiated NETs.

Regarding local, regional and distant extent of disease NENs are classified according to the American Joint Committee on Cancer/Union for International Cancer Control (AJCC/UICC) TNM staging system (8th edition) (12).

1.2 CLINICAL PRESENTATION OF NENs

1.2.1 Neuroendocrine tumors (NETs)

NETs have distinct clinical features based on their site of origin. However, an increasing proportion of NETs are incidentally diagnosed in asymptomatic patients in the context of diagnostic or surgical procedures performed for other causes, or present nonspecific or insidious symptoms that make them difficult to diagnose on clinical grounds alone. Tumor-related symptoms widely vary by primary tumor site, tumor bulk and extent of disease. Ten to twenty percent of patients may also present hormone-related symptoms. Indeed, a peculiar characteristic of NETs is their potential ability to synthesize and secrete into the systemic circulation a variety of metabolically active substances (hormones and amines such as bradykinins, tachykinins, prostaglandins, and histamine) of which serotonin is the most commonly encountered (13). More than 15 individual neuroendocrine cell types have been identified, all secreting different hormones, leading to a wide spectrum of clinical syndromes (14). The diagnosis of these syndromes is established when the clinical presentation fits a specific combination of signs and symptoms, and this is confirmed by demonstrating elevated levels of the corresponding hormone (15). When hormonal syndromes are present the tumors are defined as functioning tumors (16,17). Most GEP-NETs are sporadic, although about 5% of them arise as part of inherited familial syndromes, including multiple endocrine neoplasia type 1 (MEN-1), Von-Hippel Lindau (VHL) syndrome, tuberous sclerosis, and neurofibromatosis type 1.

1.2.1.1 Non-functioning NETs

Hormonally silent or non-functioning tumors (NF-NETs) are commonly discovered incidentally, or late in the course of the disease when they develop tumor-related symptoms related to tumor bulk or constitutional syndrome (i.e. fatigue or weight

loss), like any other neoplasms. Their wide anatomic distribution and growth rates make clinical manifestations mimic a variety of disorders. Therefore, NF-NETs tend to be diagnosed at later disease stages with larger primary tumors and often with metastatic disease. Recent studies demonstrated that vague symptoms such as abdominal pain precede the diagnosis of a gastrointestinal (GI) NET by a median of 9.2 years (18).

1.2.1.2 Functioning NETs

In most anatomical locations roughly 10% of cases are functioning NETs, except for the pancreas and ileum, where they represent 30% of cases (19).

Carcinoid syndrome (CS) is the most frequent NET hormonal syndrome, representing the clinical expression of serotonin-producing NETs. In these patients, mostly serotonin, but also histamine and the kinin peptides, reach the systemic circulation and determine characteristic clinical manifestations. Primary tumors leading to this syndrome are those not draining to the portal system (i.e. lung NETs) or those with hepatic or retroperitoneal metastasis, as a result of the bypass of hepatic metabolism. Predominantly metastasic small bowel NETs (20-30%), followed by thymic and bronchial NETs may present with CS. Pancreatic or other gastrointestinal NETs very rarely develop CS. CS consists of secretory diarrhea (70% of patients), flushing (90% of cases), venous telangiectasias (25% of cases), abdominal pain, bronchospasm (15%), and neuropsychological symptoms (20). The increased conversion of tryptophan to serotonin may lead to tryptophan deficiency with subsequent decreased protein synthesis, hypoalbuminemia and nicotinic acid deficiency leading to pellagra (5%). Carcinoid crisis is a potentially life-threatening complication of carcinoid syndrome caused by the sudden release of high levels of serotonin and other active substances in the circulation. Carcinoid crisis is characterized by severe hypotension, arrhythmias, tachycardia, flushing and bronchospasm, and can be lethal. This sudden release may be caused by tumor manipulation during surgery, tumor biopsy, induction of anesthesia or other types of intervention, such as arterial embolization, radiofrequency ablation, endoscopic procedures, among others. To prevent carcinoid crisis, adequate perioperative or peri-procedure management is of utmost importance, including the administration

of high doses of somatostatin analogues. Additionally, fibrosis is considered a hallmark of CS: a chronic exposition to high serotonin levels can induce fibrogenic responses in local or distant tissues, leading to carcinoid heart disease (CHD) and mesenteric fibrosis (21,22). Although less common, functional pancreatic tumors (F-pNETs) account for a fascinating spectrum of clinical syndromes resulting from excess tumor production of insulin, gastrin, glucagon, vasoactive intestinal peptide, or, more rarely, somatostatin.

Insulinomas are the most common F-pNETs, followed in decreasing order by gastrinomas, glucagonomas, VIPomas and somatostatinomas, pNETs causing carcinoid syndrome, and other rare hormonal syndromes (23). Insulinomas, due to excessive insulin production, present with recurrent hypoglycemic episodes, especially after fasting or heavy exercise, resulting in intermittent confusion, weakness, diaphoresis, and nausea, symptoms that are often relieved by eating. Gastrinomas, secondary to a gastrin excess, give rise to the Zollinger-Ellison syndrome, characterized by acid hypersecretion and refractory peptic ulcer disease (PUD), abdominal pain and diarrhea. Glucagonoma, due to glucagon excess, are characterized by diabetes, diarrhea, necrolytic migratory erythema and venous thrombosis. VIPomas, secondary to vasoactive intestinal peptide (VIP) hyper-secretion, are associated to the Verner–Morrison syndrome, consisting of watery diarrhea, achlorhydria and hypokalemia. Finally, somatostatinoma, which is related to an excess of somatostatin production, is characterized by diabetes, steatorrhea and cholelithiasis (23).

1.2.2 Neuroendocrine carcinomas (NEC)

NECs are rare malignancies. According to epidemiological SEER data, 90% of high grade NECs (HG-NECs) are of pulmonary origin and only 9% are extra-pulmonary (EP-NEC) (24). EP-NECs can be localized throughout the body but are most commonly encountered in the gastrointestinal (GI) and genitourinary tracts. EP-NECs are biologically aggressive neoplasms, with a median survival for all stages of 10 to 12 months with best available therapy (25,26) (24,25). Metastatic disease is present at diagnosis in about 60% of patients and confers a dismal prognosis (5

months in metastatic disease at diagnosis, as compared to 38 months in patients with a localized disease at diagnosis) (25) .

Clinical presentation comprehends constitutional symptoms such as weight loss and fatigue, and symptoms related to tumor bulk (i.e. cough, dyspnea, pain, bowel obstruction, etc..) (27).

1.3 DIAGNOSIS OF NENs

1.3.1 Histological diagnosis

To make the diagnosis of NEN, histological confirmation is essential, as recommended by international guidelines (ESMO, European Society of Medical Oncology, ENETS, European Society of Neuroendocrine Tumors, NANETS, North American Society of Neuroendocrine Tumors) (9,16,28). From a morphological point of view, NETs are characterized by an "organoid" growth pattern (with nests, trabeculae or solid) with minimal atypia and scarce necrosis, and a well differentiated morphology. NECs show diffuse, solid growth, with extensive necrosis and marked cytological atypia. NECs, depending on cell size, are further classified into three groups, small cell, large cell and mixed NECs respectively (29). Small cell NECs have an elevated nucleus to cytoplasm ratio, finely granular chromatin, poorly evident nucleoli, rounded or fusiform contour of the nucleus, "nuclear molding" or nuclear molds, thus defined nuclei deformed due to pressure from other nuclei of the same cell or neighboring cells. Large cell NECs, on the other hand, generally have a diffuse growth pattern, with cells having a round or oval morphology, evident cytoplasm, granular or vesicular nuclei, often well represented nucleoli, may present glandular features or intracytoplasmic mucin. The third group generally presents a diffuse growth pattern, a moderately increased nucleus to cytoplasm ratio, poorly defined nuclear borders, vesicular nuclei, nucleoli more evident than in small cell NECs, and absence of "nuclear molding" (30). The MiNENs, on the other hand, are characterized by the presence of two distinct neoplastic neuroendocrine and non-neuroendocrine components (31). The diagnosis of these mixed forms is not always easy, especially if they are poorly differentiated components and may require additional immunohistochemical or molecular investigations (32). In greater detail, the MiNENs are classified on the

basis of morphological criteria into three different entities: the "collision" or contrasting MiNENs, the composite forms and the anphicrine MiNENs. The first category presents the juxtaposition of two populations of neoplastic cells that coexist but remain topographically separate. The composite forms, on the other hand, consist of the integration of the two populations into one or the presence of a prominent component and a focal area of a minority component. Finally, the anphicrine MiNENs are composed of a single cell population that has the phenotype of at least two neoplasms, generally adenocarcinoma and neuroendocrine neoplasm, with cell cytoplasm containing both neuroendocrine secretory granules and mucin (33).

1.3.2 Biochemical diagnosis

NENs are a heterogeneous family of cancers in terms of tumor biology and also regarding the variety of products they can synthesize and secrete. Some of the secreted hormones are bioactive and consequently associated with a secretory syndrome. These specific hormones are useful biomarkers for the diagnosis and follow-up of patients with functioning-NETs, which overall represent only about 20% of cases. Nevertheless, non-functioning NENs may secrete compounds that are not bioactive but may be detected for diagnostic or monitoring purposes (general biomarkers). However, the majority of circulating biomarkers in NENs do not have enough sensitivity nor specificity to facilitate an early diagnosis, and a substantial proportion of patients are unfortunately still diagnosed at advanced stages of disease. Thus, although circulating biomarkers are a useful aid for diagnosis, they are not considered mandatory and are generally not enough as sole diagnostic tool to establish a NET diagnosis (34,35). Moreover, these biomarkers are all considered to be of insufficient value to accurately identify the primary tumor site or correlate with tumor burden. However, they have a consolidated role in monitoring the progress of the disease during treatment and follow-up of NEN patients (36).

1.3.2.1 General biomarkers

CgA is a heat stable, hydrophilic and acidic protein of ~460 amino acids with a molecular mass of ~70 to 85 kDa (37). Functionally, CgA is an inhibitor of catecholamine, parathormone, insulin, and leptin secretion but elevates glucagon and amylase release. In addition to its effects on endocrine organs, CgA also regulates reproductive and cardiovascular functions as well as having antimicrobial effects (38).

Determination of serum Cg A is the most commonly used test in the field of NENs (39). CgA concentrations are sensitive but nonspecific markers of NETs, with sensitivity that varies from 46% to 100% and specificity from 68% to 90% (40). In fact, although elevations in plasma CgA are principally associated with NETs, increased levels may occur in non-NE cancers, endocrine disease, gastrointestinal and renal disorders, inflammatory and cardiovascular diseases. Chronic atrophic gastritis and drugs that suppress acid secretion, particularly proton pump inhibitors (PPIs) and to a lesser extent histamine 2 receptor antagonists (H2RAs), elevate CgA as a result of compensatory hypergastrinemia and consequent gastric enterochromaffin-like neuroendocrine cell hyperplasia. Additionally, strenuous exercise and food intake may increase CgA levels. Endocrine disorders associated with elevated CgA are pheochromocytoma, hypercortisolemia, hyperthyroidism, medullary thyroid cancer, hyperparathyroidism, and pituitary tumors (except prolactinomas). The diagnostic accuracy of CgA measurement for NENs is greater for WD-NETs than for PD-NECs (41). Retrospective analyses suggest high CgA levels are associated with a poor survival (42), and prospective evidence provided by the RADIANT-1,2,3 trials have confirmed the prognostic value of CgA levels in advanced NETs (43–45). However, CgA role in NENs is limited by the lack of assay standardization leading to significant variations across different laboratories, the fact that 35-50% of NENs do not present elevated CgA levels, the lack of specific cut-off values for precise risk stratification, and the low concordance of CgA dynamic changes with tumor progression. It exerts a better overall accuracy (84%) during follow-up for the early detection of recurrence rather than in the diagnostic setting, where its clinical value is further hampered by the priorly discussed issues limiting both its specificity and sensitivity. Thus, despite

representing the best available general monoanalyte marker related to NEN (46), CgA is not very useful for diagnosis nor for therapeutic decision-making (47).
NSE is a neuron-specific isomer of the ubiquitous glycolytic enzyme 2-phospho-D-glycerate hydrolase or enolase that catalyzes the conversion of 2-phosphoglycerate to phosphoenolpyruvate. This isomer is a 78 kD gamma-homodimer and represents the dominant enolase-isoenzyme found in neuronal and neuroendocrine tissues (47). NSE is not commonly used alone in clinical practice due to its low diagnostic sensitivity of 31% (48) . Furthermore, NSE can be overexpressed also by several non-NE tumors, such as parathyroid cancer, prostate carcinoma, or neuroblastoma, and it has been correlated with high-grade disease, poor tumor differentiation and prognosis (49,50). However, early CgA/NSE responses predict treatment outcomes in patients with advanced NETs (44,51).

1.3.2.2 Specific biomarkers

The screening role for hormonal markers is justified if clinically indicated. Patients who present with symptoms of CS should undergo measurement of 24-hour urinary excretion of 5-hydroxyindoleacetic acid (5-HIAA), the primary end-product of serotonin metabolism, which is commonly used as a diagnostic test for CS with a sensitivity and specificity of 70 and >90%, respectively (28). It should be noted that several commonly prescribed drugs, certain diseases and foods may produce falsely elevated 5-HIAA levels. 5-HIAA levels are associated to prognosis, to the development of carcinoid heart disease and, to a lesser degree, to the development of mesenteric fibrosis in patients with CS. Several studies have reported similar accuracy for the determination of serum or plasma 5-HIAA levels as compared to 5-HIAA assessed in 24-hour urine samples, providing a more convenient diagnostic tool for these patients, although this assay is not yet widely available for routine clinical use (52).
In patients with a clinical presentation suggesting a functional duodenopancreatic NET such as an insulinoma, a gastrinoma, a glucagonoma, a somatostatinoma, or a VIPoma, the corresponding hormones shall be assayed in plasma (insulin, glucose and C-peptide, glucagon, gastrin, somatostatin and VIP, respectively) (53). The biochemical diagnostic criteria are briefly summarized below. For insulinoma: 72

hours fast plasma glucose <45 mg/dL; insulin ≥ 6 mU/mL; insulin/glucose ratio >0.3; C-peptide level ≥ 0.2 nmol/L; proinsulin level ≥ 5 pmol/L; absence of sulfonylurea. For gastrinoma: increased fasting serum gastrin levels off PPIs in the setting of a gastric pH <2.5; secretin stimulation test with paradoxic increase in serum gastrin by ≥ 200 pg/mL. For glucagonoma: markedly increased fasting serum glucagon level (>500 pg/mL). For VIPoma: serum VIP level >75 pg/mL. And for somatostatinoma: fasting serum somatostatin level >160 pg/mL.

1.3.2.3 Other circulating biomarkers

More recently, biomarker development is focusing on the characterization of tumor biology in peripheral blood through the analysis of circulating tumor cells (CTCs), tumor-derived DNA, mRNAs, micro-RNAs or other products that are shed into the blood stream. This allows a dynamic tumor characterization over time and has also the advantage of assessing tumor heterogeneity in a non-invasive way. Although not yet considered standard of care, this approach shall likely be incorporated in routine clinical practice in the near future (54). Among them, currently the evaluation of CTCs finds clinical use in various tumor types including prostatic, ovarian, lung and breast cancers (55). Once isolated, the CTCs are used for carrying out cytological and molecular analyses in order to obtain clinical information but also to broaden the knowledge of the various processes involved in tumor genesis and progression (56). To date, limited evidence exists about the role of CTCs in NENs. In this context, a study enrolling 79 patients with metastatic NETs of GEP or lung origin, observed that the presence of CTCs was associated with a more aggressive disease (57). Another study, including 175 NETs, suggested that CTCs are a negative prognostic factor for survival (58). These data have been confirmed by Khan and colleagues in a population of 138 advanced NETs. In this study the presence and changes in CTCs levels correlated with response to treatment and patients' outcomes (59). Therefore, further prospective studies are still needed to confirm and to validate these promising data about the utility of CTCs in NENs.

In the last years, an innovative tool called NETest, has been studied and evaluated for NETs. The NETest allows to quantify in peripheral blood through real time PCR (rt-PCR) the presence of different tumoral transcription products (mRNA) (60). The

NETest consists of a panel containing 51 genes involved in neuroendocrine tumorigenesis which together constitute a characteristic fingerprint of NEN (61). These genes were selected through a multistep process using microarray technology, which allows to verify how many and which genes are active in a specific cell type or tissue and their level of expression. By comparing tissues of NEN and other tumor histotypes with healthy tissues, genes overexpressed only in GEP-NEN were selected and, among these, those found in the blood transcriptome were subsequently identified. By integrating these genes with those already known in the literature, the currently used panel was obtained (60). Many studies have investigated the effectiveness of the NETest in identifying NENs of various origins (GEP, pulmonary, pheochromocytoma /paraganglioma), allowing the differential diagnosis with non-neuroendocrine tumors and non-neoplastic diseases (62–64). Moreover, a predictive role (particularly in terms of response to treatment with somatostatin analogues, SSAs, or peptide receptor radionuclide therapy, PRRT) for the NETest has been suggested across different studies (65). Finally, a prognostic role has also been demonstrated for this new biomarker for NET patients in several studies (62,63). Notably, the NETest has shown to be a good biomarker in predicting the outcome of NET patients undergoing radical surgery, with a significant superiority of this method over clinical-pathological criteria and blood levels of CgA (66,67).

1.3.3 Diagnostic imaging

1.3.3.1 Conventional Imaging

Diagnostic imaging is essential for the correct diagnosis, staging, therapeutic strategy design, assessment of response to therapy and for the follow-up of NENs. CT is the most recommended and used diagnostic tool in clinical practice, with an average sensitivity of 82-100% and a specificity of 83-100% (68). CT scan, thanks to its rapid acquisition process and its ability to generate multiplanar reconstructions, provides high levels of spatial resolution, which are essential for obtaining accurate details relating to the size of neoplastic lesions, the relationships with adjacent anatomical structures and their distant metastatic spread. Most NENs are visible as highly vascularized lesions and are generally more evident in the later

stages of arterial acquisition, whereas in CT images without the iodinated contrast medium NENs lesions may present the same density as the normal parenchyma, thereby limiting an accurate detection. It is therefore essential to perform CT with intravenous administration of iodinated contrast medium and a multi-phase technique, including arterial and venous acquisition phases (69). More recently, a new modality, spectral or dual energy CT (DECT) has been studied and validated. This computed tomography technique uses two separate x-ray photon energy spectra, allowing the interrogation of materials that have different attenuation properties at different energies, which provides more information on the composition of the different tissues and greater diagnostic accuracy (70).

Another commonly used imaging modality is Magnetic Resonance Imaging (MRI), which has a sensitivity and specificity of 74% and 94%, respectively, if performed after intravenous administration of contrast medium. MRI has some advantages over CT such as the lack of ionizing radiation, the use of non-iodinated contrast medium, the superiority in the analysis of soft tissues and non-hyper-vascularized lesions, and a lower inter-observer discordance. Furthermore, MRI is more adequate than CT for the study of small lesions and has higher resolution for the assessment of pancreatic NENs and metastatic liver lesions (69,71). However, MRI is more expensive and time-consuming than CT, requires improved patient collaboration (to avoid movement artefacts) and is therefore less commonly used in clinical practice (72). Trans-abdominal ultrasound (US) also plays a fundamental role in the evaluation of NEN as a first level imaging test. This technique is operator-dependent and has modest sensitivity and specificity, but can be chosen in patients with allergy to the contrast medium or in patients with contraindications to perform CT and MRI (73). The primary roles of US include the first-step diagnosis of NEN patients with advanced disease, particularly the detection of liver metastasis in patients under evaluation due to liver function test abnormalities, abdominal pain or palpable masses; the intraoperative location of tumor deposits for resection or to direct ablative therapy; the endoscopic assessment of gastroenteropancreatic or rectal tumor locoregional extension to plan adequate local therapy; or the access to pancreatic lesions or regional lymph nodes for needle-biopsy (74).

These first-line diagnostic methods are accompanied by complementary tests indicated in specific clinical contexts, such as endoscopic procedures or target

imaging as appropriate, including capsule endoscopy, entero-CT or entero-MRI in the suspicion of NEN of the small intestine, or virtual colonoscopy for the study of obstructive colorectal NE lesions. In the absence of neurological symptoms, CT or MRI of the brain are not indicated as routine investigations, since the incidence of brain metastases in EP-NECs is less than 5% (25). Bone scans to screen bone metastasis are also not indicated in asymptomatic patients.

1.3.3.2 Functional imaging

Functional imaging methods play a prominent role in NEN diagnostics and therapeutic planning. In particular, somatostatin-receptor imaging (SRI) techniques such as scintigraphy (SRS) with 99m-technetium-octreotide or 111-Indium-pentetreotide (OctreoScan®) and positron emission tomography (PET) with Gallium68-labeled somatostatin analogues (for example, 68Ga-DOTATOC, 68Ga-DOTATATE, 68Ga-DOTANOC), are essential tools for the diagnosis and staging of well differentiated NETs (75). These methods assess the expression of somatostatin receptors in neuroendocrine tumor cells, particularly of subtype 2 (SSTR 2), and are thus also useful tools to predict response to therapy targeting these receptors, such as *cold* SSAs and PRRT with radiolabelled somatostatin analogues (76). PET with Gallium68-radiolabeled SSAs has replaced Octreoscan® in many countries as it has greater sensitivity, specificity, rapidity and spatial resolution, and allows to quantify metabolic activity by means of the SUV parameter (standardized uptake value) (77).

On the contrary, in high-grade NENs the use of SRI is not routinely recommended, particularly for poorly differentiated G3 NENs, as they generally do not express somatostatin receptors (69). However, they may be considered in G3 NETs or NENs wih Ki-67 values in the low G3 range (<55%). Recently, a study conducted on a large series of NECs reported 111-Indium Octreoscan was positive in up to 45% of cases, especially in NECs with Ki67 value up to 55% (25). In high-grade EP-NECs and MiNENs, 18-fluorodeoxyglucose PET (or 18F-FDG-PET) frequently shows a high metabolic activity and this is associated with a worse prognosis. Therefore, as in other aggressive non-neuroendocrine malignancies, 18F-FDG-PET is a functional technique that allows to identify, with high

sensitivity, rapidly proliferating lesions, stratifying NENs on the basis of biological aggressivity, including G2 NETs (78). Indeed, positivity in 18F-FDG-PET may identify WD tumors with more aggressive clinical behaviour, or the presence of more aggressive clones within the same tumor. This information, together with the pattern of SSTR expression, plays a major role in the therapeutic choice and clinical management of these neoplasms.

Other PET radiotracers used in NEN diagnosis include 18F-DOPA (18F-FDOPA) and other new radiotracers as 68Ga-antagonists and 68Ga-exendin. A large literature demonstrates the high sensitivity and diagnostic accuracy of PET with 18F-DOPA for the identification of well-differentiated NENs and its superiority over conventional imaging methods (79). It must be noted, however, that the physiological distribution of 18F-DOPA at the pancreatic level limits the possibility of studying tumors in this anatomical site. Furthermore, given the reported inferiority of 18F-DOPA compared to PET-CT with Gallium68-labeled somatostatin analogues in the study of SSTR-expressing NENs (80) and the technical difficulties of its synthesis, its clinical use is mainly aimed at the study of NEN subtypes characterized by low/variable expression of SSTRs (eg neuroblastoma, pheochromocytoma, medullary thyroid carcinoma) (81). More recently, 68Gallium-labeled somatostatin antagonists (SANTs) PET tracers have also been explored. Preliminary results from preclinical and clinical studies have shown greater tumor uptake, independent of SSTR activation, and greater tumor-to-organ ratios than agonists, thereby potentially increasing sensitivity for the detection of NENs. This may be relevant for the study of NENs characterized by low or variable expression of SSTR (82) and could also have a significant impact on the effectiveness of PRRT (83). Novel radioligands targeting other NET targets are also being developed. 68 Ga-exendin is an emerging PET radiopharmaceutical that binds to the GLP-1 receptor and has been used for the identification of insulinoma (the identification of which is usually difficult due to their often small size and the fact that up to 20% do not express SSTRs). Preliminary evidence supports the role of this new radiopharmaceutical for the pre-operative identification of occult insulinoma (reported sensitivity of 97.7%) (84,85). The development of new radiotracers is a challenging and rapidly evolving field that will likely expand theranostic options for NENs in the very near future.

1.4 TREATMENT OF NENS

Management of NENs represents a clinical challenge due to their wide anatomic distribution, high number of specialists involved, heterogeneity of clinical presentation and behaviour, limited treatment options and clinical evidence, and lack of predictive biomarkers to guide management. In this context, international guidelines for NENs emphasize collaboration among diverse medical disciplines to improve patients' care and standardize diagnostic and therapeutic approaches. Ideally a multidisciplinary tumor board should include NEN-dedicated medical oncologists, endocrinologists, pneumologists, gastroenterologists, surgeons, pathologists, nurses, interventional radiologists, radiotherapists, and nuclear medicine physicians (Figure 2). A multidisciplinary approach offers the best prospect for planning optimal management and improving clinical outcomes in patients with NENs (86–88). Early referral to NEN-dedicated centers may shorten delay in diagnosis and increase the opportunity for patients to receive the best care in terms of treatment options and follow-up (86–88).

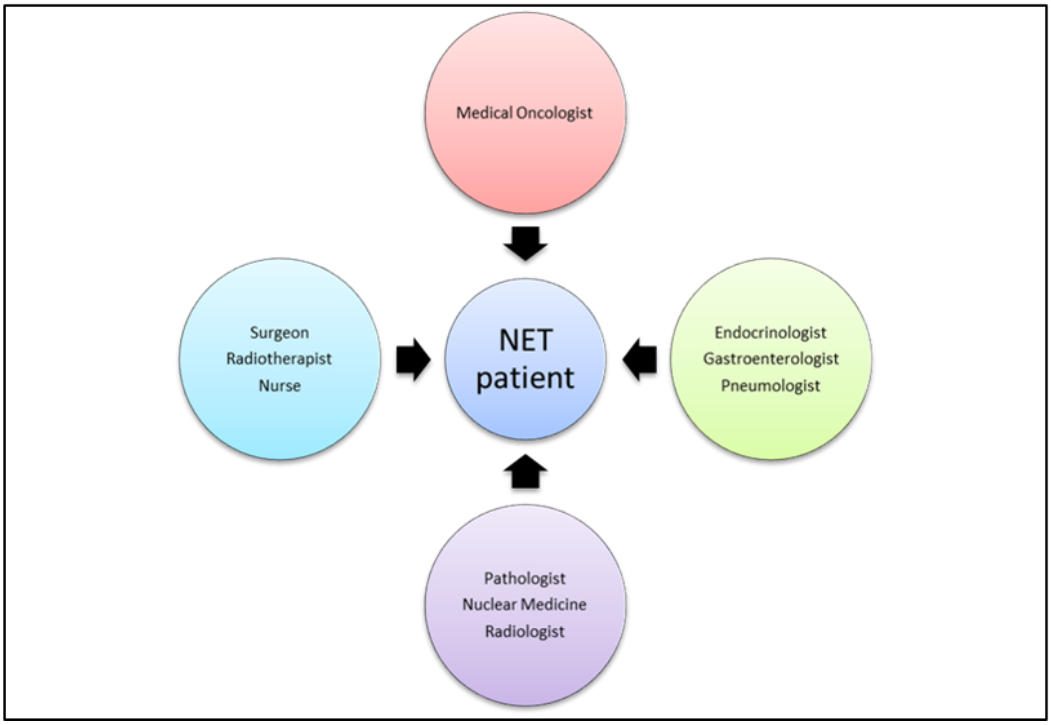

Figure 2. Multidisciplinary NET-dedicated tumor board.

1.4.1 Localized disease

1.4.1.1 Surgery

The standard of care for patients with localized NENs is surgical resection (89–95). However, depending on the primary tumor site and grade, some relevant considerations should be discussed. Surgery is curative in a high proportion of localized NETs, and more conservative approaches may be considered in small G1 well-differentiated tumors, whereas the rate of disease recurrence following surgery is very high in localized NECs, and thus adjuvant therapy is generally advised in these patients (96).

1.4.1.1.1 Small bowel NETs

Small bowel NETs are often identified incidentally during endoscopic procedures done for other causes, or alternatively present with non-specific GI symptoms, abdominal pain, GI bleeding or bowel obstruction, and thereby may undergo urgent surgery before diagnosis (97).

The optimal surgical treatment of small bowel NETs is segmental small bowel resection or ileocecectomy (for distal ileal tumors) with resection of regional lymph nodes up to the segmental branches of the superior mesenteric artery and vein (91). The abdomen should be diligently inspected for evidence of peritoneal and liver metastases, which are present in up to 20% and 60% of patients who undergo surgery for small bowel NETs, respectively (98). Careful palpation of the entire small bowel is critical to detect multifocal tumors, which often are subcentimetric in size and are detected in about 50% of cases (98). Although surgery is potentially curative, recurrence rates of over 40% have been reported after resection, and the liver is the most common site of recurrence (99). Recurrence may occur many years after the initial surgery due to the slow growth of small bowel NETs. Therefore surveillance of these patients is recommended for up to 10 years following surgery (90).

Surgery in metastatic disease should be considered in NET patients with resectable oligometastatic disease. In the presence of unresectable metastasis, surgery of the primary tumor may be indicated in selected cases, to palliate symptoms or to prevent life-threatening complications such as intestinal ischemia due to mesenteric

fibrosis or bowel obstruction or bleeding (100–102). Retrospective data suggest primary tumor resection is associated with longer survival in this setting (97,103,104), although controlled series have not demonstrated a survival advantage of this approach in asymptomatic patients with stage IV midgut NETs (105). In the presence of refractory hormonal syndrome, liver debulking surgery can also be considered to achieve syndrome control, although the benefit of R2 surgeries is controversial and the optimal resection volume is uncertain.

1.4.1.1.2 Gastric NETs

Gastric NETs are divided into three subtypes with different clinical characteristics, pathophysiology, therapeutic and prognostic implications: type I gastric NETs (70-85%) associated with chronic atrophic gastritis, type II gastric NETs (5-10%) associated with Zollinger-Ellison syndrome (ZES), usually in the context of multiple endocrine neoplasia type 1 (MEN-1)-associated gastrinomas, and type III gastric NETs, that are sporadic, and have a high rate of metastasis at diagnosis and often a poor prognosis (106).

Clinical management of localized gastric NETs mainly depends on the tumor subtype, size and grade, andextent of locoregional extension. Type I and type II gastric NETs, especially those < 1 cm in size, may be treated by endoscopic resection, or if not removed, then monitored by close endoscopic surveillance. Types I and II G1 tumors of 1–2 cm in size and those with submucosal invasion can be removed by endoscopic mucosal resection (EMR) or submucosal dissection (ESD). Small not removed lesions should be closely surveyed every 1–3 years, although there is much controversy regarding the appropriate monitoring frequency depending on tumor type, number, and size. Patients with tumors > 2 cm in size are generally considered for surgical resection (107). Surgical resection including locoregional lymph nodes is the treatment of choice for type III gastric NETs (106).

1.4.1.1.3 Appendiceal NETs

Appendiceal NETs (A-NETs) are usually incidentally discovered intraoperatively in the context of acute appendicitis. A-NETs are generally indolent tumors and appendicectomy alone is curative for stage I disease. However, some high-risk

features such as tumor size and grade, mesoappendiceal invasion, lymphovascular invasion, and perineural invasion have also been identified as risk factors for metastatic spread, although the optimal extent of surgical resection is still a matter of debate (108). Additional surgery such as right hemicolectomy is not mandatory in patients with stage IIa tumours (≤2 cm invading submucosa, muscularis propria and/or minimally (up to 3 mm) subserosa/mesoappendix or tumours >1 cm but ≤2 cm) but may be considered in young, fit patients (109). For stage IIb A-NETs, right hemicolectomy is recommended due to the increased risk of LN metastasis (110).

1.4.1.1.4 Pancreatic NETs

Surgical resection of localized disease is the mainstay of therapy for all functioning pNETs (111). However, among F-pNETs, insulinomas are unique due to their very low risk of regional or distant metastastic spread that make them suitable candidates for pancreas-sparing conservative surgical procedures. Unlike formal pancreatic surgery, such as distal pancreatectomy, central pancreatectomy, or duodeno-pancreatectomy, enucleation involves removal of just the tumor and associated capsule, sparing otherwise normal pancreatic parenchyma. A systematic review of case series with a total of more than 6200 insulinoma patients supports enucleation as the procedure of choice for most insulinomas (112). The primary goal of surgical management of non-functional pNETs is to prevent metastases and improve long-term survival (113,114). Surgical resection typically consists of formal anatomic resection of the pancreatic head (pancreaticoduodenectomy) or body/tail (distal pancreatectomy with or without splenectomy). Local invasion of nearby organs or vascular structures is not a contraindication to potentially curative resection if all macroscopic disease can be removed. However, optimal timing and extent of surgery in small incidentally detected pNETs (<2 cm) is still a matter of debate, particularly when a major pancreatic resection is required or in the context of a hereditary syndrome (MEN1, VHL) (115,116). A conservative approach seems to be safe as the majority of observed tumors did not show any significant changes during follow-up (117,118). However, large prospective studies with long-term follow-up are needed to confirm this strategy does not compromise survival.

1.4.1.1.5 Rectal NETs

According to the SEER database, rectal NETs have the best median overall survival (after appendiceal neoplasms) amongst all anatomical origins (1). The reason is that the majority of these lesions are discovered at early stages (with the majority (80-90%) being <1 cm and localised to the submucosa), often incidentally on screening colonoscopy.

The current guidelines recommend local endoscopic mucosal resection and endoscopic submucosal dissection for rectal NETs ≤10 mm in size with no risk factors for metastasis (with risk factors including size, atypical appearance, grade and depth of invasion) (119). Less than 2% and 0.7% of tumors <10mm in size, with no ulceration or depression, no muscularis invasion, no lympho-vascular invasion, and mitotic index of<2/10 HPF are associated with lymph node or distant metastases, respectively (120). However, the management of rectal NETs between 10–20 mm is more debated (121).These cases are associated with a higher risk of distant metastases (4%–30%). Each case should be discussed in the multidisciplinary tumor board and can be treated with endoscopy or surgery depending on stage, tumor grade (122), and the patient's general health status, particularly the risk of potential intervention-associated co-morbidity for slowly progressive disease (123). Finally, lesions >20 mm have a 57%–80% risk of having metastases or becoming metastatic during follow-up (124) and should be surgically managed as rectal non-neuroendocrine carcinomas with low anterior or abdominoperineal resection (125).

1.4.2 Locally inoperable/metastatic disease

1.4.2.1 Locoregional treatments

Due to their relatively indolent course, NETs are frequently diagnosed in advanced stages of disease (126), being liver metastases the most frequent site of distant spread (127). In the context of metastatic disease, the role for cytoreductive surgery is controversial. It may be considered in patients with functional tumors to facilitate hormonal syndrome control (128,129), although this strategy is not so frequently

performed to date as more effective locally ablative and systemic therapies have notably expanded in recent years.

Locoregional ablative strategies, including radiofrequency ablation (RFA), microwave ablation, embolization/chemoembolization and selective internal radiotherapy (SIRT), among others, are commonly used in patients with liver-limited disease, particularly in functioning tumors (130–133). However, no prospective large randomized trials to date have properly assessed the safety and efficacy of the different available techniques, nor their potential benefit as compared to other systemic treatment options for advanced disease.

1.4.2.2 Systemic therapy

In the metastatic setting, systemic treatment is the standard of care, both in WD NETs and in PD NECs.

In the context of WD NETs, the therapeutic armamentarium has progressively increased over the last decades, and comprehends biotherapy (somatostatin analogues, SSAs), targeted agents (such as everolimus and sunitinib), interferon, chemotherapy and radiopharmaceuticals (peptide-receptor radionuclide therapy, PRRT). For aggressive, poorly differentiated, metastatic NECs classical cytotoxic chemotherapy is the only widely available treatment (Figure 3).

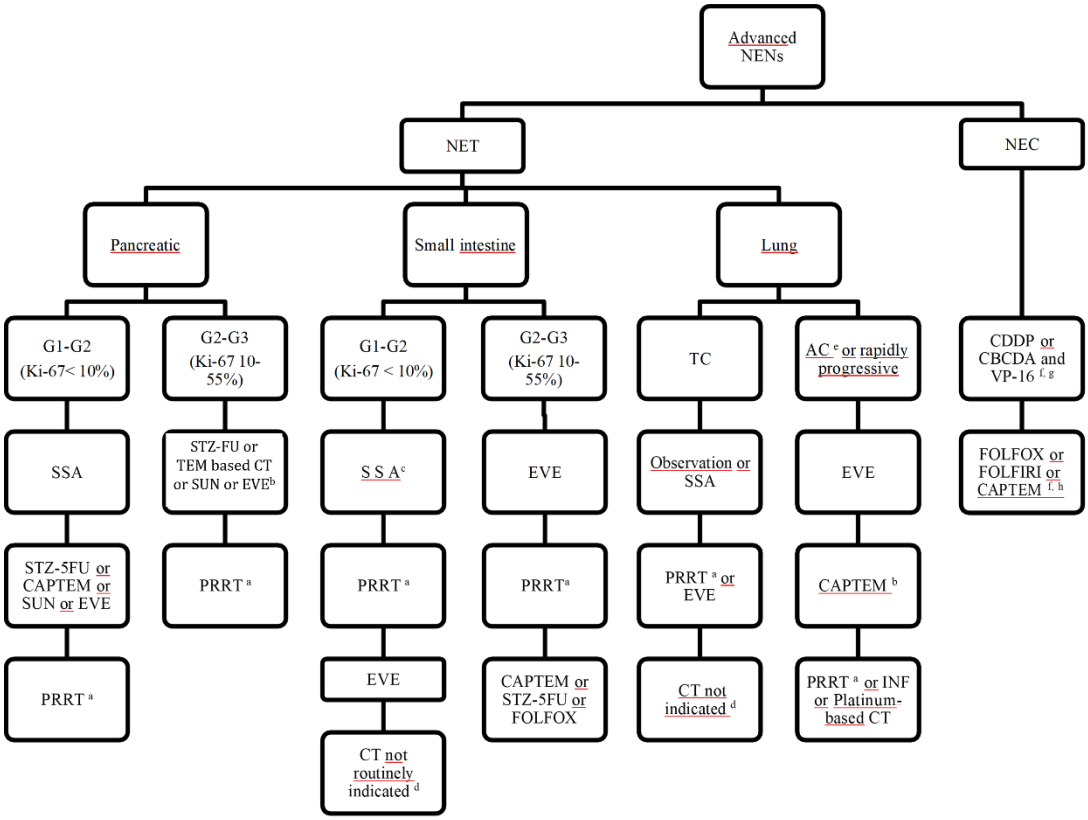

Figure 3. Therapeutic algorithm for advanced NENs. AC, atypical carcinoid; CAPTEM, capecitabine-temozolomide; CDDP, cisplatin;CBCDA, carboplatin; CT, chemotherapy; EVE, everolimus; FOLFIRI, 5-fluorouracil and irinotecan; FOLFOX, 5-fluorouracil and oxalipl- atin; INF, interferon-alfa; NENs, neuroendocrine neoplasias; NET, neuroendocrine tumor; NEC, neuroendocrine carcinoma; PRRT, pep- tide receptor radionucleotide therapy; SSA, somatostatine analogues; STZ-5FU, streptozocin-5 Fluorouracil; SUN, sunitinib; TC, typical carcinoid; VP-16, etoposide. [a]In somatostatin-receptor imaging positive tumors and/or refractory hormonal syndrome. [b]Chemotherapy preferred upfront over targeted agents in G3 NETs. [c]Watch and wait may be considered in G1 very indolent tumors, particularly in older or frailpatients. [d]CAPTEM may be considered after progression to all available treatments in selected patients with good PS and rapidly progressing tumors. [e]Chemotherapy may be considered upfront in selected patients (rapidly progressing tumors, Ki-67>20%). [f]Enrollment in clinical trials is recommended if available. [g]Carboplatin is preferred over cisplatin due to its more favorable toxicity profile. [h]The treatmentchoice should be based on response to prior therapy, toxicity profile, residual toxicity from prior chemotherapy (i.e. neurotoxicity) andpatient's comorbidities and preferences (i.e. oral vs iv)

1.4.2.2.1 SSTR-targeted therapy with somatostatin analogues (Octreotide, Lanreotide)

SSAs are synthetic octapeptides with a longer half-life than native somatostatin 14 and 28, which enabled clinical use (134). SSAs are very effective drugs for hormonal syndrome control in functioning tumors (135) (135–139), and also exert an antiproliferative effect by inducing cell cycle arrest and apoptosis, and indirectly through immunomodulatory effects and angiogenesis inhibition. Two systematic reviews and meta-analyses have reported symptomatic and biochemical responses

with SSAs in 65-74% and 39-51% of patients with CS, respectively (140,141). Moreover, in the observational SymNET study including NET patients with CS treated with lanreotide for 6 months, 76% and 73% of patients reported being completely/rather satisfied with the control of diarrhea and flushing following treatment with lanreotide for >3 months, respectively (16). SSAs also demonstrated in two randomized phase III trials to improve PFS in patients with GEP-NETs (142,143). The first one, the PROMID study, that included G1 advanced NETs of midgut origin, showed a significant improvement in time to progression for patients treated with octreotide LAR 30 mg every 4 weeks (14.3 months) as compared to patients in the placebo arm (6 months) (hazard ratio, HR 0.34, p = 0.000072) (108). The second one, the CLARINET trial, enrolled patients with advanced non-functional G1-2 GEP-NETs with a Ki-67 index <10% and a positive indium-111 pentetreotide scan (109). Treatment with lanreotide autogel significantly prolonged PFS over placebo (median not reached vs. 18 months, respectively, HR = 0.47, p = 0.0002). Although no differences in OS among treatment arms were detected in these studies (PROMID and CLARINET), the analysis was limited by crossover from the placebo group to the SSA cohort, the potential confounding effect of subsequent therapy after progression, and the low rate of events observed in this generally indolent disease. Therapy with SSAs, however, did not demonstrate a reduction of tumor load. The best clinical response obtained in all these studies was disease stabilization.

1.4.2.2.2 Peptide Receptor Radionuclide Therapy

An increasing body of evidence has demonstrated the effectiveness and safety of Peptide Receptor Radionuclide Therapy (PRRT) for NET. This strategy consists of coupling a radioisotope to a somatostatin analogue through a chelator (DOTA) to selectively target SSTR-positive NET cells. PRRT has been predominantly developed for two beta-emitting isotopes: yttrium-90 coupled to Tyr3-octreotide (90Y-DOTATOC) and lutetium-177 coupled to octreotate (177Lu-DOTATATE) (144). Upon membrane-receptor binding, the isotope is internalized and selectively delivers radioactivity to the target cell leading to DNA damage and cell death. Yttrium-90 is a β negative emitter, with a maximum β particle range of 11 mm and

a half-life of 2.7 days. Lutetium-177 is a β and γ emitter, with a maximum β particle range of 2 mm and a half-life of 6.7 days. Due to the different particle range, the potential for toxicity to adjacent healthy tissue is greater for Yttrium-90 as compared to Lutetium-177 (145). Several large retrospective series of referral centres and a randomized phase III trial have demonstrated the efficacy of PRRT in the treatment of SRI-positive NETs of various origins (144,146–149). In the NETTER-1 study, 229 patients with metastatic midgut NETs progressive to standard dose SSAs were randomized to receive 177Lu-Dotatate at a dose of 7.4 GBq every 8 weeks (4 iv infusions) plus octreotide LAR 30 mg every 4 weeks versus high doses of octreotide LAR (60 mg every 4 weeks). Median PFS was 28 months in the 177Lu-DOTATATE arm compared to 8.4 months in the control arm (HR 0.21, $p < 0.001$). A trend towards an improved OS for patients treated with 177Lu-Dotatate was also observed at the interim analysis. Based on these results, 177Lu-DOTATATE was approved by the European Medicines Agency (EMA) and the US Food and Drug Administration (FDA) for the treatment of advanced SSTR-positive GEP-NETs. More recently, mature final OS analysis have been reported with a median follow-up of 6.3 years, showing numerically greater median OS for 177Lu-DOTATATE-treated patients (48 vs 36.3 months, HR 0.84, p=0.30), although the observed differences did not reach statistical significance. However, one third of patients in the control arm received PRRT upon disease-progression (150).

1.4.2.2.3 Targeted agents

a) mTOR inhibitors

Everolimus is an oral mTOR inhibitor with a robust antitumour activity across a broad spectrum of advanced NETs, including those arising from the lung, pancreas and the GI tract, as demonstrated in several phase II/III trials (RADIANT 1,2,3,4) (43,44,151–153). Everolimus was first approved by FDA and EMA for the treatment of progressive, advanced P-NETs based on the results of the RADIANT-3 double-blind randomized trial, that showed a significant prolongation of PFS with everolimus versus placebo (11 months vs 4.6 months, respectively, HR 0.35, $p<0.0001$). More recently, everolimus was also approved in non-functional

progressive intestinal and lung NETs, based on similar results shown by the RADIANT-4 study (median PFS of 11 months with everolimus vs 3.9 months with placebo, HR 0.39, p<0.00001). Some efficacy was also shown when everolimus was combined with SSAs as compared to SSAs monotherapy in the RADIANT-2 study, conducted in patients with functional NETs, although the benefit observed was of borderline statistical significance (median PFS of 16.4 vs 11.3, HR 0.77, one sided p=0.026). The safety profile of everolimus is manageable, although around 60% of patients require dose reductions and up to 19% require treatment withdrawal due to side effects. Most common drug-related adverse events include stomatitis, rash, diarrhea, fatigue, weight loss, hyperglycemia and infections.

b) Angiogenesis inhibitors

Sunitinib maleate is a tyrosine kinase inhibitor (TKI), that can irreversibly inhibit several kinases including VEGFR and PDGFR, leading to angiogenesis inhibition and anti-tumor effects in several solid tumors (e.g., renal cell carcinoma and gastrointestinal stromal tumors), including NETs. In a multinational, randomized, double-blind, placebo-controlled phase III trial, 171 patients with progressive pNETs were allocated to receive sunitinib or placebo and best supportive care (154). The median PFS was 11.4 months in the sunitinib arm versus 5.5 months in the placebo arm (HR 0.42; p < 0.001). Five years after study closure, median OS was 38.6 months for sunitinib and 29.1 months for placebo (HR: 0.73; p = 0.094), with 69% of placebo-treated patients having crossed over to sunitinib treatment (155). The toxicity profile of sunitinib includes diarrhea, nausea, vomiting and fatigue, and less frequently hypertension, palmar-plantar erythrodysesthesia, neutropenia, and hypothyroidism. Based on this study, the drug was approved by EMA and FDA for the treatment of progressive, locally advanced inoperable or metastatic pNETs.

Another interesting angiogenesis inhibitor is Surufatinib, a TKI targeting VEGFR, FGFR and CSF1R. FGFR has been involved in primary and acquired resistance to VEGFR-targeted angiogenesis inhibitors and CSF1R is implicated in tumor immune evasion mechanisms. Surufatinib has demonstrated relevant activity in two phase III studies. First, the SANET-ep study included 198 patients with **e**xtra-

pancreatic NETs that were randomized 2:1 to receive surufatinib 300 mg daily (N=129) or placebo (N=69) (156). Median PFS per investigator assessment was 9.2 months for patients treated with surufatinib, as compared to 3.8 months for patients in the placebo group (HR 0.33; p<0.0001). The study was terminated early as it met the predefined criteria for early discontinuation at the interim analysis. The efficacy of surufatinib was seen across all subgroups and was further supported by significant improvements in secondary efficacy endpoints including ORR (10% vs 0%, p=0.0051), DCR and duration of response. The most common treatment-related grade $\geq$ 3 AEs were hypertension (36% vs 13%) and proteinuria (19% vs 0%). The second phase III clinical trial was the SANET-p study, that randomized (2:1) 264 patients with advanced pNETs to receive surufatinib or placebo (157). As the SANET-ep trial, this study was terminated early as it met the pre-specified early stopping criteria at interim analysis. Median investigator-assessed PFS was 10.9 versus 3.7 months for surufatinib- and placebo-treated patients, respectively (HR 0.49, p=0·0011). ORR was also significantly greater in patients treated with surufatinib (19%) compared to patients treated with placebo (2%) (p=0.002). Most common grade 3 or worse treatment-related AEs were hypertension (38% vs 7%), proteinuria (10% vs 2%), and hypertriglyceridaemia (7% vs none). Treatment-related serious AEs were reported in 22% (surufatinib) vs 7% (placebo) of patients. Based on these pivotal studies, that were fully conducted in Chinese population, the Chinese regulatory Medical Agency has approved surufatinib for the treatment of advanced non-pancreatic NETs and will likely be approved soon for pancreatic primaries.

Multiple other angiogenesis inhibitors are in different stages of clinical development (i.e. axitinib, pazopanib, lenvatinib, cabozantinib) but are not currently approved for the treatment of NETs.

1.4.2.2.4 Chemotherapy

Chemotherapy remains an essential component of the treatment strategy of patients with NENs, particularly for those with bulky, symptomatic or rapidly progressive tumors (generally G3 or high-G2 NENs).

In the context of NETs, chemotherapy has a well-established role in the management of those of pancreatic origin, whereas its use in lung or gastrointestinal NETs is still debated (158). In addition, randomized studies comparing the efficacy and safety of chemotherapy versus other treatment options such as targeted agents, locoregional ablative therapies or PRRT are needed to properly position chemotherapy within the treatment algorithm of NENs. A seminal randomized trial published by Moertel et al. in 1980 evaluated streptozotocin (STZ) with 5-fluorouracil (5-FU) versus STZ alone in patients with advanced islet cell carcinomas. The STZ-5FU combination showed an improved response rate as compared to single agent STZ (63 vs. 36%), and a trend towards improved survival (26 vs. 16 months) (159)). A subsequent randomized study published in 1992 by Moertel et al. (160) demonstrated that STZ plus doxorubicin was superior to STZ plus 5-FU in terms of the rate of tumor regression (69% vs. 45%, P = 0.05), time to tumor progression (20 vs. 6.9 months, P = 0.001) time to tumor progression and OS (26 vs 17 months, p=0.004). Nevertheless, the STZ-5FU regimen is most widely used as its toxicity profile is more suitable for long-term therapy. Finally, it should be noted that response rates in these trials were not assessed per current standard criteria (RECIST) and are overestimated as they also included clinical and biochemical responses. Indeed, more recent series of NET patients treated with these regimens showed lower figures than those reported in the 80-90's (161).

The combination of capecitabine and temozolomide (CAPTEM) is another widely used regimen in advanced NETs, based on response rates of up to 70% reported in small series of G1-2 NETs (162–165). More recently, a prospective randomized study demonstrated that CAPTEM (ECOG 2211) was associated with an improved PFS and OS in G1-2 metastatic pNETs when compared to temozolomide alone. Data supporting the use of CAPTEM in extrapancreatic (EP) NETs as well as in G3 NENs is scarce. Eads and colleagues are currently conducting the first prospective study to investigate the use of CAPTEM in the treatment of G3 NECs compared to platinum-based chemotherapy; however, its efficacy remains unclear (NCT02595424).

In summary, both STZ-5FU and CAPTEM are valid treatment options for P-NETs when chemotherapy is indicated, and are currently being compared head-to head in the BETTER-2 trial. The optimal integration of chemotherapy with other treatment

options in this setting is a matter of debate, and only few ongoing trials are aiming to address this relevant question (i.e. the SEQTOR trial assessing to sequencing strategies, STZ-5FU followed by everolimus upon progression or viceversa). Regarding EP-NETs, efficacy of cytotoxic chemotherapy is rather limited and thus its use cannot be recommended on a routine basis and shall be reseverd for selected patients with rapidly growing disease who have failed other more effective treatment options (158).

For PD-G3 NEC, chemotherapy remains the main therapeutic option, as these tumors are highly aggressive and associated with a very poor prognosis (median OS of 11-12 months with best available therapy). In this setting, neither debulking or cytoreductive surgery nor locoregional treatments are recommended. The most extensively explored first-line regimen is platinum-based chemotherapy, generally cisplatin (CDDP) and etoposide (VP-16). This regimen is widely adopted for HG-NEN by all guidelines (ESMO, ENETS, NCCN and NANETS,) based on small non-randomized studies dating back to the 1990s and tumor registries. ORR reported in these studies ranged from 40 to 70%, with median PFS and OS of up to 9 and 19 months, respectively (166). More recently, a retrospective tumor registry of 252 patients with advanced GI-NECs reported an ORR with first line chemotherapy of 31% (similar for cisplatin- and carboplatin-etoposide regiments) and a median OS of 11 months (25). Moreover, the authors observed that a Ki67 value greater than 55% was associated with an ORR of 42% compared to 15% in patients with a Ki67 between 20 and 55%. Median OS was 10 months and 14 months in the two groups, respectively (25). These data underline the heterogeneity of high-grade NENs, and it is increasingly recognized that there are at least two biologically distinct subgroups based on morphology and proliferative activity with different clinical course and response to therapy. These considerations are in accordance with the new WHO classification that recognizes the NET G3 category (167). As NET G3 are molecularly more similar to low grade NETs than to NECs, it is generally recommended to treat NET G3 with chemotherapy regimens or other treatment options used for NET G2, although evidence to support this statement is scarce.

There is no standard second line regimen for advanced G3 NENs, and available data in this specific setting include few small prospective studies and retrospective

data. Response rates between 20 and 40% and OS of 10-18 months have been reported with different chemotherapy schemes including combination regimens of oxaliplatin with fluoropyrimidines (XELOX, FOLFOX) (168,169) or irinotecan with fluoropyrimidines (FOLFIRI) (170). Additionally, temozolomide alone or in combination with capecitabine with or without bevacizumab was reported in heterogenous small restrospective series or small studies to induce tumor responses in up to 33% of patients and median OS of up to 22 months (171,172). Topotecan has been also proposed in analogy to the SCLC, but its activity in EPNECs has not been confirmed (173). A recent meta-analysis including 19 studies and a total of 582 patients with extra-pulmonary NECs reported limited efficacy of second-line chemotherapy in this setting, with a median ORR of 18% (range 0–50), and a median PFS and OS were 2,5 and 7,6 months, respectively (174). Alternative therapeutic strategies are currently being explored in this setting, including immunotherapy. Immune check point inhibition may be considered for the small subgroup of high grade NENs with microsatellite instability or high tumor mutational burden, and some small basket trials have reported high response rates with dual PD1 and CTLA4 blockade, particularly in lung primaries, although further studies are needed in this context before this may be considered as standard of care for these patients.

1.5 MOLECULAR BASES OF NENs

The genetic background of NENs is strongly associated with tumor differentiation and grade, functional status and primary origin (pancreatic, small bowel or lung). The majority of NENs are sporadic, although around 5% are developed in the context of hereditary syndromes. Identification of genes involved in these familiar syndromes has contributed to partially clarify some of the mechanisms involved in the pathogenesis of NETs. In addition, the omic revolution is helping to improve the molecular characterization of this heterogeneous family of tumors, both NETs and NECs.

1.5.1 Hereditary Syndromes

Neuroendocrine neoplasms (NENs) are a heterogeneous group of tumors that can arise sporadically or occur in the context of hereditary syndromes such as multiple endocrine neoplasia type 1 (MEN1), multiple endocrine neoplasia type 2 (MEN2), in the variants MEN2A and MEN2B, multiple endocrine neoplasia type 4 (MEN4), Von Hippel-Lindau disease (VHL) and neurofibromatosis type 1 (NF1) (175–177) . Hereditary NENs are generally well differentiated tumors with low proliferation rates, commonly diagnosed earlier than sporadic cancers, and often have multiple locations and can be associated with greater secretory activity (177,178). Proper recognition and referral to specialized units for familial genetic counselling is recommended for these patients.

1.5.1.1 Multiple endocrine neoplasia type 1 and 4 (MEN1 and MEN4)

MEN1 is a rare inherited tumor syndrome with autosomal dominant transmission, which is characterized by the development of parathyroid neoplasms (benign parathyroid adenomas, parathyroid hyperplasia or, more rarely, parathyroid carcinoma) resulting in primary hyperparathyroidism in over 90% of patients, pituitary adenomas (in 50% of cases), and predominantly pancreatic neuroendocrine tumors in 40-70% of patients, originally called the Werner's triad (179–181). In addition to these major clinical manifestations, multiple, although less frequent, combinations of endocrine and neuroendocrine tumors (e.g. adrenocortical tumors and NETs of non gastroenteropancreatic origin) and non-endocrine tumors (such as facial angiofibromas, collagenomas, lipomas, meningiomas) have been described in MEN1 patients (182). The annual incidence of MEN1 is estimated at 1:30,000 individuals and the prevalence is 2-3 cases per 100,000 inhabitants. Germline mutations in the MEN1 tumor suppressor gene are present in up to 85-90% of patients with MEN1 syndrome. MEN1 has a high penetrance, in fact clinical manifestations occur in 80-100% of patients with pathogenic genetic alterations (183). In the majority of cases, clinical onset of MEN1 occurs before 50 years of age, although cases up to the age of 80 years have been reported (181,184). In about 10% of cases, patients present with de novo mutations (185). There is no clear association between genotype and phenotype,

and different pathological manifestations may develop even in members of the same family (180).

A diagnosis of MEN1 is established when one of the following 3 criteria are met: development of two or more MEN1-associated endocrine tumors, development of one of the MEN1-associated tumors in a first-degree relative of a patient with a diagnosis of MEN1, and detection of a germline MEN1 mutation regardless of the presence or not of clinical, biochemical or radiological manifestations of the MEN1 syndrome (180). MEN1 mutational analysis should be offered to index cases and first-degree relatives of a MEN1 gene mutation carrier, and may be also considered in patients with suspected atypical MEN1 phenotype (individuals with parathyroid adenomas that occurred before the age of 30 or multi-glandular parathyroid disease, gastrinoma or multiple P-NETs at any age, or those who have at least two MEN1-associated tumors that are not part of the classic Werner's triad). Whenever possible, this test should be done in the first decade of life and as early as at age 5, with the aim of detecting and preventing significant morbidity and even mortality (186). All individuals should receive genetic counselling before and after the test.

More recently, a new syndrome (MEN4) has been characterized in patients with a spectrum of clinical manifestations similar to MEN1 that is caused by germline mutations in the CDKN1B gene (187). This gene encodes p27Kip1, a tumor suppressor gene that encodes a protein that inhibits cyclin/cyclin-dependent kinase complexes, thereby preventing cell cycle progression. The most common clinical manifestations in MEN4 patients are primary hyperparathyroidism followed by pituitary adenomas, seen in approximately 40% of cases, although they may also develop other types of endocrine and neuroendocrine neoplasms (i.e. bronchial carcinoids and gastric NETs) (188).

1.5.1.2 Multiple endocrine neoplasia type 2 (MEN 2)

MEN2 is an inherited autosomal dominant syndrome characterized by an increased risk of medullary thyroid carcinoma (MTC), in combination or not with pheochromocytoma (PHEO) (in ~50% of cases), parathyroid adenoma/hyperplasia with subsequent hyperparathyroidism (in < 25%) and other non-endocrine pathological features (marfanoid habitus, mucosal neuromas) (181). Almost all

cases of MEN2 are caused by germline mutations of the RET (REarranged during Transfection) proto-oncogene, located on chromosome 10 (10q11.2) (189,190). It is estimated that around 1 in 30,000 individuals have MEN2.

MEN2 includes two clinically distinct forms, MEN2A, which is the most common subtype (90-95% of cases) and MEN2B (5-10% of MEN2 cases). Nearly all MEN2 patients have either C-cell hyperplasia (CCH) or medullary thyroid cancer (MTC), and both MEN2A and MEN2B have an increased risk of PHEO (30-50%). MEN2A is also associated with an increased risk of parathyroid adenoma or hyperplasia (20-30%) and is further subclassified into four subtypes: (a) classical MEN2A, (b) MEN2A associated with cutaneous amyloid lichen (c) MEN2A associated with Hirschsprung's disease, (d) familial MTC (FMTC). FMTC occurs in families with autosomal dominant transmission of MTC, without any other endocrinopathies (191).

In MEN2, MTC is often the first manifestation of the syndrome. The penetration of MTC is greater than 90% and is the main cause of mortality. MTC classically occurs in early childhood in MEN2B patients, and in the early years of adulthood in MEN2A patients. MEN2A is more frequently associated with a multifocal and bilateral form of MTC (192). PHEO is the second most frequent endocrinopathy of MEN2 patients and is almost always benign. It is usually diagnosed in the 3rd to 4th decade and may present with involvement of both adrenal glands (193). About 25% of MEN2A patients experience parathyroid adenoma resulting in hyperparathyroidism (194). Finally, MEN2 may be associated with cutaneous amyloid lichen or Hirschsprung's disease (195). Genetic testing is recommended for individuals with a family history of FMTC, MEN2A, and MEN2B and anyone diagnosed with MTC. Mutations of the RET gene are found in over 95% of families with MEN2A or MEN2B and in more than 85% of families with FMTC (196). As for MEN1, early diagnosis is essential for the prevention and timely treatment of pathological manifestations related to the syndrome, in order to guarantee improved outcomes for affected individuals.

1.5.1.3 Von Hippel-Lindau (VHL)

VHL is an inherited condition with an incidence of 1 in 36,000 live births. VHL has a prevalence ranging from 1:38,000 to 1:91,000 individuals (197). VHL is associated with the development of benign and malignant tumors including haemangioblastomas of the retina and central nervous system, clear cell renal cell carcinomas (RCC), PHEO, pancreatic NETs and endolymphatic sac tumors (ELST).

VHL syndrome is caused by the loss of function germline mutation of the VHL gene in chromosome 3p25-26. Loss of VHL function at the cellular level results in increased expression and stabilization of the hypoxia inducible factor (HIF). The VHL / HIF protein pathway has been implicated in the tumorigenesis of numerous neoplasms, including hemangioblastomas, RCC and NETs.

VHL is subclassified into types 1 and 2 based on clinical manifestations. A high incidence of retinal hemangioblastomas (51%), CNS hemangioblastomas (46%) and RCC (33%) occurs in both types. In addition, type 2 VHLs are associated with an increased risk of PHEO/paragangliomas (20%)(198,199). The prevalence of pancreatic NETs in patients with VHL ranges from 9% to 17%, being multifocal in 32% to 53% of cases (200). Genetic counselling and testing shall be offered to individuals when VHL is suspected and, if confirmed, to their first-degree relatives (201).

1.5.1.4 Neurofibromatosis type 1 (NF 1)

NF1 or Von Reklinghausen disease is an autosomal dominant disorder associated with the development of neurofibromas, pigment lesions (café-au-lait macules, skin freckles and Lisch nodules), brain tumors (optic pathway gliomas and glioblastomas), peripheral nerve tumors (spinal neurofibromas, plexiform neurofibromas and malignant peripheral nerve sheath tumors) and skeletal abnormalities (scoliosis, tibial pseudarthrosis and orbital dysplasia) (202). NF1 patients are also at greater risk of presenting learning disorders and intellectual disabilities, and of developing neuroendocrine neoplasms such as PHEO and NETs, or non-neuroendocrine tumors such as abdominal plexiform neurofibromas (PN), rhabdomyosarcomas and GISTs.

NF1 is caused by loss-of-function mutations in the NF1 gene, a tumor suppressor gene located on chromosome 17q11.2. Neurofibromin, the cytoplasmic protein product of this gene, controls cell proliferation via p21 and the RAS and MAP kinase pathway, and is expressed in multiple tissues. The penetrance of the syndrome is complete; however, the expression of NF1 is highly variable, depending on the type of mutation (nonsense, frameshift or splice mutations or deletions are the most common), the time when the mutation occurs and the presence of molecular alterations in associated genes (203). The incidence of NF1 ranges from approximately 1: 2500 to 1: 3500 individuals.

NF1 mutation carries have a 60% life-time risk of developing a malignant tumor, especially in the nervous system. Benign tumors, in particular neurofibromas, are very common in patients with NF1 and the clinical findings of some of them, such as PN, are pathognomonic of the syndrome. The diagnosis of NF1 is mainly clinical and uses criteria initially developed in 1987 by the "NIH Consensus Conference", subsequently updated in 1997, based on the presence of at least 2 pathognomonic clinical characteristics. Due to the heterogeneity of mutations in the NF1 gene, molecular testing is complex and requires the sequencing of all coding exons and the search for deletions or rearrangements of the entire gene, especially for de novo cases. Approximately 5% of patients who meet the clinical criteria for NF1 do not have an identifiable mutation on gene sequencing.

1.5.2 Sporadic NENs

1.5.2.1 Pancreatic origin

Initial genomic studies of P-NETs by Jiao et al determined the exomic sequences of 10 sporadic P-NETs and then screened most frequently mutated genes in 58 additional tumors (204). The investigators reported a high rate of somatic inactivating mutations in genes involved in chromatin remodeling, including the MEN1 gene (44%), as menin is a component of a histone methyltransferase complex, and genes encoding two subunits of a transcription/chromatin remodeling complex, DAXX/ATRX (43%), required for incorporating the histone variant 3.3 to chromosome telomeres. Mutations in DAXX and ATRX were mutually exclusive. In addition, mutations in mTOR pathway genes were encountered in 15%

of patients (6 in TSC2, 5 in PTEN, and 1 in PIK3CA), providing a rationale for the therapeutic use of mTOR inhibitors in this tumor type, although subsequent translational studies have been unable to demonstrate a clear correlation of the molecular alterations in this pathway with greater therapeutic benefit from everolimus.

More recently, a more comprehensive genomic analysis of 98 sporadic pNETs using whole-genome sequencing was published by Scarpa et al. (205). Analysis of somatic variants and copy number variations (CNV) involved 4 main molecular pathways: DNA damage repair (MUTYH, CHEK2, BRCA2), chromatin remodeling (SETD2, MLL3), telomere maintenance (ATRX, DAXX), and activation of the mTOR signaling pathway (TSC1, TSC2, PTEN, and DEPDC5), with MEN1 having a role in all of these pathways. Of note, a larger-than-expected proportion (17%) of germline mutations were identified in these cohort of clinically sporadic pNETs, including previously unreported mutations in several DNA repair genes such as BRCA2, CHEK2 and MUTYH. Furthermore, gene expression analyses identified a subgroup of pNETs associated with hypoxia and HIF signalling. The VHL gene is associated with the regulation of hypoxia-inducible factor (HIF); loss of VHL gene expression, which leads to constitutive HIF activation and increased expression of HIF targets, such as VEGF, has been linked to the development of pNETs (206). NETs are highly vascularized tumors, and angiogenesis inhibitors (i.e. sunitinib, surufatinib) have demonstrated efficacy and are part of the treatment armamentarium of pNETs.

1.5.2.2 Small bowel origin

The first whole-exome, genome-wide sequencing of 48 SI-NETs (207) showed a low rate of somatic mutations and identified 197 protein-altering single-nucleotide variants (SNVs), affecting a large number of cancer genes that included *FGFR2*, *MEN1*, *HOOK3*, *EZH2*, *MLF1*, *CARD11*, *VHL*, *NONO*, *FANC D2*, *SMAD1* and *BRAF*. In 29% of analysed SI-NETs, there were genetic alterations in the *P13K*/*AKT*/*mTOR* pathway and mutually exclusive amplifications of *AKT1* or *AKT2* were common. Amplifications were also observed at the *PDGFRA* (platelet-derived growth factor receptor alpha) locus in 20.8% of

cases. Another recent study has detected frequent gene copy gains in *AKT1* (30.8%), *PDGFRA* (28.8%) and *KDR* (kinase insert domain receptor, involved in *VEGF* signalling; 28.8%) (208). Higher mutation rates in primary SI-NETs were associated with increased likelihood of recurrent liver metastases ($P < 0.04$) (207). In a study by Francis *et al.* ($n = 180$) including 48 cases, heterozygous frame shift mutations of the cyclin-dependent kinase inhibitor 1B gene (*CDKN1B*) were observed in 14 of 180 SI-NETs (8%) (209). *CDKN1B* is located in chromosome 12 and encodes the protein $p27^{Kip1}$, a cyclin-dependent kinase inhibitor (CKI), which main function is to control G1 to S phase cell cycle progression. The reported mutations in SI-NETs in this putative tumour suppressor gene are loss-of-function truncating mutations throughout the gene; no hotspot has been identified. The central role of CDKN1B mutations in SI-NETs has been confirmed in several other studies (209–211). Other relevant mutations found in 3.8% of cases occurred in known oncogenes such as BRAF and KRAS (involved in MAPK/ERK signalling pathway), PIK3CA (phosphatidylinositol-4,5-bisphosphate 3-kinase catalytic subunit alpha; involved in the P13K/AKT/mTOR pathway) and TP53 (tumour suppressor gene; regulator of cell proliferation and apoptosis) (208). The SRC gene (proto-oncogene; involved in cell signalling), was the most commonly amplified oncogene (23%) in the study by Banck et al. (207) and a copy gain of this gene was also evidenced in 25% of SI-NETs analysed by Simbolo et al. (208). In this study SRC copy gains were associated with poorer prognosis ($P = 0.047$). Thus, the authors suggest that copy gains of the SRC gene could potentially be a novel prognostic biomarker for SI-NETs, especially as whole-genome sequencing becomes more widely adopted in clinical practice.

1.5.2.3 Lung origin

Detailed genome/exome sequencing analysis in lung carcinoids have demonstrated that chromatin-remodelling is the most frequently altered pathway in pulmonary carcinoids. Indeed, MEN1, PSIP1 and ARID1A were recurrently mutated genes (212). Specifically, covalent histone modifiers and subunits of the SWI/SNF complex are mutated in 40% and 22% of the cases, respectively. By contrast, mutations of TP53 and RB1 are only found in 2 out of 45 cases, suggesting that

these genes are not main drivers in well-differentiated pulmonary carcinoids (212). Additionally, a recent study explored the molecular profiles of lung NENs through integrative analysis of transcriptome and methylome data, using both machine-learning (ML) techniques and multi-omics factor analyses (MOFA) (213). ML analyses showed that the molecular profiles could distinguish survival outcomes within patients with atypical carcinoid morphological features, splitting them into patients with good typical-carcinoid-like survival and patients with a clinical outcome similar to LCNEC. Unsupervised MOFA and subsequent gene-set enrichment analyses unveiled the immune system and the retinoid and xenobiotic metabolism as key deregulated processes in pulmonary carcinoids, and identified three molecular groups—clusters—of potential clinical relevance. The first group (cluster A1) presented high infiltration by dendritic cells and showed overexpression of ASCL1 and DLL3. The transcription factor ASCL1 is a master regulator that induces neuronal and neuroendocrine differentiation. It regulates the expression of DLL3, which encodes an inhibitor of the Notch pathway (214). Overexpression of ASCL1 and DLL3 is a characteristic of the SCLC of the classic subtype (214) and of type-I LCNEC. The second group (cluster A2) harboured recurrent somatic mutations in EIF1AX and showed downregulation of the SLIT1 and ROBO1 genes. In previous studies, SLIT1/ROBO1 have been associated with cell invasion inhibition by suppressing the SDF1/CXCR4 axis, and with attenuation of cell cycle progression by destruction of β-catenin and CDC42 (215). The third molecular group (cluster B) was enriched in monocytes and depleted of dendritic cells, and had the worst survival. Cluster B was also characterised by recurrent somatic mutations in MEN1, the most frequently altered gene in pulmonary carcinoids and pancreatic NETs. Low levels of OTP, high levels of ANGPTL3 and ERBB4 were also detected in this group of samples, representing potential novel targets of therapy.

1.5.2.4 Neuroendocrine carcinomas (NECs) and mixed neuroedocrine-non neuroendocrine neoplasms (MiNENs)

The molecular profile of HG-NECs differs depending on primary tumor origin and some morphological features such as cell size. Small cell NECs are molecularly more homogeneous and often characterised by the bi-allelic inactivation of both

TP53 and *RB1*. First documented in the lung (216,217), this molecular signature has subsequently been confirmed in other anatomic sites, including the digestive tract (218), the pancreas (219), the head and neck region (220), the genitourinary tract (221) and the uterine cervix (222). Additionally, the NOTCH pathway is altered in about 25% of lung small cell NECs and in some EP-NECs (222). Frequent alterations in the PI3K/PTEN/mTOR pathway can be detected in certain anatomical sites such as the uterine cervix (222). The genomics of large cell NEC are more complex and heterogeneous, and up to 40% are associated with a non-neuroendocrine component. At least two distinct molecular subtypes have been described in large cell NECs: a subgroup characterized by a 'small cell NEC-like' molecular signature, characterised by the double inactivation of TP53 and RB1, and a subgroup characterized by a 'carcinoma-like' molecular signature, that resembles the molecular profile of non-neuroendocrine tumors of similar anatomic origin (216,217). However, most available studies in HG-GEP-NECs have included small and large cell NECs of different primary sites, and not only 'pure' NECs, but also MiNENs. Thus, it is difficult to determine whether the molecular alterations reported were found in the 'pure' neuroendocrine component of a mixed tumour, or even in a whole mixed tumour without distinction between its components. Colorectal NECs might harbour mutations in KRAS (20–30%) and BRAF (7-60%), as well as MYC amplifications (223,224). Some limited preclinical studies and a few case reports suggested that BRAFV600E mutant colon NECs may benefit from BRAF inhibition (225). Furthermore, a role for microsatellite instability (MSI) has been identified for GEP NECs. MSI-GEP NECs account for approximately 1-10% of cases (226). In a study including 89 cases of GEP NECs and MiNENs (53 NECs and 36 MiNENs) (6 oesophageal, 77 gastrointestinal, 3 pancreatic and 3 gallbladder) (166), MSI was observed in 11 NEC/MANECs (12.4%) (7 intestinal and 4 gastric). A BRAF mutation was identified in 6 of 88 cases (7%) and KRAS mutations were identified in 15 cases (17%). BRAF mutations were associated with MSI ($P < 0.0008$), while KRAS status did not correlate with any clinicopathological or molecular feature (227). It was concluded that MSI identifies a subset of gastric and intestinal NECs/MANECs with distinct biology and a better prognosis. Vascular invasion ($P = 0.0003$) and MSI ($P = 0.0084$) were identified as the only independent prognostic factors on multivariable analysis (227). A recent

systematic review analysed the molecular landscape of MiNEN (228), showing that the most frequent alterations in this setting involved well-characterised cancer gene drivers and/or their protein products, such as TP53, RB1, PTEN, APC (adenomatous polyposis coli), PI3KCA, KRAS, BRAF, and MYC.

1.6 "*OMIC*" SCIENCES IN BIOMEDICINE

Advances in biomedical research and the need to improve our understanding of genotypic and phenotypic changes involved in the pathogenesis and progression of disease have boosted the development of multiple biological, technical and computational tools able to detect, identify, quantify and integrate hundreds or thousands of molecular changes and their final products, obtaining comprehensive global information from a specific patient sample in a short period of time, and enabling the holistic study of complex biological processes (Figure 4). In the oncology field, the application of these technologies provides the opportunity to identify novel biomarkers of diagnostic, prognostic and/or predictive potential, as well as novel targets for therapy that shall contribute to incorporate precision medicine in clinical practice and eventually improve patient's prognosis and quality of life.

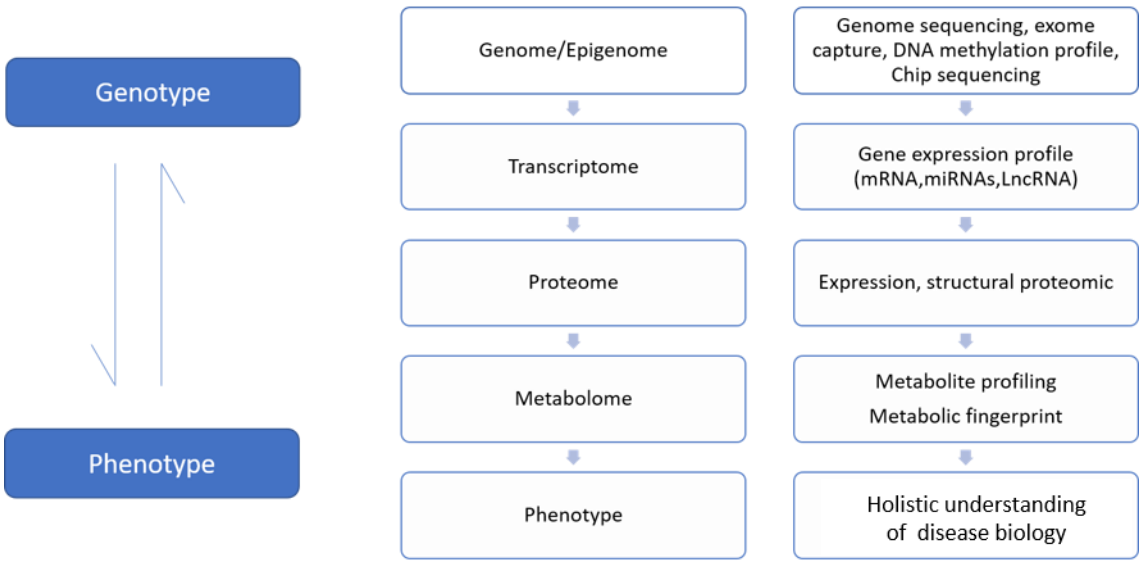

Figure 4. "Omics" waterfall

1.6.1 Metabolomics

Metabolomics is a relatively young discipline, compared to other well-established "omics", defined as the comprehensive and quantitative analysis of all metabolites, products from the metabolic reactions, which are present in cells, tissues or biofluids (blood, urine, saliva, etc) of a biological species (229). It is a powerful bioanalytical technology that directly reflects the underlying biochemical activity and state of cells/tissues, representing the molecular phenotype. Since the mid-nineties, metabolomic technology has remarkably developed (230), and consequently, has rapidly penetrated in many biomedical fields with different purposes such as diagnosis, prognosis, prediction of response to therapies and novel targets and drugs research, among others.

Metabolomics encompasses three types of analyses: i) metabolic fingerprinting, which measures a subset of the whole profile with little differentiation or quantitation of metabolites (231); ii) metabolic profiling, the quantitative study of a group of metabolites, known or unknown, within or associated with a particular metabolic pathway (232,233); and iii) target isotope-based analysis, which focuses on a particular segment of the metabolome by analysing only a few selected metabolites that comprise a specific biochemical pathway (234).

The metabolome is influenced by both exogenous and endogenous factors, such as age, gender, race, diet, presence of disease or drug exposure. Thus, a metabolomic fingerprint reflects the singularity of the biological milieu of the individual at the specific moment of sample extraction (235). As a consequence, metabolomics is a key tool for biomarker discovery and personalized medicine and has great potential to elucidate the ultimate products of genomic processes.

Over the last decade, metabolomic studies have identified several relevant biomarkers involved in complex clinical phenotypes using diverse biological systems. Most diseases result in signature metabolic profiles that reflect the sum of external and internal cellular activities (236). Different analytical techniques are used to extend the coverage of a full metabolome.

1.6.1.1 Metabolomic techniques

The most commonly used techniques are nuclear magnetic resonance (NMR) spectroscopy, capillary electrophoresis-mass spectrometry (CE-MS), liquid chromatography-mass spectrometry (LC-MS), and gas chromatography-mass spectrometry (GC-MS). The choice of the most suitable technique depends on the nature of the metabolite we want to confirm, and the speed, sensitivity, and accuracy needed. In general, metabolomic studies can be classified in two categories, untargeted and targeted analysis. The untargeted approach analyses the metabolic profiling of all metabolites ("fingerprint") of a sample. On the other side, targeted metabolomics focuses on the quantification and identification of selected metabolites, such as those involved in a specific metabolic pathway. The metabolites under investigation in targeted analysis are usually known, and the preparation of samples can be adjusted to reduce the effects of interference from associated metabolites.

1.6.1.1.1 Nuclear Magnetic Resonance (NMR)

High-resolution nuclear magnetic resonance (NMR) spectroscopy is a universal analytical tool (237). NMR represents a well-established, robust, non-invasive and reproducible method for quantifying metabolic profiles which can provide a deep overview of the human metabolome. NMR has important advantages over other analytical MS techniques, including the minimal sample preparation requirements (238) and the ability to detect multiple metabolites within a single experiment and to reuse samples (239). Additionally, NMR allows the identification of compounds with identical masses, including those with different mass isotopomer distributions. NMR is the mainstay for determining structures of unknown compounds (240). Several types of biofluids, such as blood, plasma, serum, urine, saliva, tissue/cell extracts, tumor samples, and cancer cell lines, may be used by NMR for metabolite profiling (241). NMR is commonly used in untargeted metabolomics fingerprinting studies, whereas MS techniques are considered optimum for targeted analyses.

1.6.1.1.2 Capillary electrophoresis-mass spectrometry (CE-MS)

Capillary electrophoresis is a mature separation technology that is effectively coupled with mass spectrometry (CE-MS). CE-MS has demonstrated to be a useful technique for metabolomic studies, particularly for targeted analysis (242). In this context, charged metabolites (such as amino acids, nucleotides, small organic acids, and sugar phosphates) are first separated by CE based on charge and size, and then selectively detected using MS. CE-MS presents many advantages, such as the efficient and fast separation paired with low sample consumption, its high resolution and the fact that almost any charged species can be analyzed by two methods, both cationic and anionic (243). This technique can be readily applied to various types of biological samples ranging from plasma and urine to cells and tissues (244). However, CE-MS has some limitations. First of all, CE-MS is less reproducible as compared to other MS-based techniques, such as GC-MS and LC-MS (245). CE-MS is also characterized by the lack of standard operating procedures and workflows despite new developments in sample throughput and quality control (246).

1.6.1.1.3 Liquid chromatography-mass spectrometry (LC-MS)

LC–MS represents a sensitive analytical technique that has proved to be a valuable method for the detection of serum metabolites, which has brought about great progress in targeted metabolomic analysis. LC is a separation technique in which the mobile phase is a liquid, where sample ions or molecules are dissolved. The sample with the mobile liquid will pass through a column or a plane, which is packed with a stationary phase composed of irregularly or spherically shaped particles. Separation of the compounds based on differences in ion-exchange, adsorption, partitioning, or size, which make different solutes to interact with the stationary phase to different degrees, will translate into different transit times of the different solutes through the column that can be then detected with MS with a very high resolution and a fast analysis time. LC-MS is usually utilized for the analysis of different class of glycerolipids, glycerophospholipids, lysoglycerophospholipids, sphingolipids, carnitines, fatty acyls and amides (247). This method allows the quantitative determination of these metabolites up to the picogram level (248). It is

a challenge to use LC-MS for untargeted metabolomic analysis. Indeed, heterogeneous workflows have been developed for LC-MS analysis which often involve non-standardized manual curation. This issue represents a limitation of this technique, particularly in terms of validation of the obtained results (249).

1.6.1.1.4 Gas chromatography-mass spectrometry (GC-MS)

GC-MS is the most standardized method in metabolomics, given its high sensitivity and specificity for metabolite detection (250). In fact, GC-MS has demonstrated to be a key tool both for targeted and untargeted metabolomic approaches. Through targeted analysis, GC-MS allows the identification and quantification of metabolites, including amino acids, fatty acids and sterols, among others. Additionally, GC-MS-based metabolomics allows the integration of targeted assays for absolute quantification of specific metabolites with untargeted metabolomics to discover novel compounds (251). The major difference between GC-MS and the other metabolomic techniques is that it requires the transformation of the metabolite extracts into volatile and thermally stable derivatives, which can be quantified. This analytical step requires special care to optimize the untargeted GC-MS metabolomic experimental protocol (252).

1.6.1.2 Metabolomics in oncology

In the last years, metabolomics has been applied to the discovery of tumor biomarkers for the diagnosis, treatment, and prevention of multiple solid tumors, including lung (253), pancreatic (254), gastrointestinal (255), breast (256), and prostate cancer (257), sarcoma (258) and melanoma (259,260). For lung cancer, global and targeted metabolomic studies using unbiased LC-MS in > 1,000 urine samples from patients and controls uncovered a set of urine metabolites associated with lung cancer diagnosis and prognosis (261). Novel and previously un-annotated creatine riboside (CR), and N-acetylneuraminic acid (NANA), were significantly elevated in the urine of lung cancer patients, and were also found to be enriched in tumor samples compared with adjacent non-tumor tissues, thus revealing their direct association with tumor metabolism. Both metabolites were significantly associated with a worse prognosis (261). In pancreatic cancer, the most extensively

investigated aspects of metabolic reprogramming are those associated with energy (glucose) and glutamine metabolism. Additionally, recent studies have demonstrated the potential role and relevance of other compounds including amino acids. In a prospective cohort study, elevated branched-chain amino acid levels in pre-diagnostic plasma samples were associated with more than twofold increased pancreatic cancer risk (262). Other studies showed that amino acids concentrations differed significantly between healthy controls and pancreatic cancer patients ($p < 0.05$) (263,264). Using metabolomics, several studies have identified different potential metabolomic diagnostic biomarkers for colorectal cancer, such as alterations in metabolites related to the tricarboxylic acid cycle (TCA cycle), urea cycle, glutamine metabolism, amino acids and gut flora metabolism (255,265,266). However, the metabolomic signatures generated by various investigators have been extremely heterogeneous (255).

Challenges in the development of metabolomics exist and include a simplified system to present data to end users, the coordination of multiple data streams, and the implementation of quality assurance and quality control programs. Moreover, it will be important to deal with the biologic variability between individuals in populations. Clinical studies are beginning, and the next few years should clarify whether or not metabolomics will gain its place as a complementary or even an alternative tool to genomics and proteomics in oncology.

1.6.1.3 Limitations

Metabolomic techniques are not exempt of limitations which hinder its application and inclusion in clinical practise. First of all, the complexity of the number of detected compounds and their identification. Next, changes in the concentration of metabolites may also be influenced by many disease-independent factors, including sample collection, preparation and storage, experimental process, data analysis, data description, and database standardization (267). Additionally, metabolomic analysis produce large amount of data, and it is difficult to comprehensively identify all the changed metabolites using the existing metabolite database. Considering all these aspects, metabolomics should be considered as a field of study at an early stage of development in oncology.

1.7 METABOLISM IN CANCER

1.7.1 Metabolism deregulation in cancer

During aerobic respiration, normal cells use pyruvate from glycolysis to efficiently obtain energy through the tricarboxylic acid cycle (TCA) and oxidative phosphorylation (OXPHOS). Alteration of metabolism is one of the main hallmarks of cancer. Thus, in an energy demanding situation, e.g., cancer cells, pyruvate will be derivated to lactate by lactic fermentation in the cytoplasm, obtaining low rates of energy performance (anaerobic respiration).

In 1924, Otto Warburg reported that cancer cells consume tremendous amounts of glucose, when compared with normal cells, and metabolize the majority of glucose into lactate, even in the presence of oxygen (268), phenomenon known as the Warburg effect, which represents a striking metabolic difference between cancer and normal tissues (269). This metabolic shift results in activation of numerous signalling and metabolic pathways supporting cell proliferation and survival.

However, the Warburg effect itself is not enough to sustain cancer cell proliferation. First, a cancer cell has to increase its uptake of nutrients from the environment, especially glucose and glutamine, which are the most needed nutrients for cell survival and proliferation. They provide the cancer cell, through catabolism, with sufficient pools of carbon intermediates used for synthesis of various macromolecules and for ATP production. Second, to satisfy energy needs and ensure accelerated growth and proliferation, cancer cells metabolic reprogramming also induces an increase in protein, lipid, and nucleic acid biosynthesis (270). One key source of anabolic precursors is the Krebs cycle. Several of the Krebs cycle metabolites, such as citrate, oxaloacetate/aspartate, and α-ketoglutarate/glutamate are precursors for the biosynthesis of fatty acids, nucleic acids and proteins, all of which are required for cell growth. As some of these metabolites (e.g. oxaloacetate and α-ketoglutarate) are kept low in their cellular concentration, they will have to be replenished via anaplerosis to sustain both the Krebs cycle and biosynthetic activities. This can be achieved by two anaplerotic pathways involving pyruvate carboxylation (271) and glutaminolysis (272).

1.7.2 Molecular basis of the metabolic shift in cancer cells

To date, the basis for this metabolic shift remains poorly understood, and the popularity of metabolism waned as molecular biology of cancer waxed into vogue in the 1980's with the discoveries of oncogenes and tumor suppressor genes. Research of the metabolic aspects of cancer has emerged over the past decade. Several studies have reported that oncogenic signals drive the malignant progression of cancer cells by modulating metabolic enzymes, revealing transcriptional links between oncogenic pathways and metabolism (273). The so-called metabolic plasticity or re-wiring capacity of cancer cells is one of the hallmarks of cancer. Indeed, tumors reprogram pathways of nutrient acquisition and metabolism to meet the bioenergetic, biosynthetic, and redox demands of malignant cells. Thus, interruption of one metabolic pathway, for example inhibition of the mitochondrial function, can re-wire metabolism through a compensatory increase in glycolysis.

In this context, numerous genes belonging to different pathways and with a wide range of biological functions, have been shown to contribute to cancer metabolic plasticity (274). For instance, the oncogene c-Myc transactivates most glycolytic genes, including glucose transporter 1 (Glut1) and lactate dehydrogenase A (LDHA) (275,276). Hypoxia-inducing factor 1 (HIF-1) regulates LDHA and pyruvate dehydrogenase kinase isozyme 1 (PDK1) (277). Other recent evidence has shown that mitogen signalling promotes tumor growth by modulating pyruvate kinase M2 (PKM2) (278). Forkhead Box J1 (FOXJ1), a member of the forkhead family of transcription factors, has been shown to support cancer cell growth by increasing glucose uptake and lactate production, favouring glycolysis (279). Also the phosphorylation of the mitochondrial protein Drip1 (Dynamin-related protein 1) has been associated to enhanced glycolysis and tumor growth (280). Moreover, serine synthesis plays a relevant role in the cancer metabolic shift, inhibiting aerobic glycolysis. In this context, p53 (TP53), a key tumor suppressor gene, has demonstrated to be involved in cancer cell survival through serine starvation (281). Notably, the aberrant activation of mTORC1, belonging to the PI3K-AKT-mTOR signalling pathway, leads to an anabolic growth program with a pathological increase of nucleotide, protein, and lipid synthesis (282).

A recent work has revealed remarkable flexibility in the specific pathways activated by oncogenes or loss of tumor suppressor genes in tumor cells to support these key metabolic functions (283).

All this indicates that the regulatory mechanisms underlying cellular metabolism in cancer cells are far more complex than previously believed and warrant further investigation.

What is clear is that the metabolites formed as hyper-products of cellular activity in cancer cells substantially differ from those found in normal, non-malignant cells (284,285). The metabolome expresses dynamic changes over time, concordant with evolving disease progression (286). Notably, metabolites have been demonstrated to undergo earlier and more significant changes than genes or proteins, and these changes can be measured in absolute terms. Therefore, metabolomics can be an invaluable tool for gaining insights into numerous biochemical processes including those related to cancer metabolism. In fact, metabolomics, which can be thought of as a downstream manifestation of proteomics, transcriptomics and genomics, presents potential for a relatively non-invasive liquid biopsy method that may be utilised in clinical practice in the future to diagnose and characterise cancer, assess treatment response and toxicity, and predict outcome from diagnosis (287–291). However, differential metabolite identification is a complex process in metabolomics as human metabolome has not been yet completely elucidated.

1.7.3 Metabolomics in neuroendocrine neoplasms

1.7.3.1 Preclinical NEN models

Analysis performed on NEN murine models, NEN cell lines and NEN patients have suggested the potential relevance of combined functional genomics with metabolomics in NENs. In particular, metabolic profiling could be an innovative tool for providing novel biomarkers for NEN.

Few preclinical models have been studied so far. In 2005 Ippolito and colleagues developed a transgenic murine model with transcriptional regulatory elements from mouse *Defcr2* (cryptdin-2) used to express prostatic neuroendocrine cancer cells (292). In this study, the authors carried out a GeneChip analyses of primary tumors and metastases of the mouse model as well as of prostatic neuroendocrine cell lines.

Additionally, they performed *in silico* metabolic reconstructions of NE cell metabolism from the GeneChip transcriptional profiles, and a mass spectrometric analysis of metabolites present in tumors and cancer cell extracts. First, the authors yielded a signature of 446 genes with enriched expression in the neoplastic mouse model and in prostatic NE cells. Then, targeted LC-MS analysis led to the identification of two distinct metabolic features of poor-prognosis neuroendocrine tumors. One was the activation of the glutamic acid decarboxylase-independent pathway for production of GABA. The other one was the aberrant production of imidazole-4-acetate. The authors demonstrated a connection between these two pathways. Imidazole-4-acetate can bind and activate $GABA_A$ receptors expressed by cancer neuroendocrine cells, thus providing a previously uncharacterized paradigm for NE tumor cell signaling.

In another study by Li et al, the metabolomic profile of PC-3 prostate small cell neuroendocrine carcinoma cell line was assessed (293). The authors demonstrated that glycolytic features were higher in the neuroendocrine cell line, as compared to a non-neuroendocrine prostatic cell line, suggesting a distinctive metabolism in cancer cells according to histologic tumor type.

1.7.3.2 Pheochromocytomas (PHEO) and paragangliomas (PGL)

Pheochromocytomas (PHEO) and paragangliomas (PGL) are rare neuroendocrine tumors that arise from chromaffin cells of the adrenal medulla and the sympathetic/parasympathetic neural ganglia, respectively. The majority of PHEO and sympathetic PGL are endocrine active tumors causing clinical symptoms due to excess catecholamines secretion (norepinephrine, epinephrine and dopamine, and their metabolites) (294). Mutations in succinate dehydrogenase (SDH) genes increase the risk of PPGLs and several other tumours, and specifically alterations in the B subunit (SDHB) are a risk factor for metastatic disease (295). Previous and recent genetic discoveries in PHEO/PGL research have led to the identification of PHEO/PGL-related unique metabolic abnormalities or pathways involved in oxygen sensing, hypermethylation, DNA repair, up-regulation of specific transporters and/or receptors, and particularly, Krebs cycle enzymes (296–298). These changes are tightly linked to metabolic reprogramming in PHEO/PGL, which

points out the metabolic nature of PHEO/PGL, defining this cancer as a metabolic disease.

In PGL patients with unresolved results of genetic testing, the quantification of metabolites in tumor tissue by LC-MS-based metabolomics can guide the identification of the underlying driver germline or somatic mutations (299). Identifying these driver mutations has relevant implications for the surveillance of carriers of germline-variants who are at risk of tumor development or of tumor recurrence.

Initial metabolomic studies of *ex-vivo* tumors confirmed, as expected, succinate accumulation in PGLs associated with SDH gene pathogenic variants. Metabolomics have now shown utility in clarifying SDH variants of uncertain significance, as well as in the accurate diagnosis of PPGLs associated with fumarate hydratase (FH), isocitrate dehydrogenase (IDH), malate dehydrogenase (MDH2) and aspartate transaminase (GOT2) (300).

More specifically, a characteristic metabolite profile involving high succinate:fumaratae or fumarate:malate ratios, or high levels of 2-hydroxyglutarate (2HG) in combination with high D-2-hydroxyglutarate (D-2HG)/L-2-hydroxyglutarate (L-2HG) ratios can be used to guide detection of SDHx-, FH- and IDH1/2-mutations, respectively (301,302). A particular advantage of metabolome-guided genomics is that tumors with similar phenotypic presentations in terms of metabolite accumulation or depletion can be characterized, leading to the identification of mechanisms of silencing of known PGL genes or even of novel susceptibility genes (303). In this context, a recent study has evaluated the metabolomic profiling of PHEOs/ PGLs in a large cohort of patients, both sporadic (n=48) and inherited forms (23 cases with SDHx mutation, 7 with VHL mutation, 5 with a RET mutation, 3 with a NF1 mutation and 1 with a HIF-2α mutation) by high-resolution magic angle spinning (HRMAS) nuclear magnetic resonance (NMR) spectroscopy (304). This study clearly showed a different metabolic signature in SDHx mutated versus non-SDHx mutated PHEO/PGL. SDHx mutated forms presented significantly increased levels of succinate, methionine, glutamine, and myoinositol, and decreased levels of glutamate, as compared to non-SDHx mutated cases. Thereafter, the metabolomic profile was compared between SDHx mutated tumors and sporadic cases, evidencing a higher level of succinate,

myoinositol, methionine, glutamine, taurine, and ATP in SDHx-related PHEOs/PGLs, while sporadic tumors contained larger amounts of adrenaline, noradrenaline, glutamate, ascorbate, and aspartic acid. Thus, the authors suggest the existence of a peculiar metabolic signature in SDHx-mutated PHEOs/PGLs, which clearly differs from sporadic and other inherited forms of PHEOs/PGLs, paving the way for future studies aimed to identify new biomarkers and therapeutic targets in this setting.

1.7.3.3 GEP NENs

To date, only a limited number of genomic, transcriptomic, and proteomic studies have been used to detect metabolic alterations present in GEP NENs. In 2013, Kinross JM et al, performed the first study which applied NMR metabolomic analysis to urine samples of 28 NEN patients, including 8 small bowel, 10 pancreatic and 10 NENs of other origins (305). The study included also 17 healthy control patients. The metabolomic analysis differentiated NEN and healthy samples with accuracy (R^2 Y = 0.79, Q^2 Y = 0.53, area under the curve [AUC] 0.90), showing decreased concentration of creatine, citrate, and hippurate in NEN patients with respect to healthy controls. Additionally, the analysis was able to distinguish between SI and pancreatic NENs (R^2 Y = 0.91, Q^2 Y = 0.35), and between functional and non-functional NENs (R^2 Y = 0.98, Q^2 Y = 0.77, AUC 0.6). Furthermore, the hippurate metabolism was significantly different (p value <0.0001) in metastatic patients compared to non-metastatic ones (R^2 Y = 0.72, Q^2 Y = 0.41, AUC 0.86). These results suggest that NENs present a metabolic profile that differs from healthy subjects and, also, that different subgroups of NENs (according to primary tumor origin or to the presence of a hormonal syndrome) are associated with different metabolic phenotypes.

A relevant study published in 2015 performed a cross-species integrated analysis of multi-omic profiles to stratify pNETs into subtypes with distinctive biological and clinical characteristics (306). The authors profiled and compared mRNA and miRNA transcriptomes in mouse and human pNETs, and identified different subtypes based on gene expression that were associated with distinct clinical features such as tumor stage or the presence of a hormonal syndrome. These three

subtypes, well-differentiated islet/insulinoma tumors (IT), poorly differentiated tumors associated with liver metastases, named metastasis-like primary (MLP), and a third specific gene mutation–enriched subtype were identified. Relevant differences were observed in the expression of genes involved in glucose uptake and glycolysis, such as glucose transporter *GLUT2 (SLC2A2)*, glucose 6-phosphatase (*G6PC2)*, and glucokinase (*GCK)*, which were upregulated in the IT subtype, whereas pyruvate cycling genes (such as pyruvate carboxylase, the lactate transporter MCT1 (SLC16A1) and cytoplasmic malic enzyme 1 (Me1)) were overexpressed in the MLP subtype. LC-MS-based metabolomic analysis confirmed these data, with the identification of distinctive global metabolic profiles among the defined groups.

To date, the most complete metabolic profiling of SI-NENs is represented by a study conducted in 2019 by Imperiale A et al. (307). This study analysed 94 tissue samples, including 46 SI-NETs, 18 hepatic NET metastases and 30 normal SI and liver samples. High-resolution magic angle spinning (HRMAS) NMR spectroscopy was used. Differences between primary NETs respect to normal SI tissue and primary NETs versus hepatic NET metastases were assessed. Succinate, glutathione, taurine, myoinositol and glycerol-phosphocholine were typically more abundant in NET samples, whereas normal SI specimens showed higher levels of alanine, creatine, ethanolamine and aspartate. Lower concentration of glucose, serine and glycine, and increased levels of choline-containing compounds, taurine, lactate and alanine, were found in SI-NETs with more aggressive tumors. Higher abundance of acetate, succinate, choline, phosphocholine, taurine, lactate and aspartate discriminated liver metastases from normal hepatic parenchyma. Higher levels of alanine, ethanolamine, glycerol-phosphocholine and glucose were found in hepatic NET metastases than in primary SI-NETs. These results suggest the existence of a complex metabolic reality possibly influencing tumor development and progression, and thereby clinical outcome.

Taking together all these data indicate that the dynamic analytical assessment of serum metabolomics may become a very useful tool for clinical management, providing novel potential diagnostic biomarkers, as well as a more accurate patient stratification regarding prognosis and treatment outcome, thereby enabling the identification of molecular vulnerabilities that shall lead to more effective

personalized care. However, the complex interplay within the cancer cells and with the hosting environment needs to be unravelled in depth before metabolomic profiling can be widely used in clinical practice for the management of NENs.

2. HYPOTHESIS

HYPOTHESIS

Reprogrammed metabolism encompasses the capacity of cells to respond or adapt their metabolic signalling to support and enable cell survival in unfavorable or hostile conditions. This ability is enhanced in cancer cells in order to improve their adaptive phenotype and maintain both viability and uncontrolled proliferation. Metabolic flexibility is therefore one of the key hallmarks of cancer, although the pathways involved in the metabolic plasticity of each cancer type remain to be elucidated. Metabolites are the final products of this adaptation, reflecting the aberrant changes in the genomic, transcriptomic and proteomic variability of tumors, and therefore provide useful biological and clinical information on cancer initiation and progression. This, together with the fact that metabolomics can be easily performed in readily accessible biological samples (i.e. plasma, urine), makes metabolic profiling of cancer patients a promising tool to characterize the tumor phenotype and identify novel biomarkers of potential clinical use.

Neuroendocrine neoplasms are a very heterogenous family of tumors of increasing incidence and challenging clinical management. They originate from the diffuse neuroendocrine system and can thus arise from virtually any organ and have the unique ability to secrete amines or peptide hormones that produce characteristic clinical syndromes that may seriously impair patient's quality of life and prognosis. Their low incidence, wide anatomic distribution and heterogeneous biological behaviour have hindered the efforts to decipher the molecular mechanisms involved in tumor development and progression. The recent development and increased accessibility to "omic" technologies, however, has improved our understanding of the genomic and epigenomic events driving NEN pathogenesis. However, metabolomics remains largely unexplored in these tumors.

The hypothesis of this study is that NETs present a distinct metabolomic fingerprint, and its profiling shall enable to better characterize the tumor phenotype and identify novel biomarkers associated with clinical outcome (prognostic biomarkers). Moreover, metabolic tumor phenotyping will facilitate the identification of novel dysregulated pathways involved in tumor initiation and progression, thereby unravelling molecular vulnerabilities and potential novel therapeutic targets that shall lead to more effective personalized care of these patients in the near future.

3. OBJECTIVES

OBJECTIVES

The overall objective of this study is to perform a comprehensive metabolic profiling of G1-2 extra-pancreatic NETs to better understand metabolic dysregulation in these tumors, and identify novel prognostic biomarkers of clinical use, as well as functionally characterize molecular pathways with a significant impact on patient's survival.

To this aim, the specific objectives of this study are the following:

1.- To identify plasma metabolites with a differential availability in G1-2 extra-pancreatic NET patients as compared to non-cancer individuals (controls) significantly associated with patient's survival (prognostic biomarkers).

2.- To evaluate the association between the selected prognostic metabolites and relevant clinicopathological variables, such as age, sex, BMI, hormonal syndrome, primary tumor site, grade, and concomitant medication.

3.- To assess the independent prognostic value of selected metabolites from other known clinicopathological prognostic factors and/or potentially confounding variables significantly associated with overall survival of patients with advanced G1-G2 extra-pancreatic NETs.

4.- To analyze the biological relevance of identified metabolites and dysregulated molecular pathways involved to provide further insights into the molecular mechanisms underlying NET pathogenesis and clinical behaviour.

4. MATERIAL AND METHODS

MATERIAL AND METHODS

4.1 STUDY POPULATION

The study population included 77 patients with advanced, G1-G2 well-differentiated neuroendocrine tumors of lung or gastrointestinal origin and 68 non-cancer individuals with similar distribution of gender, age and body mass index (BMI) as the control group. The NET study population belonged to the first cohort of patients of the AXINET trial (clinicalTrials.gov Identifier: NCT01744249). This trial was a phase II-III, prospective, multicenter, randomized (1:1), double-blind study to evaluate the efficacy and tolerability of axitinib and octreotide LAR versus placebo and octreotide LAR in patients with advanced G1-G2 neuroendocrine tumors (WHO 2010) of non-pancreatic origin. This study enrolled 256 patients, 106 patients in the first part of the study (Phase II), and 150 additional patients in the second part of the study (Phase III). Randomization was stratified by the time from diagnosis to study entry (> vs. $\leq$ 12 months), primary tumor origin and ki-67 index ($\leq$ 5% vs. > 5%). Treatment was continued until disease progression, unacceptable toxicity, consent withdrawal or death, whatever occurred first. The main study endpoint was progression-free survival (PFS) per investigator assessment. The study protocol was approved by the appropriate institutional review board or ethics committee at each participating institution. The study was conducted in accordance with standards of Good Clinical Practice. All patients provided written informed consent before study entry. An additional optional informed consent was required for translational studies.

4.1.1 Eligibility criteria for study entry (AXINET trial)

Patients had to fulfill all of the following eligibility criteria for study entry:

- Histologically confirmed G1-G2 well-differentiated neuroendocrine tumor (WHO 2010) of non-pancreatic origin, functioning or non-functioning.
- Ki-67 index < 20%
- Metastatic or locally advanced disease not amenable to treatment with curative intent.

- Clinical and/or radiological disease progression documented in the 12 months prior to study entry.
- Patients should have at least one measurable lesion as defined by RECIST 1.1 criteria.
- Patients should not have undergone local or regional ablative procedures (embolization, cryoablation, radiofrequency ablation, or others) in the 6 months prior to entering the study.
- Prior treatment with somatostatin analogues and/or interferon allowed
- Prior treatment allowed with up to 2 antineoplastic systemic treatment lines different from SSAs or IFN (systemic treatment included conventional cytotoxic chemotherapy or targeted agents including mTOR inhibitors, except for therapy targeting VEGF/VEGFR which was not allowed).
- Adequate organ function.
- Age ≥ 18 years.
- ECOG performance status 0-2
- Life expectancy ≥ 12 weeks
- At least 4 weeks elapsed from the end of the previous systemic treatment with resolution of all treatment-related toxicities to grade ≤ 1 according to NCI CTCAE Version 4.0 or to baseline, except for alopecia or properly treated hypothyroidism.
- No prior evidence of uncontrolled hypertension. Baseline readings of systolic blood pressure should be ≤ 150 mm Hg and baseline readings of diastolic pressure should be ≤ 90 mm Hg. Patients whose hypertension is adequately controlled with antihypertensive therapy are eligible.
- No other significant comorbidities that may interfere with the patient's ability to receive or adequately tolerate the study treatment.
- Women (or their partners) should be surgically sterilized or postmenopausal, or must agree to use an effective contraceptive method during and for at least 6 months after receiving study treatment. All fertile women should have a negative pregnancy test (serum/urine) within 7 days prior to starting study treatment. Men (or their partners) should be surgically sterilized or must agree to use an effective contraceptive method during and for at least 6 months after receiving study treatment. Lactating women may not participate in this study.

- An informed consent document stating that the patient has been informed of all pertinent aspects of the trial must be signed and dated prior to study enrolment. Patients shall be willing and able to comply with scheduled visits, treatment plans (including willingness to take axitinib or placebo according to randomization), laboratory tests, and all other study procedures**.**

4.1.2 Clinical data collection

Clinical information was prospectively collected online to electronic case report forms (CRFs) from the patient's medical history according to a previously elaborated protocol. Registered data quality was assured by onsite monitoring of source documents. The following variables were selected for the purpose of this study:

Clinical variables: age, gender, weight, height, performance status (ECOG scale), functioning tumor (yes/no), type of hormonal syndrome (in case of functioning tumor), concomitant medication

Pathological variables:

- Location of the primary tumor: gastrointestinal (esophagus, gastric, pancreas, bile duct, small intestine, appendix, colon, rectum) or lung.
- Tumor differentiation: well-differentiated or poorly differentiated.
- Proliferative index (Ki-67)
- WHO classification: NET G1 (Ki-67 < 3%) or G2 (Ki-67 from 3 to 20%) for GEP-NETs; typical carcinoid (<2 mitoses/mm2 and absence of necrosis) or atypical carcinoid (2-10 mitoses/mm2 and/or presence of necrosis) for lung NETs.
- Tumor stage at diagnosis according to TNM classification (AJCC 7th edition), including sites of metastatic disease.

Blood tests:

- Blood counts: haemoglobin concentration and absolute leucocyte, neutrophil, lymphocyte and platelet counts
- Serum chemistry profile: glucose, creatinine, urea, AST y ALT, total bilirubin, alkaline phosphatase (ALP), lactate dehydrogenase (LDH)
- Tumor markers: plasma chromogranin A levels, 24h-urinary 5-HIAA.

Treatment-related variables and clinical outcome: date of diagnosis, date of randomization, dates of treatment initiation and discontinuation, best radiological response achieved and date of best response, date of disease progression and date of death or last contact if alive.

4.2 MULTIPLATFORM METABOLIC FINGERPRINTING

Peripheral blood was extracted from NET patients prior to initiation of study treatment. Blood samples from NETs and controls were collected in sodium EDTA tubes according to standard procedures and fractionated at 3000 rpm for 5 minutes. The plasma layer was recovered in sterile cryotubes, frozen and stored until use at -80ºC.

A multiplatform non-targeted metabolomics approach was performed to provide a wide coverage of the metabolome under study. Plasma samples were analyzed according to standard protocols through different separation techniques coupled to mass spectrometry: capillary electrophoresis 7100 coupled to a MS with time-of-flight analyzer, TOF-MS 6224 (Agilent Technologies) (CE−MS), HPLC system 1290 Infinity II coupled with 6545 QTOF MS detector (Agilent Technologies) (LC−MS) and GC system 7890A coupled to a mass spectrometer 5975C (Agilent Technologies) (GC−MS) (308–310).

4.2.1 Plasma non-targeted analysis by CE–MS

Plasma samples (100 µL) were mixed with 100 µL of 0.2 M formic acid (with 5 % acetonitrile and 0.4 mM methionine sulfone as internal standard). Samples were vortex mixed for approximately 1 min and then transferred to a Centrifree Millipore (30 kDa) filter and centrifuged (2000 × g, 70 min, 4 °C). The filtered solution was transferred directly to a vial for analysis.

CE−MS analyses were performed using a capillary electrophoresis 7100 (Agilent Technologies, Wilmington, USA) coupled to an Accurate-Mass TOF−MS system 6224 (Agilent Technologies, Wilmington, USA). The coupling was equipped with an electrospray ionization source (ESI).

A new Agilent Technologies fused–silica capillary (50 µm i.d. x 100 cm total length) was conditioned with three stages of 30 minutes each of them: 1.0 M NaOH,

followed by MiliQ® water and background electrolyte (BGE) (1.0 M formic acid in 10% Methanol). Before each analysis, the BGE vial was automatically emptied and filled. The capillary was then rinsed for 5 min (950 mbar) with BGE, applying a voltage of 30 kV for 10 s in order to displace the buffer ions. Sample injections were performed during 50 s with 50 mbar pressure. After each sample injection, the BGE was injected for 20 s at 100 mbar pressure. The separation conditions included 25 mbar of pressure and 30 kV of voltage. Data were acquired in ESI+ with a scan rate of 1.00 spectra/sec and the mass range from m/z 74 to 1000. The sheath liquid consisted of 50% methanol, 50 % water and 10 µL of reference standards (0.25 µM purine, (m/z 121.0509) + 0.25 µM HP-0921 (m/z 922.0098)) using a flow rate of 0.6 mL/min (1:100 split). The drying gas temperature was maintained at 200°C with a flow rate of 10 L/min; the nebulizer pressure was set to 10 psig, voltage 3,500 V, fragmentor voltage 125 V, and skimmer 65 V.

In-source fragmentation was used to fragment molecules and obtain product ions to confirm the tentative annotation of the metabolite (in-source collision-induced dissociation (IS-CID))(311,312). The samples were re-analyzed using the same conditions but increasing up to 200 V the fragment voltage allowing the fragmentation of molecules in the ESI source and the mass range from m/z 50 to 1000. Thus, additional information useful to elucidate the structure with a single-stage mass analyzer was provided.

4.2.2 Plasma non-targeted analysis by LC–MS

Samples were treated for plasma deproteinization and metabolites extraction. 100 µL of plasma was mixed with 300 µL of cold (-20 °C) mixture of MeOH:EtOH (1:1, v/v). Samples were vortex-mixed for 1 min, incubated on ice for 5 min and centrifuged for 20 min at 16000 x g at 4 °C. The resulting supernatant was then transferred directly to a vial for analysis.

LC−MS analysis was performed on a UHPLC system 1290 Infinity II (313)(Agilent Technologies, Waldbronn, Germany) coupled with 6545 QTOF MS detector in positive and negative ESI modes. For the separation, a volume of 0.5 µL was injected onto a Zorbax Extended-C18 Rapid Resolution column (Agilent Technologies, 2.1×50 mm, 1.8 µm) thermostated at 60 °C. The flow rate was 0.6

mL/min with a mobile phase composed of water with 0.1% formic acid for A and ACN with 0.1% formic acid for B. The chromatography gradient started from 5% B for the first min increasing to 80% B in 6.0 min, then to 100% by 11.5 min and the starting condition was returned in 0.5 min allowing re-equilibration until 15.0 min.

Data were collected in positive and negative ESI ionization modes in separate runs and operated in the range from m/z 100 to 1000, and m/z 40 to 1000 for MS analysis and MS/MS analysis, respectively. The nozzle voltage was set to 1000 V, and the capillary voltage was 3000 V with a scan rate of 1.5 scans/s (positive mode) or -4000 V with a scan rate of 1.0 scan/s (negative mode). The drying gas was heated up to 250 °C and flowed at a rate of 12 L/min, pressure 52.0 psi. Additional heating was applied using sheath heated gas up to 370 ºC with a flow of 11 L/min for improving the ionization.

The MS/MS analysis was performed with the same chromatographic and spectrometric conditions used for the primary analysis. According to the prior determined accurate mass and retention time, ions of interest were targeted by collision-induced dissociation (CID) fragmentation on the fly, using a narrow isolation width (approx. 1.3 Da). For internal mass correction during data acquisition, two reference masses were infused continuously to the system over the course of the whole analysis: m/z 121.0509 (protonated purine) and m/z 922.0098 protonated hexakis (1H,1H,3H-tetrafluoropropoxy) phosphazine (HP-921) in positive ionization mode, whereas m/z 112.9856 (proton-abstracted TFA anion) and m/z 966.0007 (formate adduct of HP921) for the negative mode.

4.2.3 Plasma non-targeted analysis by GC–MS

For GC–MS analysis, protein precipitation was performed by treatment with cold acetonitrile (1:3) followed by vortex-mix for 2 min and let stand on ice for 5 min. Samples were centrifuged at 15,400 x g for 10 min at 4 °C. For methoximation reaction, 100 µl of the supernatant were transferred to a GC vial and evaporated to complete dryness by Speedvac concentrator (314)(SpeedVac Concentrator System, Thermo Fisher Scientific, Waltham, MA) and then, 10 µL of O-methoxyamine hydrochloride (15 mg/mL) in pyridine solution was added to the dried sample and

thoroughly mixed for 1 min on a vortex mixer. Methoxymation reaction was carried out in darkness at room temperature for 16 h. For silylation process, 10 µL of BSTFA/TMCS (99:1) was added as catalyst and vortex-mixed for 5 min. Capped vials were heated in an oven for 1 h at 70 °C. Finally, 100 µL of heptane containing C18:0 methyl ester (10 mg/L) as internal standard (IS) was added to each sample and vortex-mixed prior GC analysis.

The analysis was performed by GC system (Agilent Technologies 7890A) coupled to a mass spectrometer with triple-Axis detector (5975C, Agilent Technologies). Two microlitres of derivatized plasma samples were automatically injected by an Agilent autosampler (7693) in split mode (split ratio 1:10) through an Agilent ultra-inert deactivated glass wool split liner. An Agilent GC column DB5-MS (30 m length, 0.25 mm i.d, and 0.25 µm film of 95% dimethyl/5% diphenylpolysiloxane) with a precolumn (10 m J&W integrated with Agilent 122-5532G) was used for compound separation. Carrier gas flow rate (He) was set approximately at 1 mL/min after performing Retention Time Locking (RTL) and, injector and transfer line temperatures at 250 °C and 280 °C, respectively. The initial column oven temperature was set at 60 °C (held for 1 minute), rose to 325 °C at 10 °C/min during 26.5 min, and hold at this temperature for 10 minutes before cooling down for the next injection. MS detection was performed with electron impact ionization (EI) with 70 eV of energy and 230 °C in filament source.

Mass spectra were collected over a mass range of m/z 50–600 at a scan rate of 2 spectra/s. Internal standard C18:0 methyl ester (10 mg/L) and, for retention index determination, a mixture of n-alkanes (C8-C28) dissolved in n-hexane were injected prior to the samples. Data were acquired using Agilent MSD ChemStation Software (Agilent Technologies) (315,316).

The analysis was carried out by randomising the samples for each platform run. For equipment performance and reproducibility determination, several replicates were analysed from a homogeneous pool containing a small equal amount of all the samples (Quality Controls, QC). These QCs were treated like the rest of the samples. They were injected at the beginning of the batch (10 injections) to equilibrate the system and every ten samples to monitor the stability of the analysis

4.3 DATA PROCESSING

The raw data obtained by CE−MS were processed with MassHunter Profinder software version B.08.00 (317), applying the Molecular Feature Extraction (MFE) to clean of background noise and unrelated ions. Coeluting adducts of the same feature (+H+, +Na+, and neutral loss of water) were searching by MFE where all the features (ions) were aligned across the samples using mass and retention time (RT). Therefore, a final spectrum for each compound group was built to continue with the next step, the re-extraction of the batch files. Batch Recursive Feature Extraction (RFE) refines the quality of the target list for the Find by Ion (FbI) function by improving the quality of the final list of compounds. By RFE, using both the mass and the RT of the previous MFE results, a final compound group list was generated, and the verification of the correct integration of extracted ion chromatogram was inspected for each feature, through all the samples, one by one. The raw data collected by LC−MS were reprocessed by the molecular feature extraction (MFE) with Mass Hunter Qualitative (B.06.00, Agilent Software). The MFE algorithm enables us to clean data background noise and creates a final list of possible components. As a way of finding coeluting adducts of the same feature, data were reprocessed using DA Reprocessor Offline Utilities B.05.00 (Agilent) for ions such as [M]+, [M+H]+, [M+Na]+ in positive ionization, [M−H]-, [M+HCOOH-H]−, [M+Cl]- in negative ion mode, and neutral loss of water in both polarities. Data were aligned and filtered using Mass Profiler Professional software (B.14.9 Agilent Software).

GC−MS data treatment started with a thorough inspection of the total ion chromatograms (TIC) of experimental samples with examination of the overall quality of analytical performance. Raw data files were converted to the appropriate format for quantitative analysis through MassHunter Workstation GC-MS Translator (B.04.01). Agilent MassHunter Unknowns Analysis Tool 7.0 was used for deconvolution and metabolite identification. The assignment of a chemical identity was done by searching via two specific libraries: Fiehn, 2008 version, and "in house" plasma spectral library from CEMBIO based on Fiehn and NIST (National Institute of Standards and Technology, library 2.2 version 2014) libraries. This identity was granted comparing their retention indices and retention times, and spectrum extracted after deconvolution with each compound included in the

libraries. Afterward the data was aligned with MassProfiler Professional (B.14.9 Agilent Software) (318) and exported to Agilent MassHunter Quantitative Analysis (B.07.00) for target ion assignation and obtaining the abundance of compounds with the inspection of the correct integration of peaks. Finally, the data matrix with the final abundance of each metabolite was generated.

To ensure valid measurements, data matrix obtained after data reprocessing for each platform were filtered according to the variation in the abundance of the compounds in QC samples, expressed as standard deviation relative, and only those with RSD<30% were kept.

4.3.1 Data analysis

The three hyperparameters that determine the accuracy of the within-batch effects elimination were: i) the tolerance threshold (ε) 5% of the median of distribution of QC values, ii) the penalty term (C) median of the distribution of QC samples and iii) the kernel width (γ) logspace (0,3) 20 values.

OPLS-DA models were validated for every platform using response of permutation test through 999 permutations. This test assesses whether the specific classification of individuals in the two designed groups is significantly better than any other random classification into two arbitrary groups. Permutation tests show the validity and degree of overfitting for model. The R^2 and Q^2 distribution is compared to the original (unperturbed)) data when the Y data is randomly permutated. At the same time, the X data is left intact. The resulting validation plot represents on the y-axis the R^2 and Q^2 values of the original and permuted models, while the x-axis represents the correlation coefficients between both models. The points were fitted via the regression line. Model validity should have higher R^2 and Q^2 values of the original models than of the permutated models (319).

4.3.2 Annotation and compound identification

An initial tentative identification of features from LC−MS and CE−MS based on the m/z of the compounds showing significant differences in class separation was performed by CEU Mass Mediator tool (311). Tentative annotation covered, beside the accurate mass matching with the mass error set to 10 ppm for LC−MS and 20 ppm for CE−MS, isotopic distribution determination and manual checking of the

possible ions and adducts. For CE−MS, fragments, dimers or ringing artefacts were removed from the dataset as described in Godzien et al. (308) Spectra at high fragmentor voltage (200 V) were used to confirm CE−MS annotations. As a result, fragmentation spectra were obtained and ion-source fragmentation characteristic patterns were studied. For this purpose, an in-house database created by CEMBIO of 515 fragments has been used together with its ions, adducts and multimers, which is available in CEU Mass Mediator (CMM) (320) and includes a relative migration time library.

To confirm the annotation of the compounds, LC−MS/MS analysis was carried out, repeating the experiment. The data independent analysis (DIA) was performed with the same chromatographic and spectrometric conditions used for the primary analysis. According to the prior determined accurate mass and retention time, ions of interest were targeted by collision-induced dissociation (CID) fragmentation, using a narrow isolation width (approx. 1.3 Da). Precursor ions were targeted with different fixed collision energies at 20 and 40eV, for separate runs to obtain collision energy-specific MS/MS spectra.

The identification of each metabolite was achieved by manual MS/MS spectra interpretation. Comparison of the fragmentation pattern based on fragmentation mechanism and mass differences, was done against the MS/MS from standard compound when available or spectral matching with spectra available in Metlin database (321) and MetFrag (322) for *in silico* fragmentation for computer assisted identification of metabolite mass spectra.

4.4 STATISTICAL ANALYSIS OF CLINICAL VARIABLES

Descriptive statistics were used to characterize the most relevant clinical, biochemical and pathological features of the study population. The association of categorical variables was assessed by the chi-squared test or Fisher’s exact test, when appropriate. The distribution of quantitative variables among study groups was evaluated by parametric (Student's t) or non-parametric (Kruskal-Wallis or Mann-Whitney) tests as required for each variable.

Overall survival (OS) was calculated from the date of randomization into the study to the date of death from any cause or of last contact in living patients. Progression-

free survival (PFS) was calculated from the date of treatment initiation within the AXINET trial to the date of disease progression or the last contact in patients without progression. The Kaplan-Meier product limit method was used to estimate PFS and OS, and differences observed among patient subgroups were assessed by the log-rank test. Statistical significance was established at $P \leq 0.05$.

The prognostic value for PFS and OS was analyzed for each identified metabolite (N=155) with a differential availability in NET patients ($P<0.05$) when compared to non-cancer individuals, considering their expression as a continuous variable, by univariate Cox regression method collected in the package of R survival (323) 3.2-7. The adjusted p-value for multiple testing was estimated by the False Discovery Rate (FDR) method (324,325). We also evaluated the potential prognostic impact of identified metabolites considered as categorical variables, with the median value as the cut-off point (> or ≤ median), using the Kaplan-Meier estimator and log-rank test to assess the statistical significance. Metabolites with a significant impact ($P<0.05$) on PFS or OS were selected (N=35) for further association analyses. The potential association of selected metabolites (N=35) with most relevant clinicopathological features (gender, age, BMI, grade, primary tumor origin and tumor functionality) and most common concomitant medications was assessed by the Chi-square or Fisher's exact tests, as appropriate. Drug classes selected for association analyses were those taken by >10% of patients at study entry, and included the following: antihypertensives, analgesics, nonsteroidal anti-inflammatory drugs, diuretics, antiaggregants, anxiolytics, H2-receptor blockers, and lipid-lowering medications. Statistical significance was established at $P<0.05$.

To evaluate the independent prognostic value of selected metabolites both for PFS and OS, adjusted for other potential confounding variables such as gender, age, BMI, grade, tumor functionality, primary tumor location (gastroenteric, pulmonary or other) and concomitant medication if appropriate, a multivariate analysis was performed using the Cox proportional hazards method. All analyses were performed using SPSS software version 21 and R software version. 3.6.1.

4.5 METABOLITE PATHWAY ANALYSIS (MPA) AND METABOLITE SET ENRICHMENT ANALYSIS (MSEA).

In order to identify aberrant molecular pathways in NET patients we analysed our data by Metabolite Pathway Analysis (MPA) and Metabolite SetEnrichment Analysis (MSEA) using MetaboAnalyst (326) 4.0 platform (http://www.metaboanalyst.ca/). The databases of reference employed were KEGG *homo sapiens* (Oct 2019) and SMPD (327).

4.6 HEATMAP AND HIERARCHICAL CLUSTERING

Heatmaps were conducted with the $\log_{10}$ value of each metabolite levels in the plasma samples. Unsupervised hierarchical clustering was performed for metabolites and patients using Pearson correlation and average as linkage method. Both were conducted using the Morpheus Software (328) (Broad Institute; https://software.broadinstitute.org/morpheus).

5. RESULTS

RESULTS

5.1 BASELINE CHARACTERISTICS OF THE STUDY POPULATION

The study population included 77 plasma samples from patients with advanced G1-G2 extra-pancreatic neuroendocrine tumors enrolled in the AXINET trial (EUDRACT:2011-001550-29) and 68 non-cancer individuals, as control cohort. The most relevant clinicopathological characteristics of the NET study population are summarized in Table 1.

Globally, we included 49 patients with neuroendocrine tumors of GEP origin, 19 of pulmonary origin, 7 of unknown primary and 2 from other primary sites. Among patients with GEP tumors, 1 was of gastric origin, 1 of duodenal origin, 39 of small intestine, 2 of colon, and 6 of rectum. All tumors were well-differentiated, 31.2% had non-functioning tumors, 32.5% were grade 1 (G1) and over two thirds (67.5%) were grade 2 (G2). The median time from diagnosis to study entry was 14.1 months (range: 0.1-223.1 months).

Forty percent of patients had not received any prior systemic therapy, whereas 44.2% and 15.6% had received one or more prior lines of treatment, respectively. Among pre-treated patients, 40 of them had received SSA, 10 chemotherapy, 4 interferon and 8 everolimus. One third (33.4%) of patients had undergone a surgical resection of the primary tumor.

The median age at diagnosis was 63 years (range: 37 to 83 years), and the majority of patients were male (54.5%). The median BMI of NET patients was 25.9 (range 17.2- 52.5). About one third of patients (36.4%) presented a normal weight (BMI 18.5–24.9), 33.8% had overweight (BMI 25.0–29.9) and 24.7% obesity (BMI>30). The distribution of gender, age and body mass index (BMI) was similar in the NET and control cohorts, as detailed in Table 2.

Most relevant biochemical abnormalities observed in NET patients (urinary 5-HIAA, and plasma chromogranin A, LDH, ALT, AST, glycemia, creatinine and urea) are summarized in Table 3. The general neuroendocrine plasma biomarker chromogranin A was elevated in 71.4% of cases and in 59.7% of patients the elevation was greater than two times the upper limit of normal. 5-HIAA was

elevated in 66.2% of patients and greater than two times the upper limit of normal in 55.8%. One third of patients presented hyperglycemia, and the majority of patients had renal and liver function tests within the normal range.

Table 1. Clinico-pathological characteristics of the study population.

Features	N (%)
Age (years)	
Median value (range)	63 (38-83)
BMI	
Median value (range)	25.9 (17.2- 52.5)
BMI	
Underweight (BMI < 18.5)	1 (1.3%)
Normal weight (BMI 18.5–24.9)	28 (36.4%)
Overweight (BMI 25.0–29.9)	26 (33.8%)
Obesity (BMI>30)	19 (24.7%)
Unknown	3 (3.9%)
Gender	
Female	34 (45.5%)
Male	42 (54.5%)
ECOG	
0	49 (63.6%)
1	28 (36.4%)
Localization of primary tumor	
Gastric	1 (1.3%)
Duodenum	1 (1.3%)
Jejunum-ileum	39 (50.6%)
Colon	2 (2.6%)
Rectum	6 (7.8%)
Lung	19 (24.7%)
Unknown primary	7 (9.1%)
Others	2 (2.6%)
Grade	
G1 (Ki-67<3%)	25 (32.5%)
G2 (Ki-67 3-20%)	52 (67.5%)
Ki67 (%)	
≤5	51 (66.2%)
>5	26 (33.8%)
Functioning Tumor	
Yes (Carcinoid Syndrome)	24 (31.2%)
No	53 (68.8%)
Time from diagnosis to study entry	
≤12 months	33 (40.3%)
>12 months	44 (57.1%)
Prior systemic treatment	
No	31 (40.3%)
1 line	34 (44.2%)
≥ 2 lines	12 (15.6%)
Prior SSA	
Yes	40 (51.9%)
No	37 (48.9%)

Features	N (%)
Prior Chemotherapy	
Yes	10 (13.0%)
No	67 (87.0%)
Prior PRRT	
Yes	0 (0.0%)
No	77 (100%)
Prior Interferon	
Yes	4 (5.2%)
No	73 (94.8%)
Prior Everolimus	
Yes	8 (10.4%)
No	69 (89.6%)
Prior Radiotherapy	
Yes	2 (2.6%)
No	75 (97.4%)
Prior Locoregional Therapy	
Yes	8 (10.4%)
No	69 (89.6%)
Prior Surgery	
Yes	34 (44.2%)
No	43 (55.8%)
Exitus	
Yes	39 (50.6%)
No	38 (49.4%)

BMI: Body Mass Index, SSA: Somatostatin analogues, PRRT: Peptide receptor radionuclide therapy

Table 2. Distribution of age, gender and body mass index in NET and control patients.

	Neuroendocrine Tumors (Study Cohort) N= 77	Non-cancer Individuals (Control Cohort) N= 68
Gender (N (%))		
Female	35 (45.5%)	41 (60.3%)
Male	42 (54.5%)	27 (39.7%)
Age (years)		
Median value (range)	63 (37-83)	61.7 (38-83)
BMI		
Median value (range)	25.9 (17.2-52.5)	26.8 (20.7–35.9)

BMI: Body Mass Index

Table 3. Biochemical parameters of the NET cohort.

Blood parameter	N (%)
Chromogranin A > ULN	
Yes	55 (71.4%)
No	13 (16.9%)
Unknown	9 (11.7%)
Chromogranin A > 2xULN	
Yes	46 (59.7%)
No	22 (28.6%)
Unknown	9 (11.7%)
5-HIAA > ULN	
Yes	51 (66.2%)
No	14 (18.2%)
Unknown	12 (15.6%)
5-HIAA > 2xULN	
Yes	43 (55.8%)
No	22 (28.6%)
Unknown	12 (15.6%)
LDH > ULN	
Yes	14 (18.2%)
No	54 (70.1%)
Unknown	9 (11.7%)
Alkaline Phosphatase >ULN	
Yes	11 (14.4%)
No	61 (79.1%)
Unknown	5 (6.5%)
AST > ULN	
Yes	7 (9.1%)
No	70 (90.9%)
ALT > ULN	
Yes	8 (10.4%)
No	69 (89.6%)
Glycemia > ULN	
Yes	25 (32.5%)
No	51 (66.2%)
Unknown	1 (1.3)
Creatinine > ULN	
Yes	8 (10.4%)
No	69 (89.6%)
Urea > ULN	
Yes	11 (14.3%)
No	65 (84.4%)
Unknown	1 (1.3%)

ALT: Alkaline Phosphatase; AST: aspartate aminotransferase; 5-HIAA: 5-Hydroxyindoleacetic acid; ULN: Upper Limit of Normal

5.2 SURVIVAL ANALYSIS BY CLINICO-PATOLOGICAL FEATURES

With a median follow-up of 46 months (range: 2-96), 55 (71.4%) patients had progressed and 39 (50.6%) had died. The median progression free survival (PFS) was 13.7 months (range: 2.4-93.7) and the 1-year PFS rate was 55.8%. The median OS was 49.0 months (range: 2.4-96.4), and 53.5% were alive at 5 years (5-year OS). The 1-year PFS rate from study entry was significantly higher for patients that had received no prior systemic therapy (76.8 %) than for those that had been treated with 1 (56.0%) or more than 1 (25.0%) prior lines of treatment (*p=0.01*). PFS was also greater for patients with a shorter time from diagnosis to study entry (1-year PFS rate of 69.7 % vs. 45.5 % for patients with 12 months or less versus more than 12 months, respectively, *p=0.02*). PFS (% at 1 year) per primary tumor site was greater for small bowel NETs (62.5%), followed by NETs from other gastrointestinal sites (gastric, colorectal) (55.6%), the lung (52.6%) or those of unknown origin (42.9%). The 5-year OS rate after study entry was significantly greater in women than in men (69.8 % vs. 40.1%, *p=0.05*) and for patients naïve from previous systemic therapy (67.7 % vs. 23.5% vs. 33.3% for patients with 0, 1 or more than 1 prior lines of therapy, respectively; *p=0.001).* There were no statistically significant differences in patient survival based on age or grade, although survival rates were numerically higher in younger patients and low grade tumors (G1). In addition, no significant survival differences were observed by BMI, presence or not of a hormonal syndrome, or chromogranin A and 5-HIAA levels. All these data are summarized in Table 4.

Table 4. Univariate PFS and OS analysis by clinico-pathological features.

		PFS (% at 1 y)				OS (% at 5 y)			
Feature	**N**	Median (months)	%	**HR**	**P**	Median (months)	%	**HR**	**P**
All patients	77	13.7	55.8 %			49.0	57.1 %		
Gender					*0.43*				***0.05***
Female	34	18.5	61.9 %	*0.76*		NA	69.8 %	*0.50*	
Male	42	13.0	57.6 %			45.9	40.1 %		
Age					*0.25*				*0.28*
≤ median value	39	27.4	61.5%	*0.50*		76.2	59.6 %	*0.70*	
> median value	38	11.9	50.0%			54.5	46.4 %		
BMI					*0.63*				*0.26*
Underweight (BMI < 18.5)	1	8.4	0.0 %	*2.22*	*0.44*	81.9	100.0 %	*0.00*	*0.97*
Normal weight (BMI 18.5–24.9)	28	11.7	46.4 %	*REF*		43.6	28.6 %	*REF*	
Overweight (BMI 25.0–29.9)	26	13.7	61.5%	*0.74*	*0.46*	68.6	50.0%	*0.55*	*0.09*
Obesity (BMI>30)	19	17.1	63.2%	*0.71*	*0.45*	76.2	52.6%	*0.52*	*0.10*
Tumor location					*0.23*				*0.30*
Small Intestine	40	17.1	64.1 %	*REF*		76.2	58.0 %	*REF*	
Lung	19	12.3	55.6 %	*1.26*	*0.47*	NA	56.1 %	*1.13*	*0.73*
GI other	9	16.5	55.6 %	*1.26*	*0.47*	33.8	33.3 %	*1.72*	*0.29*
Unknown	7	9.6	57.1 %	*1.29*	*0.59*	NA	64.3 %	*0.55*	*0.42*
Other	2	4.4	0.0 %	*5.69*	***0.02***	5.1	0.0 %	*2.89*	*0.11*
Time from dx to study entry					***0.02***				*0.27*
≤ 12 months	33	28.1	69.7 %			76.2	61.1 %		
> 12 months	44	11.7	45.5 %	*1.88*		52.5	48.0 %	*1.43*	
Prior systemic treatment					***0.010***				***0.001***
No	31	NA	76.8%	*REF*		NA	67.7 %	*REF*	
1 line	34	27.4	56.0%	*2.29*	***0.003***	37.0	23.5 %	*2.70*	***0.03***
> 1 line	12	8.0	25.0%	*4.19*	*0.14*	43.6	33.3 %	*1.57*	*0.64*
Ki67 (%)					*0.34*				*0.65*
<5	39	17.2	59.0%	*REF*		77.8	54.7%	*REF*	
5-9	23	18.2	60.9%	*0.70*	*0.43*	54.5	43.6%	*1.38*	*0.36*
10-20	15	8.8	46.7%	*1.42*	*0.36*	76.2	39.6%	*1.78*	*0.68*

		PFS (% at 1 y)				OS (% at 5 y)			
Feature	**N**	Median (months)	%	**HR**	**P**	Median (months)	%	**HR**	**P**
Grade					*0.48*				*0.65*
G1	25	21.0	68.0 %	*0.81*		68.8	53.8 %	*0.85*	
G2	52	11.9	50.0%			76.2	53.0 %		
Hormonal Sd					*0.31*				*0.77*
Yes	24	13.0	54.2 %	*1.33*		68.6	55.9 %	*0.90*	
No	53	14.4	56.6 %			76.2	52.6 %		
Crg-A > ULN					*0.16*				*0.74*
Yes	55	14.4	54.5 %	*1.77*		76.2	53.3 %	*1.16*	
No	13	50.8	76.9 %			77.8	68.4 %		
5HIAA > ULN					*0.53*				*0.99*
Yes	51	14.4	58.8 %	*1.27*		77.8	60.5 %	*0.99*	
No	14	21.0	64.3 %			NA	54.2 %		

BMI: Body Mass Index; Crg-A: Chromogranin A; dx: diagnosis; 5HIAA: 5-Hydroxyindoleacetic acid; Sd: Syndrome; ULN: Upper Limit of Normal

5.3 METABOLIC PROFILE OF NEUROENDOCRINE TUMORS

5.3.1 Plasma metabolomic profiling of patients with NETs.

The metabolite fingerprint was assessed using a multiplatform LC-MS, GC-MS and CE-MS approach to analyze the plasma of 77 patients with advanced NETs and of 68 non-cancer individuals (controls). Data obtained was used for multivariate analysis of unsupervised principal components (PCAs) to verify system stability, performance and reproducibility of sample treatment procedures, as priorly reported (329). For multivariate analysis in each platform, unsupervised PCA models were built to observe natural clustering of NETs and controls, and OPLS-DA models were also conducted to model differences between groups (Figure 5, A-D). Clear separation between NETs and non-cancer individuals for all analytical techniques were shown in the applied models. After data processing as previously described, univariate statistical analysis revealed the following individually significant differential metabolites between NETs and controls: 75 compounds in CE–MS, 150 in LC–MS ESI (+), 296 in LC–MS ESI (-) and 19 in GC–MS (330). These variables were annotated and/or identified as described in "*Annotation and compound identification*" in the material and methods section. The integration of metabolic data acquired by different analytical platforms resulted in 155 identified metabolites with a differential availability in NET patients as compared to non-cancer individuals ($p<0.05$). Metabolite identification of some specific metabolites (arginine, glutamine, phenylalanine, among others) across more than one analytical platform significantly increases the confidence of metabolite identification (Supplementary Table 1).

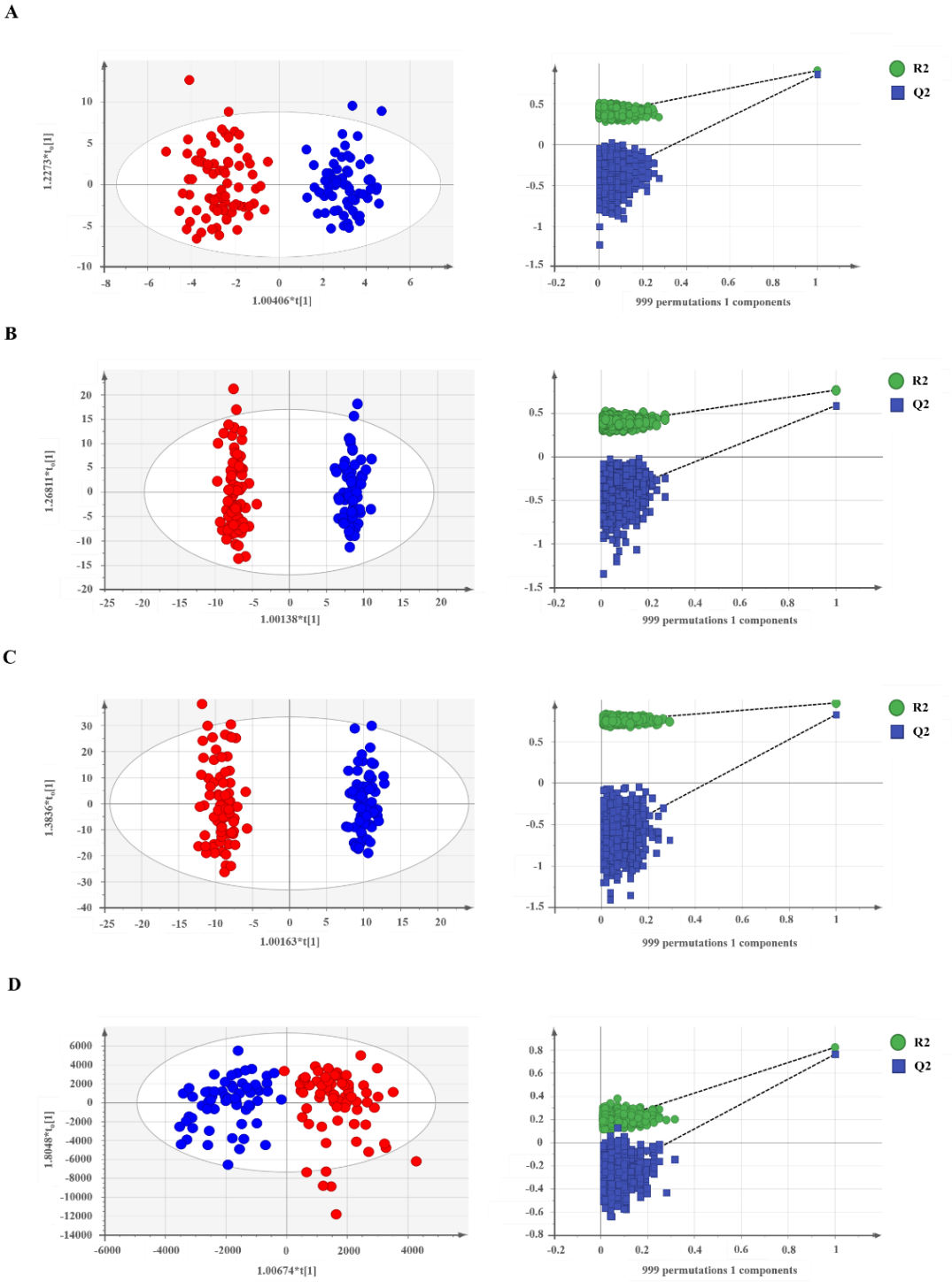

Figure 5. OPLS-DA supervised models and permutation tests in NET and non-cancer patients. Supervised models show a clear separation between NET patients and non-cancer individuals. A-D) OPLS-DA score plots and permutation tests of OPLS-DA models for each platform through 999 permutations. Panel A for CE-MS data (R2 = 0.872, Q2 = 0.843); panel B, LC−MS/ESI(+) data (R2 = 0.954, Q2 = 0.871); panel C, LC−MS/ESI(-) data (R2 = 0.885, Q2 = 0.788); and panel D, GC-MS data (R2 = 0.781, Q2 = 0.744). Red dots, NETs (N= 77); blue dots, non-cancer individuals (N= 68).

5.3.2 Prognostic impact of differential metabolites in NET patients.

We assessed the prognostic impact of the 155 identified metabolites with a differential availability in NET patients (*p<0.05*), when compared to non-cancer individuals. Each metabolite was analysed both as a continuous and as a dichotomic variable (categorized as high or low according to their median value) to explore their potential impact on patient´s survival. Thirty-four metabolites were significantly associated with PFS (N=16) and/or OS (N=27). The metabolites that correlated with PFS were the following: Cys-Gly disulphide, Glu-Hyp, Glu-Lys/Ɛ-Glu-Lys, Glu-Lys/Ɛ-Glu-Lys 2, methionine S-oxide, suberylglycine, pyranose (glucose/altrose/galactose/talose), eicosapentaenoic acid, 3-hydroxy-5-octenoylcarnitine, LPA (13:0), LPC (22:1), LPE (22:6), PG (28:0), 3-hydroxydodecanoic acid, urocanate nicotinamide N-oxide, 5-hydroxyindoleacetic acid. The following metabolites were associated with OS: dimethyl-arginine (symmetric), Glu-Hyp, Glu-Lys/Ɛ-Glu-Lys 2, pyroglutamine, Ser-Ala, suberylglycine, Thr-Gly, pyranose (glucose/altrose/galactose/talose), eicosapentaenoic acid, MG(20:0), N-palmitoyl glutamic acid, 3-hydroxy-5-octenoylcarnitine, 3-hydroxy-5-tetradecenoylcarnitine, linoleyl carnitine, LPC (16:0)-OH, LPC (22:1), methylimidazole, urocanate nicotinamide N-oxide, 5-hydroxyindoleacetic acid, N-(4-coumaroyl)-homoserine lactone, 4-methylcatechol, 1-methyladenosine, SM (36:0), biliverdin, cholestane-3.7.12.24.25-pentol, cortisone acetate, ecdysone 25-O-D-glucopyranoside. There were 9 metabolites associated with both PFS and OS: Glu-Hyp, Glu-Lys/Ɛ-Glu-Lys 2, suberylglycine, pyranose (glucose/altrose/galactose/talose), eicosapentaenoic acid, 3-hydroxy-5-octenoylcarnitine, LPC (22:1), urocanate nicotinamide N-oxide and 5-hydroxyindoleacetic acid. The association significance of these 34 metabolites with PFS and/or OS is detailed in Table 5. Table 6 summarizes PFS-rates at 1 year and OS-rates at 5 years by metabolite abundance classified as “low” or “high” according to their median values.

The main characteristics of the 34 selected metabolites according to the Human Metabolome Database (HMDB) (www. hmdb.ca) are provided in Supplementary Table 2.

Table 5. Metabolites with significant impact on PFS and OS evaluated as continuous or categorized variables according to median values.

	PFS				OS			
	Continuous		Median		Continuous		Median	
	P	*FDR*	*P*	*FDR*	*P*	*FDR*	*P*	*FDR*
Amino acids, peptides, and analogues								
Cys-Gly disulphide	***0.026***	*0.586*	*X*	*X*	*X*	*X*	*X*	*X*
Dimethyl-Arginine (symmetric)	*X*	*X*	*X*	*X*	***0.002***	*0.108*	***0.0113***	*0.342*
Glu-Hyp	***0.034***	*0.624*	***0.042***	*0.561*	***0.033***	*0.399*	*X*	*X*
Glu-Lys/Ɛ-Glu-Lys	***0.019***	*0.586*	***0.016***	*0.508*	*X*	*X*	*X*	*X*
Glu-Lys/Ɛ-Glu-Lys 2	***0.023***	*0.586*	***0.002***	*0.168*	*X*	*X*	***0.016***	*0.365*
Methionine S-oxide	*X*	*X*	***0.000***	*0.099*	*X*	*X*	*X*	*X*
Pyroglutamine	*X*	*X*	*X*	*X*	*0.041*	*0.419*	*X*	*X*
Ser-Ala*	*X*	*X*	*X*	*X*	*X*	*X*	***0.037***	*0.436*
Suberylglycine	***0.024***	*0.586*	***0.027***	*0.561*	***0.022***	*0.399*	*X*	*X*
Thr-Gly*	*X*	*X*	*X*	*X*	*X*	*X*	***0.037***	*0.436*
Carbohydrates and CH conjugates								
PYRANOSE (glucose/altrose /galactose /talose)	*X*	*X*	***0.043***	*0.561*	*X*	*X*	***0.033***	*0.436*
Fatty Acyds								
Eicosapentaenoic acid	***0.020***	*0.586*	*X*	*X*	***0.023***	*0.399*	***0.045***	*0.436*
MG(20:0)	*X*	*X*	*X*	*X*	***0.023***	*0.399*	***0.024***	*0.421*
N-palmitoyl glutamic acid*	*X*	*X*	*X*	*X*	*X*	*X*	***0.027***	*0.421*
3-Hydroxy-5-octenoylcarnitine	***0.026***	*0.586*	***0.008***	*0.462*	***0.000***	*0.071*	***0.002***	*0.255*
3-Hydroxy-5-tetradecenoylcarnitine*	*X*	*X*	*X*	*X*	*X*	*X*	***0.027***	*0.421*
Linoleyl carnitine	*X*	*X*	*X*	*X*	***0.037***	*0.412*	*X*	*X*
Glycerophospholipids								
LPC (16:0)-OH	*X*	*X*	*X*	*X*	*X*	*X*	*X*	*X*
LPA (13:0)	***0.041***	*0.648*	***0.034***	*0.561*	*X*	*X*	*X*	*X*
LPC (22:1)	***0.010***	*0.586*	***0.013***	*0.508*	***0.002***	*0.108*	***0.015***	*0.365*
LPE (22:6)	*X*	*X*	***0.046***	*0.561*	*X*	*X*	*X*	*X*
PG (28:0)	*X*	*X*	***0.047***	*0.561*	*X*	*X*	*X*	*X*

	PFS				OS			
	Continuous		Median		Continuous		Median	
	P	***FDR***	***P***	***FDR***	***P***	***FDR***	***P***	***FDR***
Hydroxy acids and derivatives								
3-Hydroxydodecanoic acid	***0.036***	*0.624*	*X*	*X*	*X*	*X*	*X*	*X*
Imidazoles								
Methylimidazole	*X*	*X*	*X*	*X*	***0.030***	*0.399*	*X*	*X*
Urocanate Nicotinamide N-oxide	*X*	*X*	***0.029***	*0.561*	***0.048***	*0.443*	***0.010***	*0.342*
Indoles and derivatives								
5-Hydroxyindoleacetic acid	*X*	*X*	***0.046***	*0.561*	*X*	*X*	*X*	*X*
Lactones								
N-(4-Coumaroyl)-homoserine lactone	*X*	*X*	*X*	*X*	***0.004***	*0.124*	***0.004***	*0.255*
Phenols								
4-Methylcatechol	*X*	*X*	*X*	*X*	***0.031***	*0.399*	*X*	*X*
Purine nucleosides								
1-Methyladenosine	*X*	*X*	*X*	*X*	***0.000***	***0.017***	***0.004***	*0.255*
Sphingolipids								
SM (36:0)	*X*	*X*	*X*	*X*	*X*	*X*	*X*	*X*
Steroids and steroid derivatives								
Biliverdin	*X*	*X*	*X*	*X*	*X*	*X*	*X*	*X*
Cholestane-3.7.12.24.25-pentol	*X*	*X*	*X*	*X*	***0.026***	*0.399*	*X*	*X*
Cortisone acetate	*X*	*X*	*X*	*X*	***0.043***	*0.419*	*X*	*X*
Ecdysone 25-O-D-glucopyranoside	*X*	*X*	*X*	*X*	***0.025***	*0.399*	*X*	*X*

CH: carbohydrates; FDR: false discovery rate. OS: Overall Survival. PFS: Progression free survival

Table 6. PFS and OS by metabolite abundance classified as "Low" or "High" by the median value.

		PFS (% at 1 year)				OS (% at 5 years)			
	N	**Median (months)**	**%**	***HR***	***P***	**Median (months)**	**%**	***HR***	***P***
Amino acids, peptides and analogues									
Cys-Gly disulphide									
Low	37	10.9	43.2 %	*1.7*	*0.1*	77.8	54.4 %	*1.0*	*0.9*
High	40	18.8	67.5 %			66.3	53.0 %		
Dimethyl-Arginine (symmetric)									
Low	36	17.2	58.3 %	*0.9*	*0.8*	81.9	68.2 %	*0.4*	***0.009***
High	41	13.7	53.7 %			45.5	40.0 %		
Glu-Hyp									
Low	38	26.4	60.5 %	*0.6*	*0.2*	81.9	66.7 %	*0.5*	***0.05***
High	39	12.4	51.3 %			45.5	40.7 %		
Glu-Lys/Ɛ-Glu-Lys									
Low	38	25.8	60.5 %	*0.6*	*0.2*	81.9	62.4 %	*0.6*	*0.2*
High	39	12.4	51.3 %			54.5	44.9 %		
Glu-Lys/Ɛ-Glu-Lys 2									
Low	37	28.1	64.9 %	*0.5*	***0.09***	NA	64.5 %	*0.5*	***0.08***
High	40	11.5	47.5 %			52.4	42.6 %		
Methionine S-oxide									
Low	38	27.8	63.2 %	*0.4*	***0.03***	NA	63.4 %	*0.6*	*0.1*
High	39	11.9	48.7 %			45.9	44.0 %		
Pyroglutamine									
Low	38	13.1	56.4 %	*0.9*	*0.8*	81.9	66.2 %	*0.5*	***0.04***
High	39	13.7	55.3 %			43.6	41.1 %		
Ser-Ala*									
Low	36	16.6	61.1 %	*0.7*	*0.3*	77.8	60.3 %	*0.7*	*0.2*
High	41	12.4	51.2 %			56.9	47.1 %		
Suberylglycine									
Low	38	24.7	60.5 %	*0.6*	*0.2*	NA	67.7 %	*0.5*	***0.06***
High	39	12.3	51.3 %			49.0	39.3 %		
Thr-Gly*									
Low	36	16.6	61.1 %	*0.7*	*0.3*	77.8	60.3 %	*0.7*	*0.2*
High	41	12.4	53.7 %			56.9	47.1 %		
Carbohydrates/carbohydrate conjugates									
PYRANOSE (glucose/altrose /galactose/talose)									
Low	34	17.2	67.6 %	*0.4*	***0.04***	76.2	62.8 %	*0.5*	***0.03***
High	39	11.5	43.6 %			45.5	42.5 %		

		PFS (% at 1 year)				OS (% at 5 years)			
	N	**Median (months)**	**%**	***HR***	***P***	**Median (months)**	**%**	***HR***	***P***
Fatty Acyls									
Eicosapentaenoic acid									
Low	37	27.4	62.2 %	*0.7*	*0.3*	NA	60.8 %	*0.9*	*0.7*
High	40	11.9	50.0 %			56.9	47.8 %		
MG (20:0)									
Low	69	13.7	62.5 %	*0.9*	*0.9*	72.7	56.2 %	*0.4*	***0.03***
High	8	12.4	55.1 %			37.0	29.2 %		
N-palmitoyl glutamic acid*									
Low	38	18.5	56.4 %	*0.7*	*0.4*	77.8	63.7 %	*0.5*	***0.05***
High	39	13.0	55.3 %			43.6	42.9 %		
3-hydroxy-5-octenoylcarnitine									
Low	38	26.4	71.1 %	*0.5*	***0.05***	NA	75.3 %	*0.3*	***0.001***
High	39	9.7	41.0 %			41.7	31.2 %		
3-Hydroxy-5-tetradecenoylcarnitine*									
Low	38	18.5	56.4 %	*0.7*	*0.4*	77.8	63.7 %	*0.5*	***0.05***
High	39	13.0	55.3 %			43.6	42.9 %		
Linoleyl carnitine									
Low	37	18.2	59.5 %	*0.9*	*0.8*	NA	63.9 %	*0.6*	*0.1*
High	40	12.3	52.5 %			54.5	43.6 %		
Glycerophospholipids									
LPC (16:0)-OH									
Low	37	25.8	62.2 %	*0.6*	*0.2*	77.8	67.5 %	*0.6*	*0.1*
High	40	11.9	50.0 %			49.0	40.6 %		
LPA (13:0)									
Low	55	14.5	58.2 %	*0.8*	*0.7*	77.8	59.5 %	*0.5*	***0.04***
High	22	11.7	50.0 %			41.7	38.6 %		
LPC (22:1)									
Low	34	27.4	62.9 %	*0.8*	*0.5*	81.9	76.5 %	*0.3*	***0.001***
High	38	11.7	47.4 %			45.9	34.3 %		
LPE (22:6)									
Low	37	25.8	62.2 %	*0.7*	*0.4*	81.9	63.8 %	*0.6*	*0.1*
High	40	11.8	50.0 %			54.5	43.6 %		
PG (28:0)									
Low	37	24.7	67.6 %	*0.7*	*0.3*	81.9	60.0 %	*0.7*	*0.2*
High	40	11.7	45.0 %			56.9	47.6 %		

		PFS (% at 1 year)				OS (% at 5 years)			
	N	**Median (months)**	**%**	***HR***	***P***	**Median (months)**	**%**	***HR***	***P***
Hydroxy acids and derivatives									
3-Hydroxydodecanoic acid									
Low	37	12.4	60.0 %	*1.0*	*0.9*	56.9	47.0 %	*1.5*	*0.1*
High	40	14.5	51.4 %			77.8	59.2 %		
Imidazoles									
Methylimidazole									
Low	36	13.0	55.6 %	*0.9*	*0.7*	81.9	67.4 %	*0.4*	***0.01***
High	41	13.7	56.1 %			43,6	41.1 %		
Urocanate Nicotinamide N-oxide									
Low	38	24.7	60.5 %	*0.6*	*0.1*	NA	61.6 %	*0.6*	*0.1*
High	39	12.4	51.3 %			49.0	45.4 %		
Indoles and derivatives									
5-Hydroxyindoleacetic acid									
Low	38	25.8	60.5 %	*0.7*	*0.4*	NA	63.6 %	*0.5*	***0.08***
High	39	12.4	51.3 %			45.5	43.4 %		
Lactones									
N-(4-Coumaroyl)-homoserine lactone									
Low	38	17.2	55.3 %	*1.1*	*0.6*	NA	72.0 %	*0.4*	***0.01***
High	39	13.7	56.4 %			43.6	34.8 %		
Phenols									
4-Methylcatechol									
Low	38	11.9	50.0 %	*1.5*	*0.1*	81.9	64.0%	*0.6*	*0.1*
High	39	21.0	61.5 %			45.9	43.4%		
Purine nucleosides									
1-Methyladenosine									
Low	38	18.1	56.4 %	*0.8*	*0.7*	81.9	74.3 %	*0.3*	***0.001***
High	39	13.7	55.3 %			39.5	33.2 %		
Sphingolipids									
SM (36:0)									
Low	36	10.9	44.4 %	*1.5*	*0.2*	45.9	41.8 %	*1.7*	***0.07***
High	41	25.8	65.9 %			NA	63.6 %		
Steroids and steroid derivatives									
Biliverdin									
Low	37	26.4	64.9 %	*0.7*	*0.3*	81.9	74.3 %	*0.4*	***0.004***
High	40	11.7	47.5 %			41.7	34.5 %		

		PFS (% at 1 year)				OS (% at 5 years)			
	N	**Median (months)**	**%**	***HR***	***P***	**Median (months)**	**%**	***HR***	***P***
Cholestane-3,7,12,24,25-pentol									
Low	38	18.2	57.9 %	*0.9*	*0.7*	81.9	62.6 %	*0.6*	***0.09***
High	39	13.0	53.8 %			52.5	43.9 %		
Cortisone acetate									
Low	38	11.4	44.7 %	*1.5*	*0.2*	45.9	44.1 %	*1.6*	*0.1*
High	39	18.1	66.7 %			77.8	62.7 %		
Ecdysone 25-O-D-glucopyranoside									
Low	37	13.7	60.0 %	*0.9*	*0.8*	54.5	47.4 %	*1.4*	*0.2*
High	40	13.7	51.4 %			81.9	59.5 %		

HR: Hazard Ratio, OS: Overall Survival, PFS: Progression free survival

5.3.3 Association of prognostic metabolites with clinical features and concomitant drugs in NET patients

We explored the potential associations between each prognostic metabolite and relevant clinical variables (gender, age, BMI, tumor grade, primary tumor site, presence or not of a hormonal syndrome) and concomitant drugs administered to more than 10% of patients at the time of study entry (analgesics, non-steroidal anti-inflammatory agents (NSAIDS), antihypertensives, diuretics, antiaggregants, anxiolytics, H2-receptor blockers and lipid-lowering agents). Fourteen metabolites were associated with at least one clinical characteristic and 14 metabolites were associated with at least one drug class.

Specifically, pyroglutamine (*p=0.002*), LPA(13:0) (*p=0.011),* methylimidazole (*p=0,000*), 4-methylcatechol (*p=0.030*) and SM(36:0) (*p=0.045*) were associated with gender; eicosapentaenoic acid (*p=0.001*), LPC(16:0)-OH (*p=0.016*), LPE(22:6) (*p=0,004*) and methylimidazole (*p=0.029*) were associated with age; dimethyl-arginine symmetric (*p=0.005*), suberylglycine (*p=0.020*), LPC(22:1) (*p=0.017*) and 1-methyladenosine (*p=0.036*) were associated with BMI; cholestane-3,7,12,24,25-pentol (*p=0.025*) and ecdysone 25-O-D-glucopyranoside (*p=0.025*) were associated with grade; LPC(22:1) (*p=0.050*) was associated with primary tumor site; and methylimidazole (*p=0.049*) was associated with the tumor functionality (Table 7).

Regarding concomitant medication, Glu-Hyp (*p=0.040*), Ser-Ala (*p=0.015*) and LPE(22:6) (*p=0.033*) were associated with analgesics; SM(36:0) (*p=0.040*) was associated with NSAIDS; 4-methylcatechol (*p=0.029*) was associated with antihypertensives; pyranoses (glucose/altrose/galactose/talose) (*p=0.005*) were associated with diuretics; methylimidazole (*p=0.040*) and cortisone acetate (*p=0.023*) were associated with antiaggregants; eicosapentaenoic acid (*p=0.002*) was associated with anxiolytics; LPC(22:1) (*p=0.055*), 5-hydroxyindoleacetic acid (*p=0.007*), N-(4-coumaroyl)-homoserine lactone (*p=0.033*) and biliverdin (*p=0.058*) were associated with H2-receptor blockers; and dimethyl-arginine (symmetric) (*p=0.050*), LPA(13:0) (*p=0.007*) and N-(4-coumaroyl)-homoserine lactone (*p=0.029*) were associated with lipid-lowering agents.

Table 7. Association of prognostic metabolites with relevant clinical features and concomitant drugs in NET patients.

	Clinical variables							Concomitant Drug Classes						
Compound	**Sex**	**Age**	**BMI**	**Grade**	**Primary site**	**Functioning**	**Analgesic**	**NSAIDS**	**Antihypertensive**	**Diuretic**	**Antiaggregant**	**Anxiolytic**	**H2-receptor blockers**	**Lipid-lowering agents**
Amino acids, peptides, and analogues														
Dimethyl-Arginine (symmetric)			***0.005***											***0.050***
Glu-Hyp							***0.040***							
Pyroglutamine	***0.002***													
Ser-Ala*							***0.015***							
Suberylglycine			***0.020***											
Carbohydrates and carbohydrate conjugates														
PYRANOSES (glucose/altrose /galactose /talose)										***0.005***				
Fatty Acyls														
Eicosapentaenoic acid		***0.001***										***0.002***		
Glycerophospholipids														
LPC (16:0)-OH		***0.016***												
LPA (13:0)	***0.011***													***0.007***
LPC (22:1)			***0.017***		***0.050***								***0.055***	
LPE (22:6)		***0.004***					***0.033***							

	Clinical variables							Concomitant Drug Classes						
Compound	**Sex**	**Age**	**BMI**	**Grade**	**Primary site**	**Functioning**	**Analgesic**	**NSAIDS**	**Antihypertensive**	**Diuretic**	**Antiaggregant**	**Anxiolytic**	**H2-receptor blockers**	**Lipid-lowering agents**
Imidazoles														
Methylimidazole	***0.000***	***0.029***				***0.049***					***0.040***			
Indoles and derivatives														
5-Hydroxy-indoleacetic acid													***0.007***	
Lactones														
N-(4-Coumaroyl)-homoserine lactone													***0.033***	***0.029***
Phenols														
4-Methylcatechol	***0.030***								***0.029***					
Purine nucleosides														
1-Methyladenosine			***0.036***											
Sphingolipids														
SM(36:0)	***0.045***							***0.040***						
Steroids and steroid derivatives														
Biliverdin													***0.058***	
Cholestane-3.7.12.24.25-pentol				***0.025***										
Cortisone acetate											***0.023***			
Ecdysone 25-O-D-glucopyranoside				***0.025***										

5.3.4 Multivariate analysis confirms selected metabolites as independent prognostic factors in NET patients

Multivariate analyses were performed for each of the 34 metabolites significantly associated with PFS (16) and/or OS (27) (see section 3.2), adjusted by gender, age (as continuous variable), grade, primary tumor site, and time from randomization to study entry (as continuous variable). In addition, BMI, tumor functionality and concomitant drugs were also included in the model only for metabolites for which a significant association was identified (see section 3.3). In the PFS multivariate analysis, Glu-Hyp (*p=0.018*), Glu-Lys/Ɛ-Glu-Lys 2 (*p=0.006*), Methionine S-oxide (*p=0.012*), 3-hydroxy-5-octenoylcarnitine (*p=0.018*) and PG (28:0) (*p=0.050*) demonstrated to be independent prognostic factors (Table 8). In the OS multivariate model, Glu-Hyp (*p=0.011*), Glu-Lys/Ɛ-Glu-Lys 2 (*p=0.004*), MG(20:0) (*p=0.054*), N-palmitoyl glutamic acid (*p=0.045*), 3-hydroxy-5-octenoylcarnitine (*p=0.001*), 3-hydroxy-5-tetradecenoylcarnitine (*p=0.045*), LPC (22:1) (*p=0.002*), 5-hydroxyindoleacetic acid (*p=0.041*), 1-methyladenosine (*p=0.006*), biliverdin (*p=0.019*) and ecdysone 25-O-D-glucopyranoside (*p=0.051*) retained independent statistical significance (Table 9). Thus, 5 and 11 metabolites showed an independent impact on patients' outcomes in terms of PFS and OS, respectively. Three of them, Glu-Hyp, Glu-Lys/Ɛ-Glu-Lys 2 and 3-hydroxy-5-octenoylcarnitine, showed a significant impact on both PFS and OS. PFS and OS curves for these 13 independent prognostic metabolites are depicted in Figure 6.

Table 8. Metabolites with significant impact on PFS (univariate and multivariate analysis).

	Univariate				Multivariate	
	Continuous		Median		Median	
	P	***FDR***	***P***	***FDR***	***P***	***HR***
Amino acids, peptides, and analogues						
Cys-Gly disulphide	*0,026*	*0,586*	*X*	*X*	*0,186*	*1,503*
Glu-Hyp	*0,035*	*0,624*	*0,042*	*0,561*	***0,018***	*0.486*
Glu-Lys/Ɛ-Glu-Lys	*0,019*	*0,586*	*0,016*	*0,508*	*0,085*	*0,577*
Glu-Lys/Ɛ-Glu-Lys 2	*0,023*	*0,586*	*0,002*	*0,168*	***0,006***	*0,411*
Methionine S-oxide	*X*	*X*	*0,000*	*0,099*	***0,012***	*0,448*
Suberylglycine	*0,0248*	*0,586*	*0,027*	*0,561*	*0,353*	*0,757*
Carbohydrates and carbohydrate conjugates						
PYRANOSE (glucose/altrose /galactose /talose)	*X*	*X*	*0,043*	*0,561*	*0,577*	*0,836*
Fatty Acyls						
Eicosapentaenoic acid	*0,020*	*0,586*	*X*	*X*	*0,767*	*0,906*
3-hydroxy-5-octenoylcarnitine	*0,026*	*0,586*	*0,008*	*0,462*	***0,018***	*0,508*
Glycerophospholipids						
LPA (13:0)	*0,041*	*0,648*	*0,035*	*0,561*	*0,066*	*0,571*
LPC (22:1)	*0,010*	*0,586*	*0,013*	*0,508*	*0,069*	*0,546*
LPE (22:6)	*X*	*X*	*0,046*	*0,561*	*0,315*	*0,715*
PG (28:0)	*X*	*X*	*0,047*	*0,561*	***0,050***	*0,560*
Hydroxy acids and derivatives						
3-Hydroxydodecanoic acid	*0,036*	*0,624*	*X*	*X*	*0,564*	*0,840*
Imidazoles						
Urocanate Nicotinamide N-oxide	*X*	*X*	*0,029*	*0,561*	*0,210*	*0,702*
Indoles and derivatives						
5-Hydroxyindoleacetic acid	*X*	*X*	*0,046*	*0,561*	*0,170*	*0,603*

FDR: *false discovery rate*; OS: *Overall Survival;* PFS: *Progression free survival*

Table 9. Metabolites with significant impact on OS (univariate and multivariate analysis).

	Univariate				Multivariate	
	Continuous		Median		Median	
	P	***FDR***	***P***	***FDR***	***P***	***HR***
Amino acids, peptides, and analogues						
Dimethyl-Arginine (symmetric)	*0.002*	*0.108*	*0.011*	*0.352*	*0.228*	*0.620*
Glu-Hyp	*0.033*	*0.399*	*X*	*X*	***0.011***	*0.393*
Glu-Lys/Ɛ-Glu-Lys 2	*X*	*X*	*0.016*	*0.365*	***0.004***	*0.353*
Pyroglutamine	*0.041*	*0.419*	*X*	*X*	*0.270*	*0.656*
Ser-Ala*	*X*	*X*	*0.037*	*0.436*	*0.694*	*0.870*
Suberylglycine	*0.022*	*0.399*	*X*	*X*	*0.222*	*0.651*
Thr-Gly*	*X*	*X*	*0.037*	*0.436*	*0.518*	*0.802*
Carbohydrates and carbohydrate conjugates						
PYRANOSE (glucose/altrose /galactose /talose)	*X*	*X*	*0.033*	*0.436*	*0.554*	*0.802*
Fatty Acyls						
Eicosapentaenoic acid	*0.023*	*0.399*	*0.045*	*0.436*	*0.596*	*0.809*
MG(20:0)	*0.0238*	*0.399*	*0.024*	*0.421*	***0.054***	*0.359*
N-palmitoyl glutamic acid*	*X*	*X*	*0.027*	*0.421*	***0.045***	*0.493*
3-hydroxy-5-octenoylcarnitine	*0.000*	*0.071*	*0.002*	*0.255*	***0.001***	*0.292*
3-Hydroxy-5-tetradecenoylcarnitine*	*X*	*X*	*0.027*	*0.421*	***0.045***	*0.493*
Linoleyl carnitine	*0.037*	*0.412*	*X*	*X*	*0.259*	*0.668*
Glycerophospholipids						
LPC (16:0)-OH	*X*	*X*	*X*	*X*	*0.650*	*0.853*
LPC (22:1)	*0.002*	*0.108*	*0.015*	*0.365*	***0.002***	*0.293*

	Univariate				Multivariate	
	Continuous		Median		Median	
	P	***FDR***	***P***	***FDR***	***P***	***HR***
Imidazoles						
Methylimidazole	*0.030*	*0.399*	*X*	*X*	*0.278*	*0.646*
Urocanate nicotinamide N-oxide	*0.048*	*0.443*	*0.010*	*0.352*	*0.071*	*0.573*
Indoles and derivatives						
5-Hydroxyindoleacetic acid	*X*	*X*	*X*	*X*	***0.041***	*0.471*
Lactones						
N-(4-Coumaroyl)-homoserine lactone	*0.004*	*0.124*	*0.004*	*0.255*	*0.098*	*0.514*
Phenols						
4-Methylcatechol	*0.031*	*0.399*	*X*	*X*	*0.529*	*0.789*
Purine nucleosides						
1-Methyladenosine	*0.000*	***0.017***	*0.004*	*0.255*	***0.006***	*0.348*
Sphingolipids						
SM (36:0)	*X*	*X*	*X*	*X*	*0.247*	*1.511*
Steroids and steroid derivatives						
Biliverdin	*X*	*X*	*X*	*X*	***0.019***	*0.417*
Cholestane-3,7,12,24,25-pentol	*0.026*	*0.399*	*X*	*X*	*0.258*	*0.663*
Cortisone acetate	*0.043*	*0.419*	*X*	*X*	*0.654*	*1.175*
Ecdysone 25-O-D-glucopyranoside	*0.025*	*0.399*	*X*	*X*	***0.051***	*2.039*

FDR: false discovery rate, OS: Overall Survival, PFS: Progression free survival

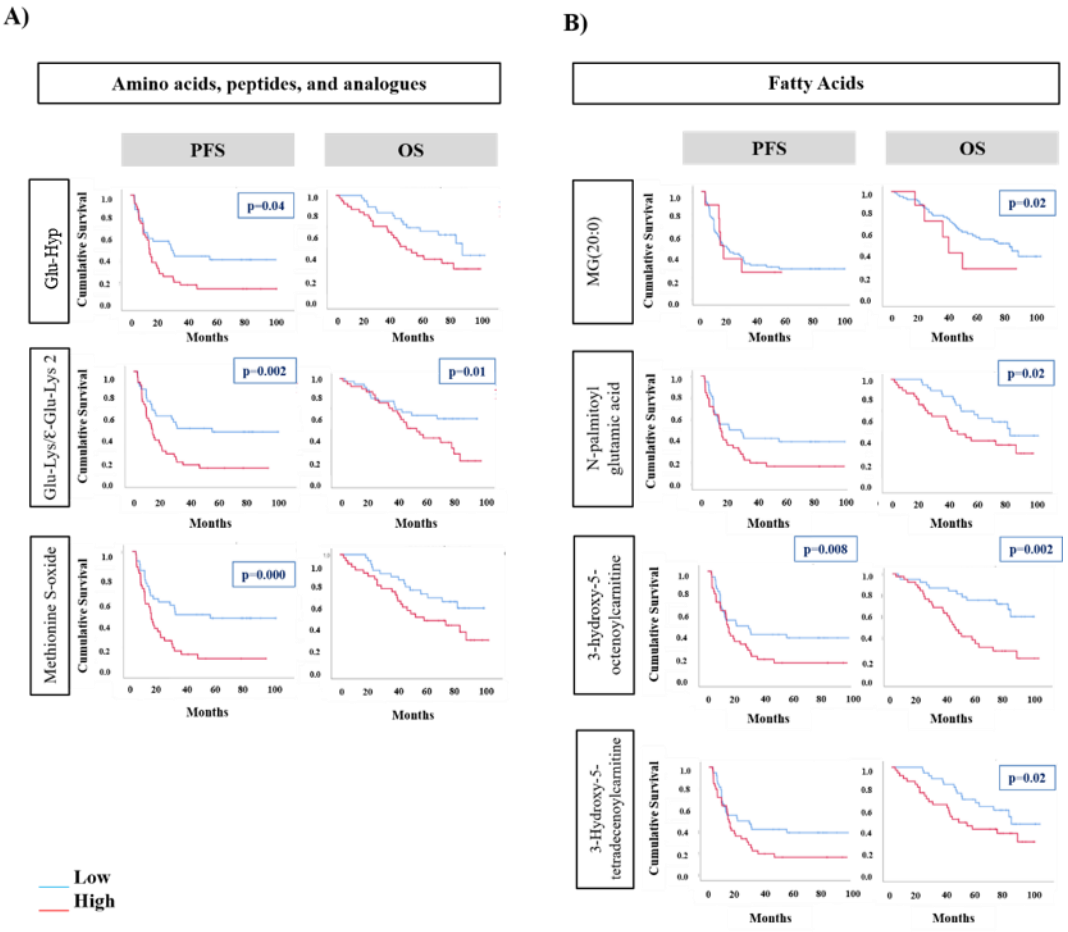
A)
Amino acids, peptides, and analogues
PFS
OS
Glu-Hyp
Glu-Lys/ε-Glu-Lys 2
Methionine S-oxide
Cumulative Survival
Months
p=0.04
p=0.002
p=0.01
p=0.000
Low
High
B)
Fatty Acids
PFS
OS
MG(20:0)
N-palmitoyl glutamic acid
3-hydroxy-5-octenoylcarnitine
3-Hydroxy-5-tetradecenoylcarnitine
p=0.02
p=0.02
p=0.008
p=0.002
p=0.02

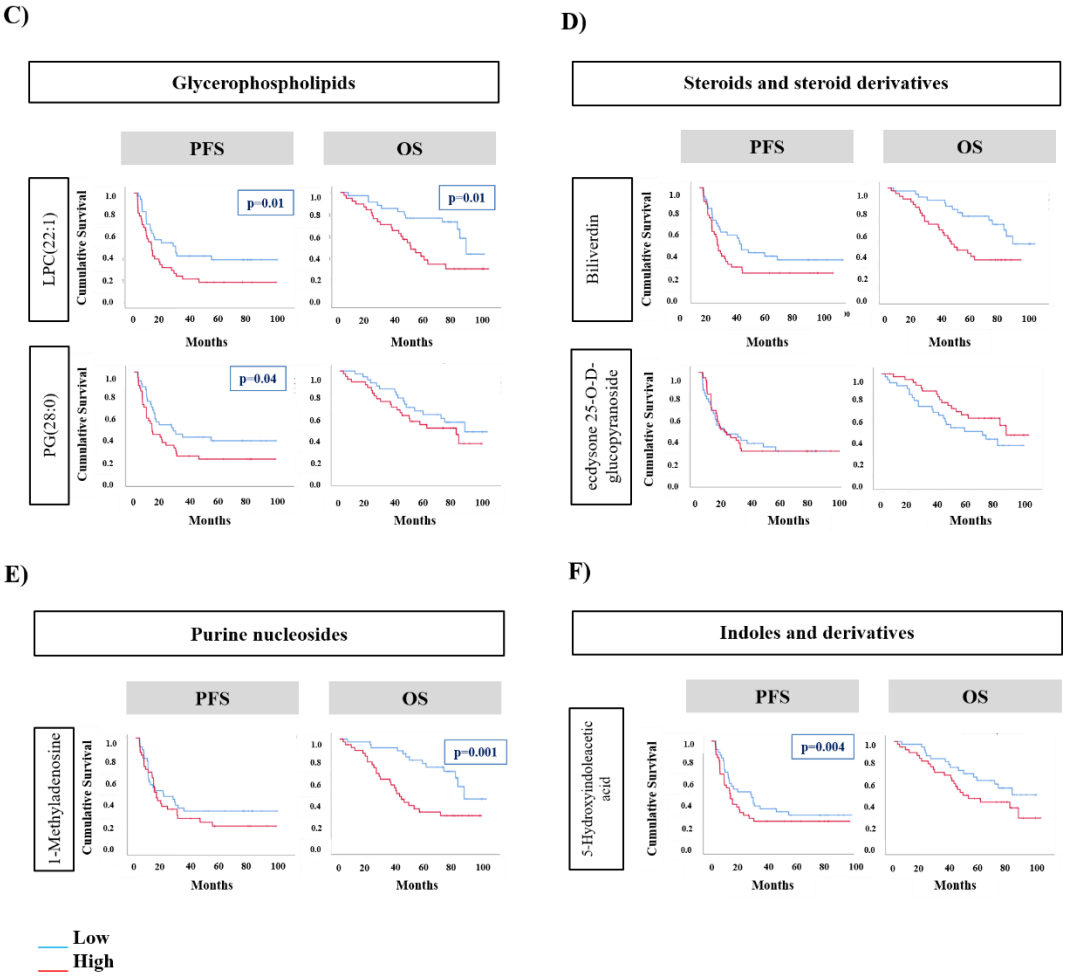

Figure 6. Kaplan-Meier survival curves of the 13 metabolites with an independent impact on patient's survival in terms of PFS and/or OS. The selected metabolites are grouped according to their biochemical nature: A) Amino acids, peptides and analogues (Glu-Hyp, Glu-Lys/Ɛ-Glu-Lys 2 and Methionine S-oxide); B) Fatty acids (MG (20:0), N-palmitoyl glutamic acid, 3-hydroxy-5-octenoylcarnitine and 3-hydroxy-5-tetradecenoylcarnitine); C) Glycerophospholipids (LPC (22:1) and PG (28:0)); D) Steroids and steroid derivatives (biliverdin and ecdysone 25-O-D-glucopyranoside); E) Purine nucleosides (1-methyladenosine and F) Indoles and derivatives (5-hydroxyindoleacetic acid); *P-values* are reported where significant at the corresponding univariant cox regression analysis.

5.4 PROGNOSTIC METABOLITES IDENTIFY NOVEL DYSREGULATED ONCOGENIC PATHWAYS IN NET PATIENTS.

We performed a functional analysis with the 34 prognostic metabolites to identify enriched signalling pathways in NET patients. Metabolite Set Enrichment Analysis (MSEA) showed several enriched molecular pathways in NETs. These pathways are related to alpha linolenic and linoleic acid, porphyrin, methionine and tryptophan metabolism (Figure 7A). Additionally, we performed a MSEA of the 13 metabolites with an independent impact on PFS and/or OS (Figure 7B) that showed two main enriched pathways related to porphyrin and tryptophan metabolism.

Metabolite Pathway Analysis (MPA) with all 34 prognostic metabolites showed that histidine metabolism, sphingolipid metabolism, porphyrin metabolism, biosynthesis of unsaturated fatty acids, glycerophospholipid metabolism and tryptophan metabolism were the most commonly dysregulated pathways in NET patients (Figure 8A). MPA performed with the 13 selected independent metabolites confirmed that methionine, porphyrin and tryptophan metabolisms were the most relevant dysregulated pathways in these patients (Figure 8B). The 5 metabolites with a significant impact on PFS were associated with methionine and tryptophan metabolism, whereas the 11 metabolites with a significant impact on OS were associated with porphyrin and tryptophan metabolism. Consistently, pathway analysis performed only with the 3 common metabolites with a significant impact on both PFS and OS evidenced a relevant dysregulation of tryptophan metabolism.

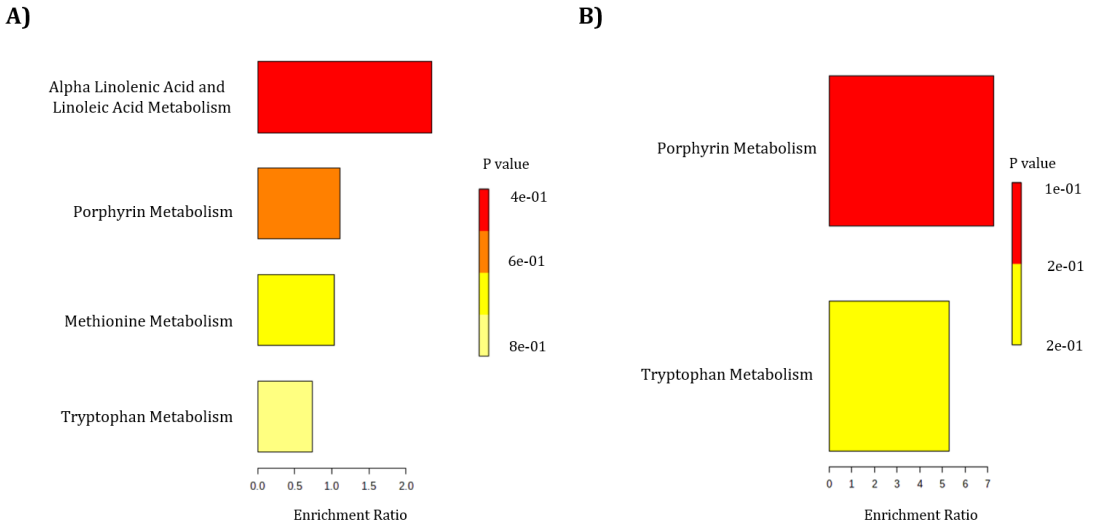

Figure 7. Metabolite Set Enrichment Analysis (MSEA) of selected plasma metabolites in patients with advanced NETs. A) MSEA of the 34 prognostic metabolites significantly associated with PFS and/or OS in univariate analysis, and B) MSEA of the 13 metabolites with an independent impact on PFS and/or OS in multivariate analysis. The x-axis represents the fold enrichment of each metabolite set and the bar colour indicates the raw *P-value*.

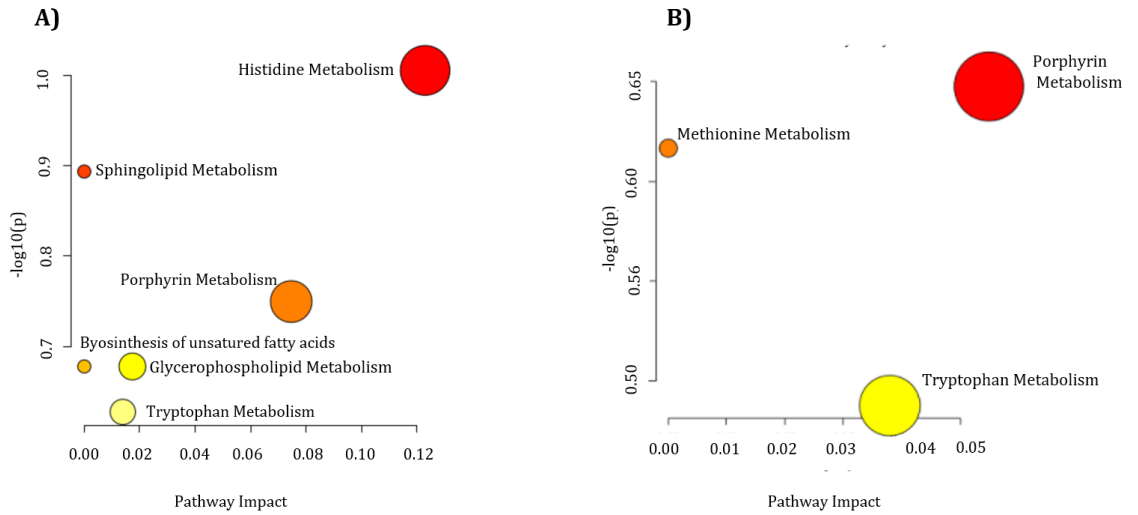

Figure 8. Metabolite Pathway Analysis (MPA) of selected plasma metabolites in patients with advanced NETs. A) MPA of the 34 prognostic metabolites significantly associated with PFS and/or OS in univariate analysis, and B) MPA of the 13 metabolites with an independent impact on PFS and/or OS in multivariate analysis. Metabolite Pathway Analysis (MPA) representing the significantly enriched pathways (*FDR < 0.05*) by availability of selected metabolites in plasma of NET patients. The x-axis indicates the impact of matched metabolites of our dataset on the pathway from the topology analysis. The -log $_{10}$ *(p-value)* is plotted in the y-axis and shows the pathway enrichment significance. Circle size represents the impact factor of matched metabolites in the pathway, and circle colour the pathway enrichment significance (*p-value*).

5.5 HEATMAP OF SELECTED METABOLITES AND IMPACT ON SURVIVAL

To identify metabolite profiles that define biological and prognostic subgroups of NET patients, we performed an unsupervised analysis of the 13 selected metabolites with an independent impact on PFS and/or OS. First, we performed the unsupervised heatmap cluster plot of the 5 metabolites with an independent impact on PFS which identified 2 distinct clusters, a smaller one (cluster 1) encompassing 26 NET patients and the other one (cluster 2) including the remaining 51 patients (Figure 9A, left side). These clusters did not seem related to classical clinical features such as primary tumor site, tumor function or grade as illustrated in Figure 9A. Remarkably, the identified clusters presented a significant impact on PFS, with a PFS rate at 1 year of 64.7% vs 38.5% for cluster 2 versus cluster 1 (HR:0.56, *p=0.045*) (Figure 9A, right side). Second, we performed an unsupervised heatmap cluster plot of the 11 metabolites with an independent impact on OS, that identified 4 different clusters: cluster 1 was the smallest subgroup with only 4 patients, cluster 2 encompassing 12 patients, cluster 3 included the majority of cases (n=52), and cluster 4 included the remaining 9 patients (Figure 9B, left side). No clear association was found between metabolic clusters and most relevant clinical features as depicted in Figure 9B. Cluster 4 was associated with an improved OS when compared with the other 3 clusters (Figure 9B, right side) of borderline statistical significance at univariate analysis (HR:0.14, *p=0.073*). OS rate at 5 years was 50.0%, 63.6%, 45.5% and 88.9% for clusters 1, 2, 3 and 4, respectively.

Finally, we performed an unsupervised heatmap of the 3 selected metabolites with an independent impact both on PFS and OS (Figure 10, upper side), that stratified patients in 3 prognostic groups (Figure 10). In terms of PFS, outcome was significantly different by metabolic cluster, with PFS rates at 1 year of 47.4%, 15.4% and 71.1% for clusters 1, 2 and 3, respectively (*p=0.003*). Regarding OS, cluster 3 was associated with the best prognosis, with OS rates at 5 years of 32.5%, 27.7% and 69.7% for clusters 1, 2 and 3, respectively (*p=0.003*). Multivariate analysis including age, gender, grade, functionality, primary tumor location, and time from randomization to study entry as covariables confirmed the metabolite clusters as a significant independent predictor of outcome both for PFS and OS (*p=0.012* and *p=0.007*, respectively) (Table 10).

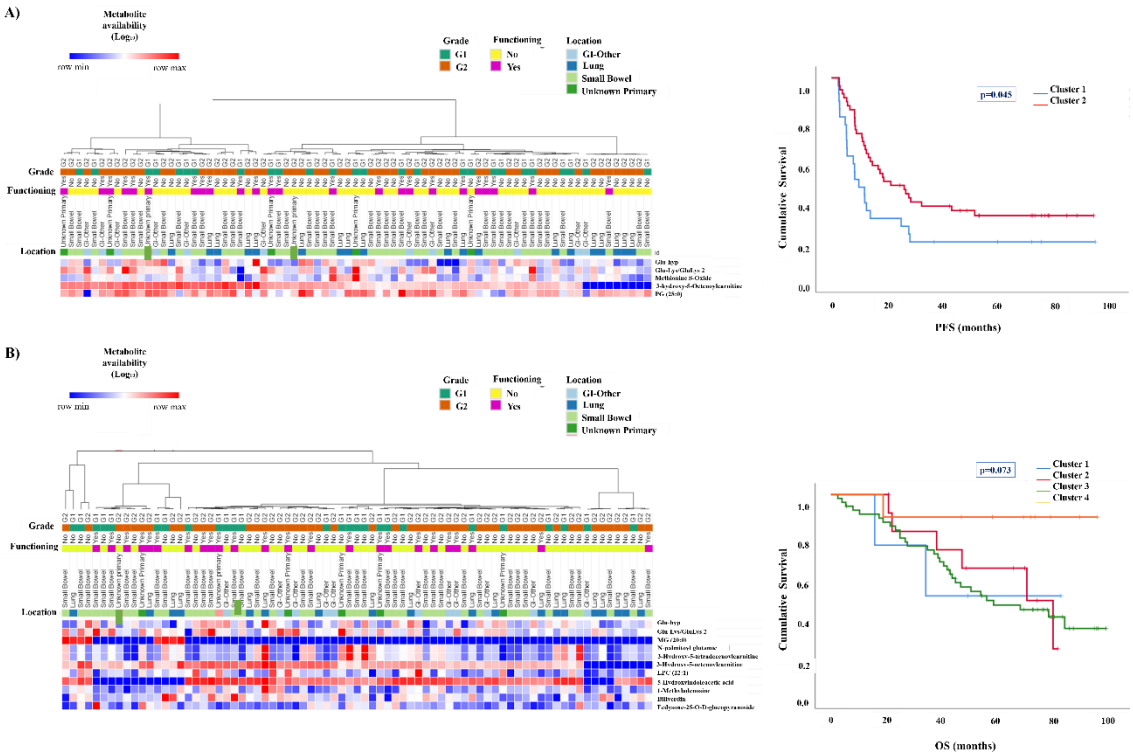

Figure 9. Heatmap of the the 5 selected metabolites with an independent impact on PFS A) and of the 11 selected metabolites with an independent impact on OS B) and their Kaplan-Meiers survival graphs. A) Unsupervised hierarchical heatmaps of the 5 metabolites with impact on PFS. All samples (n=77) are shown in columns and metabolites in rows. Hierarchical clustering was performed on rows and columns using One minus Pearson correlation metric and average as linkage method. Individual values are coded as colors, ranging from blue (row minimum) to red (row maximum). This heatmap showed two clusters with a significant impact on progression-free survival at the univariant analysis. B) Unsupervised hierarchical heatmaps of the 11 selected metabolites with impact on OS. All samples (n=77) are shown in columns and metabolites in rows. Hierarchical clustering was performed on rows and columns using One minus Pearson correlation metric and average as linkage method. Individual values were coded as colors, ranging from blue (row minimum) to red (row maximum). This heatmap showed four clusters, with the fourth cluster presenting the best OS. *P-values* are reported at the corresponding univariant cox regression analysis.

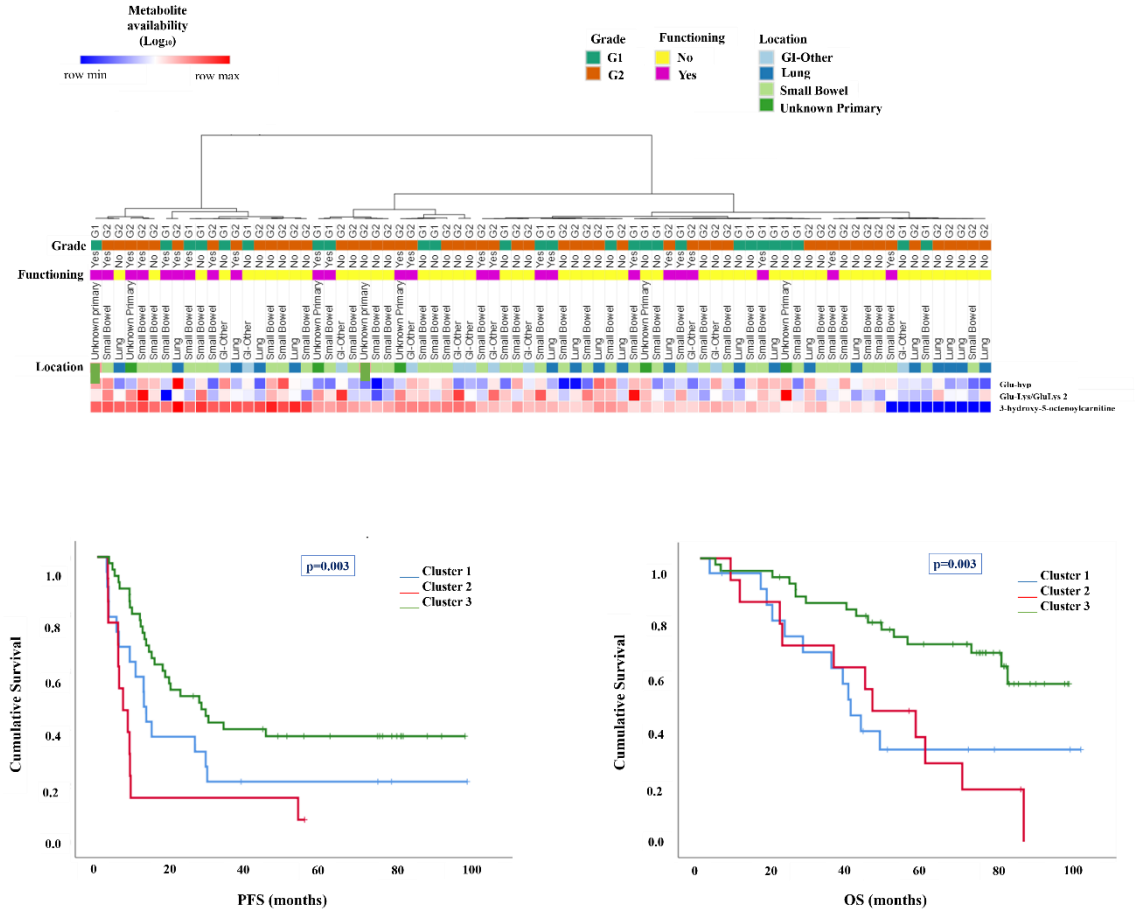

Figure 10. Heatmap of the 3 selected metabolites with an independent impact both on PFS and OS and their Kaplan-Meiers survival curves. Unsupervised hierarchical heatmap of the 3 metabolites with a significant impact on PFS and OS. All samples (n=77) are shown in columns and metabolites in rows. Hierarchical clustering was performed on rows and columns using One minus Pearson correlation metric and average as linkage method. Individual values are coded as colours, ranging from blue (row minimum) to red (row maximum). The three clusters clearly stratified patients in terms of PFS and OS, with cluster 3 representing the subgroup of patients with the best outcomes. *P-values* are reported at the corresponding univariant cox regression analysis.

Table 10. Multivariate analysis assessing the impact of the 3-metabolite cluster on PFS and OS.

	PFS		OS	
Feature	***HR***	***P***	***HR***	***P***
Metabolic Cluster (3 metabolites)		***0,012***		***0,007***
Cluster 3 "good prognosis"	*REF*	*--*	*REF*	--
Cluster 1 "intermediate prognosis"	*1,559*	*0,201*	*2,901*	***0,001***
Cluster 2 "poor prognosis"	*3,720*	***0,001***	*3,960*	***0,021***
Gender (male vs female)	*0,639*	*0,146*	*0,270*	***0,002***
Age	*1,011*	*0,464*	*1,017*	*0,295*
Primary tumor location		*0,311*		*0,480*
Small bowel	*REF*	--	*REF*	--
GI other	*1,033*	*0,943*	*1,749*	*0,253*
Lung	*1,425*	*0,366*	*1,065*	*0,906*
Unknown primary	*1,583*	*0,377*	*0,689*	*0,655*
Other	*4,738*	*0,056*	*3,549*	*0,139*
Grade (G2 vs G1)	*1,036*	*0,914*	*0,858*	*0,701*
Functioning (no vs yes)	*1,216*	*0,575*	*1,096*	*0,829*
Time from randomization to study entry	*1,007*	***0,041***	*0,999*	*0,857*

G1: Grade 1; G2: Grade 2; OS: Overall Survival, PFS: Progression free survival; REF: reference.

6. DISCUSSION

DISCUSSION

Neuroendocrine neoplasms (NENs) comprise a heterogeneous family of rare tumours with steadily increasing incidence and prevalence (1–3). NENs display a wide anatomic distribution and a great biological heterogeneity, facts that have complicated their study and, consequently, their clinical management. Although relevant advances have been recently achieved in the molecular characterization of NENs, metabolomics remains largely unexplored. Metabolic flexibility is one of the key hallmarks of cancer and metabolites are the final products of this adaptation (270). Metabolites thus reflect the aberrant changes in the genomic, transcriptomic and proteomic variability of tumors and provide useful biological information on cancer initiation and progression (331–333). Moreover, the metabolomic profile can be easily performed in readily accessible biological samples (plasma, urine), making metabolic profiling of cancer patients a promising tool to characterize the tumor phenotype and identify novel biomarkers of potential clinical use. Systems medicine approaches integrating high-throughput "-omic" technologies into diagnostic platforms have indeed enabled the detailed analysis of metabolic networks (known as metabolomics) in several cancers of high incidence, prevalence and mortality (334–337), but these do not include neuroendocrine neoplasms (NENs).

In this context, the overall objective of our work was to perform a comprehensive metabolic profiling of G1-2 extra-pancreatic NETs to better understand metabolic dysregulation in these tumors, and identify novel prognostic biomarkers of clinical use, as well as to functionally characterize molecular pathways with a significant impact on patient's survival. To this aim, we analyzed the metabolomic fingerprint by means of a multiplatform untargeted approach (LC-MS, GC-MS and CE-MS) in plasma samples of 77 advanced extra-pancreatic NETs and of 68 non-oncologic individuals (control cohort), matched per age, gender and body mass index (BMI). The integrated analysis of metabolic data acquired by the different analytical platforms enabled the identification of 155 compounds with differential availability in plasma of NETs compared with controls. We then analyzed the prognostic value of these 155 metabolites and identified 34 metabolites significantly associated with

patients' outcome (PFS and/or OS). Functional analysis performed with the 34 prognostic metabolites by MSEA revealed enriched pathways involved alpha linolenic and linoleic acid, porphyrin, methionine and tryptophan metabolism. Moreover, MPA confirmed porphyrin and tryptophan metabolism as relevant dysregulated metabolic pathways, and also identified the biosynthesis of unsaturated fatty acids, and histidine, sphingolipid and glycerophospholipid metabolism as additional pathways implicated in NET prognosis.

This is to our knowledge the most comprehensive metabolic profiling study performed to date in NETs. The results of this work demonstrate that NET patients have a distinct metabolomic profile that reflects the molecular dysregulation of these neoplasms and provides new relevant information on disease biology of potential clinical application. Indeed, we have identified a set of 34 metabolites that may be used as prognostic biomarkers to improve patient stratification beyond classical clinical and pathological prognostic factors, and pathway analysis of these set of prognostic metabolites have enabled the identification of dysregulated pathways involved that may facilitate the development of new therapeutic strategies in the future.

In particular, 10 of these 34 metabolites are related to an essential pathway involved in the metabolic shift of cancer cells, the tricarboxylic acid cycle (TCA cycle): 3 belong to the amino acids, peptides and analogues class (Glu-Hyp, Glu-Lys/Ɛ-Glu-Lys and Glu-Lys/Ɛ-Glu-Lys 2), 1 belongs to the carbohydrates and carbohydrate conjugates group (pyranose (glucose/altrose/galactose/talose)) and 6 to the fatty acids class (eicosapentaenoic acid, MG(20:0), N-palmitoyl glutamic acid, 3-hydroxy-5-octenoylcarnitine, 3-hydroxy-5-tetradecenoylcarnitine, and linoleyl carnitine). Several studies support that the TCA cycle plays an important role in tumorigenesis in different tumor types by sustaining mitochondrial metabolism (338,339). Cancer cells can adapt to the availability of various fuels, as well as to microenvironmental conditions like hypoxia and acidosis, thanks to the metabolic versatility provided by this mitochondrial input, that confers the cancer cell a survival advantage (340). Consistent with this, in our study higher levels of glutamine, glucose and fatty acids, which represent the main fuel of the TCA cycle, are associated with decreased survival. The relevance of the TCA cycle

dysregulation in NETs is also supported by a previous study by Imperiale et al. (304) In this study, the metabolic profile of 46 small intestinal NET primary tumors and 18 liver NET metastasis assessed by 1H-NMR spectroscopy, as compared to 30 normal small intestine and liver samples, suggested alterations of different metabolites related to the TCA cycle in NETs, such as a higher abundance of succinate, and an up-regulation of choline-containing compound metabolism, suggesting either accumulation or excess depletion of these metabolites for aberrant cell membrane turnover. In line with these observations, it is well known the importance of TCA cycle alterations in the tumorigenesis of PHEOs and PGLs. SDH catalyse sequential steps in the TCA cycle (341) and SDH mutations are associated with hereditary predisposition syndromes that increase the risk to develop this subgroup of rare NETs. Evidence from several studies support the utility of metabolomic profiling in this setting, providing relevant information about functionality of the SDH complex and other Krebs cycle enzymes also involved in the pathogenesis of these tumors, such as fumarate hydratase (FH) and isocitrate dehydrogenase (IDH), through measurements of precursor and product metabolites involved in the TCA cycle (299,300,302). Moreover, authors propose incorporation of metabolome data into the PPGLs diagnostics algorithm to guide genetic testing and variant interpretation and to help identify rare cases with pathogenic variants in FH and IDHx.

Our study also demonstrated a characteristic lipidome in NETs, mainly represented by the enrichment of glycerophospholipids (5 of 34 prognostic metabolites), fatty acids (6 of the 34 selected metabolites) and steroids/steroid derivatives (4 of the 34). More specifically, oxidized lysoglycerophospholipids (oxLPCs) were found with increased abundances in NETs indicating a strong oxidative stress in these tumors (329). Increasing evidence is arising supporting the role of oxidized lipids in cancer metabolism, paving the way for new and exciting therapeutic opportunities, together with a more profound comprehension of the metabolic wiring of cancer cells (342–344). However, further knowledge of the dependence of cancer cells on oxidized lipids will be necessary to refine rational approaches to develop new therapeutic strategies that target lipid catabolism.

In addition, some of the 34 selected metabolites may contribute to the angiogenesis switch that is another hallmark of cancer (345). Targeting angiogenesis has been successfully explored as a therapeutic strategy in a wide spectrum of solid tumors, including NETs. NETs are typically vascularized tumors and angiogenesis dysregulation play an essential role in the development and progression of these tumors (346). In our study, greater arginine's abundance correlated with a worse survival. Arginine is the main source of nitric oxide, which is deeply involved in the regulation of angiogenesis, cancer initiation and progression, but also restricts cancer proliferation and invasion, and contributes to the anti-tumor immune response (347). Therefore, and consistent with the results of our study, the regulation of nitric oxide via the synthesis and availability of its precursor, arginine, is strongly linked to cancer biology. Moreover, biliverdin also contribute to angiogenesis through the upregulation of VEGFA, VEGFC, IL-1β and IL-8 (348,349). In our series, a greater abundance of biliverdin was associated with a worse prognosis. Overall, these findings further support the relevant role that angiogenesis plays in the pathogenesis of NETs.

To further assess the independent prognostic value of the 34 identified metabolites, we performed a multivariate analysis to adjust for other potentially confounding factors, including clinicopathological variables of known prognostic value (age, sex, tumor grade, primary tumor location, time from randomization to study entry) and other variables potentially associated with metabolite abundance (BMI, sex, hormonal syndrome and concomitant medication). Thirteen of 34 metabolites retained statistical significance in the multivariate analysis ($p<0.05$), 5 had an independent impact on PFS (Glu-Hyp ($p=0.018$), Glu-Lys/Ɛ-Glu-Lys 2 ($p=0.006$), methionine S-oxide (p=0.012), 3-hydroxy-5-octenoylcarnitine ($p=0.018$) and PG (28:0) ($p=0.050$)), and 11 were independently associated with OS (Glu-Hyp ($p=0.011$), Glu-Lys/Ɛ-Glu-Lys 2 ($p=0.004$), MG(20:0) ($p=0.054$), N-palmitoyl glutamic acid ($p=0.045$), 3-hydroxy-5-octenoylcarnitine ($p=0.001$), 3-hydroxy-5-tetradecenoylcarnitine ($p=0.045$), LPC (22:1) ($p=0.002$), 5- hydroxyindoleacetic acid ($p=0.041$), 1-methyladenosine ($p=0,006$), biliverdin ($p=0.019$) and ecdysone 25-O-D-glucopyranoside ($p=0.051$)). Three of them, Glu-Hyp, Glu-Lys/Ɛ-Glu-Lys 2 and 3-hydroxy-5-octenoylcarnitine, had a significant impact both on PFS and OS.

We then performed two exploratory unsupervised clustering analyses, one with the 5 metabolites associated with PFS and another one with the 11 metabolites associated with OS, that stratified NET patients into 2 and 4 clusters, respectively. PFS was significantly better in cluster 2 versus cluster 1 (PFS at 1 year: 64.7% vs 38.5%, HR:0.56, *p=0.045*). Metabolite clusters also identified a subgroup of patients (cluster 4) that was associated with improved OS when compared with the other 3 clusters that was of borderline statistical significance (OS rate at 5 years: 50.0%, 63.6%, 45.5% and 88.9% for clusters 1, 2, 3 and 4, respectively, HR:0.14, *p=0.073*).

Finally, we performed an unsupervised clustering of the 3 common metabolites with an independent impact on both PFS and OS, that stratified patients in 3 distinct prognostic groups: 1) Cluster 3 was associated with **good prognosis** (PFS rate at 1 year of 71.1% and OS rate at 5 years of 69.7%); 2) Cluster 1 was associated with **intermediate prognosis** (PFS rate at 1 year of 47.4% and OS rate at 5 years of 32.5%), and 3) Cluster 2 was associated with **poor prognosis** (PFS rate at 1 year of 15.4% and OS rate at 5 years of 27.7%) (*p=0.003* for PFS and OS). Multivariate analysis confirmed metabolic clusters were independently associated with both PFS (p=0.012) and OS (p=0.007).

MSEA and MPA of the 13-metabolite signature identified methionine, porphyrin and tryptophan metabolism as the most relevant dysregulated pathways in these patients. PFS metabolites (N=5) were associated with methionine and tryptophan metabolism, and OS metabolites (N=11) were associated with porphyrin and tryptophan metabolism. Thus, tryptophan metabolism was common to both clinical outcomes, which was confirmed by pathway analysis performed only with the 3 metabolites with a significant impact on both PFS and OS.

Porphyrin metabolism is a key dysregulated pathway in cancer (350,351). An aberrant porphyrin metabolism has been demonstrated in several tumor types, such as hepatocellular carcinoma (352), acute lymphoblastic leukaemia, non-Hodgkin's lymphoma and Hodgkin's disease (353). Porphyrin-induced oxidative stress is thought to be the major mechanism of porphyrin-mediated cell damage, primarily caused by reactive oxygen species generated through type I/II photosensitized reactions of porphyrins (354). Furthermore, porphyrin accumulation has been

reported to cause significant lipid peroxidation (355) thereby compromising cell survival. Porphyrins have also demonstrated to cause a cellular energy imbalance by aggregating key glycolytic enzymes, leading to mitochondrial dysfunction with a deep effect on cell growth (356). Moreoever, some recent evidence has suggested an antiproliferative effect of porphyrins in NETs (357,358). Indeed, cationic porphyrins decreased cell viability and induced apoptosis in human small intestinal NET and medullary thyroid carcinoma cell lines (36-37).

In our study, some of the selected metabolites, Glu-Hyp (glutamyl-hydroxyproline) and biliverdin, are associated with porphyrin metabolism. The first one, Glu-Hyp, which is involved in the porphyrin biosynthesis pathway, is a source of glutamate to erythrocytes and it is important for the amino acid glutathione synthesis (359). In our series, a higher abundance of this metabolite was associated with a worse survival. The second one, biliverdin, is a heme derivative that is converted to the powerful antioxidant molecule bilirubin by the biliverdin reductase-A (BVR-A), the main isoform of BVR (a dual-specificity kinase upstream activator of the insulin/insulin growth factor-1 (IGF-1) and mitogen-activated protein kinase (MAPK) signalling pathways). Up-regulation of BVR-A occurs as an adaptive response to oxidative stress and inflammation (360). Therefore, BVR-A has been hypothesized to have a cytoprotective activity (361). The conversion of biliverdin to bilirubin by BVR has been demonstrated to determine cell protection due to direct and indirect antioxidant actions of bilirubin (362). In our study, high levels of biliverdin resulted associated with worse survival, indirectly confirming a protective role for BVR. Therefore, further studies are needed to determine the relevance and significance of porphyrin metabolism dysregulation in NET patients.

A second dysregulated pathway which emerged from our MPA and MSEA analyses was methionine metabolism. Methionine is an essential amino acid that plays a key role in mammalian metabolism. Besides its essential role in protein synthesis, methionine is also involved in epigenetic regulation (DNA methylation), nucleotide biosynthesis, cell detoxification (glutathione), membrane lipid homeostasis, and several other signalling pathways controlled by methylation. The role of this pathway in the metabolic shift of cancer cells is well established. In addition to the Warburg effect, other metabolic changes occur in cancer cells to maintain their

long-term survival, and the dependence on methionine is one of them, known as the Hoffman effect. Cancer cells are not able to proliferate when methionine is replaced with its metabolic precursor, homocysteine, as a consequence of an increased demand for methionine-derived metabolites. However, tumor cells are able to synthesize methionine from homocysteine, suggesting that their dependence on exogenous methionine reflects a general need for altered metabolic flow through methionine-related pathways (363). Interesting preclinical data from breast cancer described that methionine sulfoxide reductase A (MsrA), enzyme responsible for reversing the oxidation of methionine, functioning as ROS scavenger, was down-regulated in neoplastic breast cells (364). The reduction of MsrA levels results in an increase in cell proliferation and extracellular matrix degradation, leading to a more aggressive cellular phenotype, both *in vivo* and *in vitro*. Authors explain that the underlying molecular mechanisms involve increased ROS levels, resulting in a reduction of phosphatase and tensin homolog deleted on chromosome ten (PTEN) protein, and an activation of the phosphoinositide 3-kinase pathway (PI3K). They also observed that MsrA down-regulation induced VEGF up-regulation, enhancing thereby tumoral angiogenesis. Consistent with these findings, we have found that higher levels of methionine S-oxide correlated with a poor outcome of NET patients, suggesting that the regulation of methionine availability could be a useful strategy in limiting cancer growth (363). Methionine S-oxide is the oxide derivative of methionine that is a biomarker of many relevant biological processes such as oxidative stress (365), inflammation (366), necrosis (367) and hypoxia (368), and has been implicated in a wide spectrum of human diseases including cancer (369–372) .

The third main dysregulated pathway identified in our study was the tryptophan metabolism. Tryptophan catabolism has been firmly established as a powerful mechanism of innate and adaptive immune tolerance, thereby maintaining immune homeostasis and preventing autoimmunity. Dysregulation of this pathway has been involved in different types of cancers (373,374), including NETs. The most relevant identified mechanism is related to its roll in tumor immune evasion (375,376). The enzyme indoleamine-2,3-dioxygenase (IDO), expressed in tumor cells or antigen-presenting cells, which has a fundamental role in tryptophan catabolism, has been identified as an essential suppressor of antitumor immune responses through

tryptophan depletion and accumulation of immunosuppressive tryptophan catabolites. This has been documented in several types of gastrointestinal malignancies such as colorectal, gastric, pancreatic, esophageal, and GI stromal tumors (377), bladder cancer (378), clear cell renal cell carcinoma (379) and gynaecological cancers (380).

More specifically, tryptophan metabolism plays a crucial role in NETs. Serotonin (5-hydroxytryptamine, 5-HT), a biogenic monoamine, is the most relevant metabolically active substance in functioning NETs and is produced from the essential amino acid tryptophan (381). Excess tumor production and secretion of serotonin causes the carcinoid syndrome (CS), that is characterized by flushing and diarrhea, and less commonly carcinoid heart disease, bronchoconstriction and pellagra. Approximately 20% of NET patients present CS, most commonly small intestinal NETs, with a negative impact on patients' outcomes and quality of life (13). In patients with NET and CS, the metabolism of tryptophan is altered, with approx. 60% of all dietary tryptophan being consumed by tumor cells for serotonin synthesis (382). Tryptophan depletion may cause pellagra due to niacin deficiency in severe cases.

5-Hydroxyindoleacetic acid, also known as 5-hydroxyindole-3-acetate or 5-HIAA, is the primary metabolite of serotonin degradation in the liver. Notably, the urine quantitation of 5-HIAA is the most sensitive and specific test for the diagnosis of CS (13,20). The prognostic role of this biomarker has been extensively evaluated (383). Higher 5-HIAA doubling time was associated with a higher risk of progression and mortality in NET patients (384). Other studies have also confirmed the independent negative prognostic value of 5-HIAA in this setting (385). Consistent with the existing literature data, in our study higher levels of 5-HIAA were associated with a worse prognosis of NET patients. Moreover, higher values of MG (20:0), that has been shown to induce serotonin secretion in preclinical models (386), were also associated with a worse prognosis in our series.

Interestingly, recent data have linked carnitine and tryptophan metabolism (387). Tryptophan degradation enhances carnitine palmitoyltransferase I activity and fatty acid oxidation, and also exerts fatty acid-dependent effects in human alloreactive CD4+ T-cells. L-carnitine is an essential metabolite, critical for the bidirectional

transport of long-chain fatty acids and the acyl coenzyme A between the cytosol and the mitochondria, which has been considered a bottleneck in the metabolism control of cancer cells (388,389). Recent reports suggest that the carnitine system is essential for the metabolic adaptation of cancer cells, which obtain energy from beta-oxidation of lipids. Thus, low levels of carnitine in plasma of NET patients may be related to an active carnitine system in tumor mitochondria and the upregulation of beta-oxidation pathways, a process which results in the esterification of L-carnitine to form acylcarnitine derivatives. Additional functions of the carnitine system, besides its essential role in the mitochondrial metabolism of fatty acids, also includes the removal of excess acyl groups from the body and the modulation of coenzyme A homeostasis. Acylcarnitines are therefore not only by-products of the enzymatic carnitine transfer system, but also provide indirect evidence of altered mitochondrial metabolism. In our study, greater abundance of both 3-hydroxy-5-tetradecenoylcarnitine and 3-hydroxy-5-octenoylcarnitine, an O-acylcarnitine, were associated with a worse prognosis. Our data, in agreement with the existing literature, suggest that NET tumor cells not only utilize the precursors of carnitine biosynthesis but also increase carnitine expenditure, producing increased levels of these acylcarnitine derivatives.

One of the strengths of our study is that it was performed in plasma samples of a homogeneous population of 77 patients with G1-2 advanced extra-pancreatic NETs, uniformly and prospectively collected and analyzed. Moreover, identification of some metabolites (arginine, glutamine, phenylalanine, among others) across more than one analytical platform, and their validation through a target analysis with a different analytical platform in the same cohort (330) significantly increases the confidence of metabolite identification. Furthermore, the robust statistical analysis performed allowed the reliable identification of 13 metabolites with a significant impact on PFS and/or OS, independent of other well stablished clinical and pathological prognostic factors, thereby enabling further stratification of patients in 3 distinct prognostic groups to further assist physicians in clinical decisions. However, the results of our study should be further investigated in an independent NET patient cohort to validate our results. In addition, metabolomic profiling of patients with exocrine tumors of similar tissue origin (lung and gastrointestinal carcinomas) and also of patients with NETs of

other primary sites (i.e. pancreatic NETs) would also help validate the described metabolic prognostic signature, and confirm its potential prognostic value for advanced low-grade NETs. Moreover, complementary -omic approaches, such as exome, transcriptome or methylome tumor profiling of these patients are needed to further understand the underlying mechanisms involved in metabolic dysregulation in NETs. In particular, the metabolomic profile could be combined with complementary analytical approaches in plasma, such as cell-free nucleic acids profiling, that might be particularly useful for early diagnostics and patient stratification for personalized clinical management. Plasma -omic profiling has the additional advantage of providing a dynamic characterization of disease biology, which could be eventually utilized, beyond accompanying diagnostics, for targeted prevention or screening, individualized treatment strategies, therapeutic monitoring and prediction of patient´s outcome.

7. CONCLUSIONS

CONCLUSIONS

1. A comprehensive plasma metabolomic profiling was performed in a prospective cohort of 77 patients with advanced G1-2 extra-pancreatic NETs (study cohort) and 68 non-cancer individuals (controls) through a multiplatform LC-MS, GC-MS and CE-MS untargeted metabolomic approach. The integration of metabolic data acquired by different analytical platforms resulted in 155 identified metabolites with a differential availability in NET patients ($p<0.05$), when compared to non-cancer individuals.

2. Among the 155 differential compounds identified, 34 metabolites were significantly associated with PFS (16) and/or OS (27). Multivariate analysis confirmed 13 of these metabolites were significantly associated with PFS (5) and/or OS (11) ($p<0.05$), independent from other known prognostic or confounding factors such as age, gender, tumor grade, primary tumor location, time from diagnosis to study entry, BMI, tumor functionality and concomitant medication.

3. The unsupervised clustering analysis of the 3 metabolites with an independent impact on both PFS and OS (Glu-Hyp, Glu-Lys/Ɛ-Glu-Lys 2 and 3-hydroxy-5-octenoylcarnitine) revealed 3 clusters that stratified patients in 3 distinct prognostic groups: 1) Cluster 3 was associated with *good prognosis* (PFS rate at 1 year of 71.1% and OS rate at 5 years of 69.7%); 2) Cluster 1 was associated with *intermediate prognosis* (PFS rate at 1 year of 47.4% and OS rate at 5 years of 32.5%), and 3) Cluster 2 was associated with *poor prognosis* (PFS rate at 1 year of 15.4% and OS rate at 5 years of 27.7%) ($p=0.003$ for PFS and OS). Multivariate analysis confirmed metabolic clusters were independently associated with both PFS (p=0.012) and OS (p=0.007).

4. Metabolite Set Enrichment Analysis (MSEA) and Metabolite Pathway Analysis (MPA) of the 13-metabolite signature identified methionine, porphyrin and tryptophan metabolism as the most relevant dysregulated pathways associated with the prognosis of NET patients.

5. The results of our study demonstrate that NET patients have a distinct metabolomic profile that provides new relevant information on disease biology of potential clinical application. Indeed, we have identified a metabolomic signature that improves the prognostic stratification of patients beyond classical prognostic factors for clinical decisions. In addition, new enriched metabolic pathways identified may open innovative avenues of clinical research that may foster the development of new therapeutic strategies. Nevertheless, further prospective studies are needed to confirm our results and validate these encouraging data.

8. REFERENCES

REFERENCES

1. Dasari A, Shen C, Halperin D, Zhao B, Zhou S, Xu Y, et al. Trends in the Incidence, Prevalence, and Survival Outcomes in Patients With Neuroendocrine Tumors in the United States. JAMA Oncol. 2017 Oct 1;3(10):1335–42.

2. Garcia-Carbonero R, Capdevila J, Crespo-Herrero G, Díaz-Pérez JA, Martínez del Prado MP, Alonso Orduña V, et al. Incidence, patterns of care and prognostic factors for outcome of gastroenteropancreatic neuroendocrine tumors (GEP-NETs): results from the National Cancer Registry of Spain (RGETNE). Ann Oncol. 2010 Sep;21(9):1794–803.

3. Yao JC, Hassan M, Phan A, Dagohoy C, Leary C, Mares JE, et al. One hundred years after 'carcinoid': epidemiology of and prognostic factors for neuroendocrine tumors in 35,825 cases in the United States. J Clin Oncol Off J Am Soc Clin Oncol. 2008 Jun 20;26(18):3063–72.

4. Toni R. The neuroendocrine system: organization and homeostatic role. J Endocrinol Invest. 2004;27(6 Suppl):35–47.

5. Montuenga LM, Guembe L, Burrell MA, Bodegas ME, Calvo A, Sola JJ, et al. The diffuse endocrine system: from embryogenesis to carcinogenesis. Prog Histochem Cytochem. 2003;38(2):155–272.

6. Tischler AS. The dispersed neuroendocrine cells: the structure, function, regulation and effects of xenobiotics on this system. Toxicol Pathol. 1989;17(2):307–16.

7. Rindi G, Klimstra DS, Abedi-Ardekani B, Asa SL, Bosman FT, Brambilla E, et al. A common classification framework for neuroendocrine neoplasms: an International Agency for Research on Cancer (IARC) and World Health Organization (WHO) expert consensus proposal. Mod Pathol Off J U S Can Acad Pathol Inc. 2018 Dec;31(12):1770–86.

8. Shia J, Tang LH, Weiser MR, Brenner B, Adsay NV, Stelow EB, et al. Is nonsmall cell type high-grade neuroendocrine carcinoma of the tubular gastrointestinal tract a distinct disease entity? Am J Surg Pathol. 2008 May;32(5):719–31.

9. Strosberg JR, Coppola D, Klimstra DS, Phan AT, Kulke MH, Wiseman GA, et al. The NANETS consensus guidelines for the diagnosis and management of poorly differentiated (high-grade) extrapulmonary neuroendocrine carcinomas. Pancreas. 2010 Aug;39(6):799–800.

10. Uccella S, La Rosa S, Metovic J, Marchiori D, Scoazec J-Y, Volante M, et al. Genomics of High-Grade Neuroendocrine Neoplasms: Well-Differentiated Neuroendocrine Tumor with High-Grade Features (G3 NET) and Neuroendocrine Carcinomas (NEC) of Various Anatomic Sites. Endocr Pathol. 2021 Mar;32(1):192–210.

11. Travis WD, Brambilla E, Burke AP, Marx A, Nicholson AG. Introduction to The 2015 World Health Organization Classification of Tumors of the Lung, Pleura,

Thymus, and Heart. J Thorac Oncol Off Publ Int Assoc Study Lung Cancer. 2015 Sep;10(9):1240–2.

12. Chen L, Zhou Z, Chen J. [Interpretation and evaluation of the American Joint committee on Cancer (AJCC) 8th Edition Staging System for patients with gastroenteropancreatic neuroendocrine tumors]. Zhonghua Wei Chang Wai Ke Za Zhi Chin J Gastrointest Surg. 2017 Sep 25;20(9):972–6.

13. Ito T, Lee L, Jensen RT. Carcinoid-syndrome: recent advances, current status and controversies. Curr Opin Endocrinol Diabetes Obes. 2018 Feb;25(1):22–35.

14. Kidd M, Modlin IM, Bodei L, Drozdov I. Decoding the Molecular and Mutational Ambiguities of Gastroenteropancreatic Neuroendocrine Neoplasm Pathobiology. Cell Mol Gastroenterol Hepatol. 2015 Mar;1(2):131–53.

15. Kaltsas GA, Besser GM, Grossman AB. The diagnosis and medical management of advanced neuroendocrine tumors. Endocr Rev. 2004 Jun;25(3):458–511.

16. Pavel M, Öberg K, Falconi M, Krenning EP, Sundin A, Perren A, et al. Gastroenteropancreatic neuroendocrine neoplasms: ESMO Clinical Practice Guidelines for diagnosis, treatment and follow-up. Ann Oncol Off J Eur Soc Med Oncol. 2020 Jul;31(7):844–60.

17. Auernhammer CJ, Spitzweg C, Angele MK, Boeck S, Grossman A, Nölting S, et al. Advanced neuroendocrine tumours of the small intestine and pancreas: clinical developments, controversies, and future strategies. Lancet Diabetes Endocrinol. 2018 May;6(5):404–15.

18. Basuroy R, Bouvier C, Ramage JK, Sissons M, Srirajaskanthan R. Delays and routes to diagnosis of neuroendocrine tumours. BMC Cancer. 2018 Nov 16;18(1):1122.

19. Vinik AI, Chaya C. Clinical Presentation and Diagnosis of Neuroendocrine Tumors. Hematol Oncol Clin North Am. 2016 Feb;30(1):21–48.

20. Rubin de Celis Ferrari AC, Glasberg J, Riechelmann RP. Carcinoid syndrome: update on the pathophysiology and treatment. Clin Sao Paulo Braz. 2018 Aug 20;73(suppl 1):e490s.

21. Davar J, Connolly HM, Caplin ME, Pavel M, Zacks J, Bhattacharyya S, et al. Diagnosing and Managing Carcinoid Heart Disease in Patients With Neuroendocrine Tumors: An Expert Statement. J Am Coll Cardiol. 2017 Mar 14;69(10):1288–304.

22. Modlin IM, Shapiro MD, Kidd M. Carcinoid tumors and fibrosis: an association with no explanation. Am J Gastroenterol. 2004 Dec;99(12):2466–78.

23. Ito T, Igarashi H, Jensen RT. Pancreatic neuroendocrine tumors: clinical features, diagnosis and medical treatment: advances. Best Pract Res Clin Gastroenterol. 2012 Dec;26(6):737–53.

24. Dasari A, Mehta K, Byers LA, Sorbye H, Yao JC. Comparative study of lung and extrapulmonary poorly differentiated neuroendocrine carcinomas: A SEER database analysis of 162,983 cases. Cancer. 2018 Feb 15;124(4):807–15.

25. Sorbye H, Welin S, Langer SW, Vestermark LW, Holt N, Osterlund P, et al. Predictive and prognostic factors for treatment and survival in 305 patients with advanced gastrointestinal neuroendocrine carcinoma (WHO G3): the NORDIC NEC study. Ann Oncol Off J Eur Soc Med Oncol. 2013 Jan;24(1):152–60.

26. Lee SS, Lee J-L, Ryu M-H, Chang HM, Kim TW, Kim WK, et al. Extrapulmonary small cell carcinoma: single center experience with 61 patients. Acta Oncol Stockh Swed. 2007;46(6):846–51.

27. Conte B, George B, Overman M, Estrella J, Jiang Z-Q, Mehrvarz Sarshekeh A, et al. High-Grade Neuroendocrine Colorectal Carcinomas: A Retrospective Study of 100 Patients. Clin Colorectal Cancer. 2016 Jun;15(2):e1-7.

28. Oberg K, Couvelard A, Delle Fave G, Gross D, Grossman A, Jensen RT, et al. ENETS Consensus Guidelines for Standard of Care in Neuroendocrine Tumours: Biochemical Markers. Neuroendocrinology. 2017;105(3):201–11.

29. La Rosa S, Sessa F. High-grade poorly differentiated neuroendocrine carcinomas of the gastroenteropancreatic system: from morphology to proliferation and back. Endocr Pathol. 2014 Jun;25(2):193–8.

30. La Rosa S. Challenges in High-grade Neuroendocrine Neoplasms and Mixed Neuroendocrine/Non-neuroendocrine Neoplasms. Endocr Pathol. 2021 Mar 31;

31. Volante M, Rindi G, Papotti M. The grey zone between pure (neuro)endocrine and non-(neuro)endocrine tumours: a comment on concepts and classification of mixed exocrine-endocrine neoplasms. Virchows Arch Int J Pathol. 2006 Nov;449(5):499–506.

32. Klöppel G. Neuroendocrine Neoplasms: Dichotomy, Origin and Classifications. Visc Med. 2017 Oct;33(5):324–30.

33. de Mestier L, Cros J, Neuzillet C, Hentic O, Egal A, Muller N, et al. Digestive System Mixed Neuroendocrine-Non-Neuroendocrine Neoplasms. Neuroendocrinology. 2017;105(4):412–25.

34. Oberg K, Krenning E, Sundin A, Bodei L, Kidd M, Tesselaar M, et al. A Delphic consensus assessment: imaging and biomarkers in gastroenteropancreatic neuroendocrine tumor disease management. Endocr Connect. 2016 Sep;5(5):174–87.

35. Ferolla P, Faggiano A, Mansueto G, Avenia N, Cantelmi MG, Giovenali P, et al. The biological characterization of neuroendocrine tumors: the role of neuroendocrine markers. J Endocrinol Invest. 2008 Mar;31(3):277–86.

36. Zatelli MC, Torta M, Leon A, Ambrosio MR, Gion M, Tomassetti P, et al. Chromogranin A as a marker of neuroendocrine neoplasia: an Italian Multicenter Study. Endocr Relat Cancer. 2007 Jun;14(2):473–82.

37. Konecki DS, Benedum UM, Gerdes HH, Huttner WB. The primary structure of human chromogranin A and pancreastatin. J Biol Chem. 1987 Dec 15;262(35):17026–30.

38. Modlin IM, Gustafsson BI, Moss SF, Pavel M, Tsolakis AV, Kidd M. Chromogranin A--biological function and clinical utility in neuro endocrine tumor disease. Ann Surg Oncol. 2010 Sep;17(9):2427–43.

39. Kos-Kudła B, Blicharz-Dorniak J, Strzelczyk J, Bałdys-Waligórska A, Bednarczuk T, Bolanowski M, et al. Diagnostic and therapeutic guidelines for gastro-entero-pancreatic neuroendocrine neoplasms (recommended by the Polish Network of Neuroendocrine Tumours). Endokrynol Pol. 2017;68(2):79–110.

40. Schürmann G, Raeth U, Wiedenmann B, Buhr H, Herfarth C. Serum chromogranin A in the diagnosis and follow-up of neuroendocrine tumors of the gastroenteropancreatic tract. World J Surg. 1992 Aug;16(4):697–701; discussion 701-702.

41. Cimitan M, Buonadonna A, Cannizzaro R, Canzonieri V, Borsatti E, Ruffo R, et al. Somatostatin receptor scintigraphy versus chromogranin A assay in the management of patients with neuroendocrine tumors of different types: clinical role. Ann Oncol Off J Eur Soc Med Oncol. 2003 Jul;14(7):1135–41.

42. Nanno Y, Toyama H, Matsumoto I, Otani K, Asari S, Goto T, et al. Baseline plasma chromogranin A levels in patients with well-differentiated neuroendocrine tumors of the pancreas: A potential predictor of postoperative recurrence. Pancreatol Off J Int Assoc Pancreatol IAP Al. 2017 Apr;17(2):291–4.

43. Yao JC, Phan AT, Chang DZ, Wolff RA, Hess K, Gupta S, et al. Efficacy of RAD001 (everolimus) and octreotide LAR in advanced low- to intermediate-grade neuroendocrine tumors: results of a phase II study. J Clin Oncol Off J Am Soc Clin Oncol. 2008 Sep 10;26(26):4311–8.

44. Pavel ME, Hainsworth JD, Baudin E, Peeters M, Hörsch D, Winkler RE, et al. Everolimus plus octreotide long-acting repeatable for the treatment of advanced neuroendocrine tumours associated with carcinoid syndrome (RADIANT-2): a randomised, placebo-controlled, phase 3 study. Lancet Lond Engl. 2011 Dec 10;378(9808):2005–12.

45. Yao JC, Shah MH, Ito T, Bohas CL, Wolin EM, Van Cutsem E, et al. Everolimus for advanced pancreatic neuroendocrine tumors. N Engl J Med. 2011 Feb 10;364(6):514–23.

46. Baudin E. Gastroenteropancreatic endocrine tumors: clinical characterization before therapy. Nat Clin Pract Endocrinol Metab. 2007 Mar;3(3):228–39.

47. Lamberts SW, Hofland LJ, Nobels FR. Neuroendocrine tumor markers. Front Neuroendocrinol. 2001 Oct;22(4):309–39.

48. Nobels FR, Kwekkeboom DJ, Coopmans W, Schoenmakers CH, Lindemans J, De Herder WW, et al. Chromogranin A as serum marker for neuroendocrine neoplasia: comparison with neuron-specific enolase and the alpha-subunit of glycoprotein hormones. J Clin Endocrinol Metab. 1997 Aug;82(8):2622–8.

49. Sansone A, Lauretta R, Vottari S, Chiefari A, Barnabei A, Romanelli F, et al. Specific and Non-Specific Biomarkers in Neuroendocrine Gastroenteropancreatic Tumors. Cancers. 2019 Aug 4;11(8).

50. Baudin E, Gigliotti A, Ducreux M, Ropers J, Comoy E, Sabourin JC, et al. Neuron-specific enolase and chromogranin A as markers of neuroendocrine tumours. Br J Cancer. 1998 Oct;78(8):1102–7.

51. Yao JC, Pavel M, Phan AT, Kulke MH, Hoosen S, St Peter J, et al. Chromogranin A and neuron-specific enolase as prognostic markers in patients with advanced pNET treated with everolimus. J Clin Endocrinol Metab. 2011 Dec;96(12):3741–9.

52. Adaway JE, Dobson R, Walsh J, Cuthbertson DJ, Monaghan PJ, Trainer PJ, et al. Serum and plasma 5-hydroxyindoleacetic acid as an alternative to 24-h urine 5-hydroxyindoleacetic acid measurement. Ann Clin Biochem. 2016 Sep;53(Pt 5):554–60.

53. Öberg K. Management of functional neuroendocrine tumors of the pancreas. Gland Surg. 2018 Feb;7(1):20–7.

54. Modlin IM, Bodei L, Kidd M. Neuroendocrine tumor biomarkers: From monoanalytes to transcripts and algorithms. Best Pract Res Clin Endocrinol Metab. 2016 Jan;30(1):59–77.

55. Mader S, Pantel K. Liquid Biopsy: Current Status and Future Perspectives. Oncol Res Treat. 2017;40(7–8):404–8.

56. Sundling KE, Lowe AC. Circulating Tumor Cells: Overview and Opportunities in Cytology. Adv Anat Pathol. 2019 Jan;26(1):56–63.

57. Khan MS, Tsigani T, Rashid M, Rabouhans JS, Yu D, Luong TV, et al. Circulating tumor cells and EpCAM expression in neuroendocrine tumors. Clin Cancer Res Off J Am Assoc Cancer Res. 2011 Jan 15;17(2):337–45.

58. Khan MS, Kirkwood A, Tsigani T, Garcia-Hernandez J, Hartley JA, Caplin ME, et al. Circulating tumor cells as prognostic markers in neuroendocrine tumors. J Clin Oncol Off J Am Soc Clin Oncol. 2013 Jan 20;31(3):365–72.

59. Khan MS, Kirkwood AA, Tsigani T, Lowe H, Goldstein R, Hartley JA, et al. Early Changes in Circulating Tumor Cells Are Associated with Response and Survival Following Treatment of Metastatic Neuroendocrine Neoplasms. Clin Cancer Res Off J Am Assoc Cancer Res. 2016 Jan 1;22(1):79–85.

60. Modlin IM, Kidd M, Bodei L, Drozdov I, Aslanian H. The clinical utility of a novel blood-based multi-transcriptome assay for the diagnosis of neuroendocrine tumors of the gastrointestinal tract. Am J Gastroenterol. 2015 Aug;110(8):1223–32.

61. Modlin IM, Drozdov I, Kidd M. The identification of gut neuroendocrine tumor disease by multiple synchronous transcript analysis in blood. PloS One. 2013;8(5):e63364.

62. Filosso PL, Kidd M, Roffinella M, Lewczuk A, Chung K-M, Kolasinska-Cwikla A, et al. The utility of blood neuroendocrine gene transcript measurement in the diagnosis of bronchopulmonary neuroendocrine tumours and as a tool to evaluate surgical resection and disease progression. Eur J Cardio-Thorac Surg Off J Eur Assoc Cardio-Thorac Surg. 2018 Mar 1;53(3):631–9.

63. Malczewska A, Witkowska M, Makulik K, Bocian A, Walter A, Pilch-Kowalczyk J, et al. NETest liquid biopsy is diagnostic of small intestine and pancreatic neuroendocrine tumors and correlates with imaging. Endocr Connect. 2019 Mar 1;

64. Pęczkowska M, Cwikla J, Kidd M, Lewczuk A, Kolasinska-Ćwikła A, Niec D, et al. The clinical utility of circulating neuroendocrine gene transcript analysis in well-differentiated paragangliomas and pheochromocytomas. Eur J Endocrinol. 2017 Feb;176(2):143–57.

65. Bodei L, Kidd M, Modlin IM, Severi S, Drozdov I, Nicolini S, et al. Measurement of circulating transcripts and gene cluster analysis predicts and defines therapeutic efficacy of peptide receptor radionuclide therapy (PRRT) in neuroendocrine tumors. Eur J Nucl Med Mol Imaging. 2016 May;43(5):839–51.

66. Modlin IM, Frilling A, Salem RR, Alaimo D, Drymousis P, Wasan HS, et al. Blood measurement of neuroendocrine gene transcripts defines the effectiveness of operative resection and ablation strategies. Surgery. 2016 Jan;159(1):336–47.

67. Genç CG, Jilesen APJ, Nieveen van Dijkum EJM, Klümpen H-J, van Eijck CHJ, Drozdov I, et al. Measurement of circulating transcript levels (NETest) to detect disease recurrence and improve follow-up after curative surgical resection of well-differentiated pancreatic neuroendocrine tumors. J Surg Oncol. 2018 Jul;118(1):37–48.

68. Öberg K, Sundin A. Imaging of Neuroendocrine Tumors. Front Horm Res. 2016;45:142–51.

69. Garcia-Carbonero R, Garcia-Figueiras R, Carmona-Bayonas A, Sevilla I, Teule A, Quindos M, et al. Imaging approaches to assess the therapeutic response of gastroenteropancreatic neuroendocrine tumors (GEP-NETs): current perspectives and future trends of an exciting field in development. Cancer Metastasis Rev. 2015 Dec;34(4):823–42.

70. Hardie AD, Picard MM, Camp ER, Perry JD, Suranyi P, De Cecco CN, et al. Application of an Advanced Image-Based Virtual Monoenergetic Reconstruction of Dual Source Dual-Energy CT Data at Low keV Increases Image Quality for Routine Pancreas Imaging. J Comput Assist Tomogr. 2015 Oct;39(5):716–20.

71. Thoeni RF, Mueller-Lisse UG, Chan R, Do NK, Shyn PB. Detection of small, functional islet cell tumors in the pancreas: selection of MR imaging sequences for optimal sensitivity. Radiology. 2000 Feb;214(2):483–90.

72. Owen NJ, Sohaib SA, Peppercorn PD, Monson JP, Grossman AB, Besser GM, et al. MRI of pancreatic neuroendocrine tumours. Br J Radiol. 2001 Oct;74(886):968–73.

73. Rockall AG, Reznek RH. Imaging of neuroendocrine tumours (CT/MR/US). Best Pract Res Clin Endocrinol Metab. 2007 Mar;21(1):43–68.

74. Sundin A, Arnold R, Baudin E, Cwikla JB, Eriksson B, Fanti S, et al. ENETS Consensus Guidelines for the Standards of Care in Neuroendocrine Tumors: Radiological, Nuclear Medicine & Hybrid Imaging. Neuroendocrinology. 2017;105(3):212–44.

75. Buchmann I, Henze M, Engelbrecht S, Eisenhut M, Runz A, Schäfer M, et al. Comparison of 68Ga-DOTATOC PET and 111In-DTPAOC (Octreoscan) SPECT in patients with neuroendocrine tumours. Eur J Nucl Med Mol Imaging. 2007 Oct;34(10):1617–26.

76. Ruf J, Heuck F, Schiefer J, Denecke T, Elgeti F, Pascher A, et al. Impact of Multiphase 68Ga-DOTATOC-PET/CT on therapy management in patients with neuroendocrine tumors. Neuroendocrinology. 2010;91(1):101–9.

77. Ambrosini V, Campana D, Bodei L, Nanni C, Castellucci P, Allegri V, et al. 68Ga-DOTANOC PET/CT clinical impact in patients with neuroendocrine tumors. J Nucl Med Off Publ Soc Nucl Med. 2010 May;51(5):669–73.

78. Binderup T, Knigge U, Loft A, Federspiel B, Kjaer A. 18F-fluorodeoxyglucose positron emission tomography predicts survival of patients with neuroendocrine tumors. Clin Cancer Res Off J Am Assoc Cancer Res. 2010 Feb 1;16(3):978–85.

79. Ambrosini V, Morigi JJ, Nanni C, Castellucci P, Fanti S. Current status of PET imaging of neuroendocrine tumours ([18F]FDOPA, [68Ga]tracers, [11C]/[18F]-HTP). Q J Nucl Med Mol Imaging Off Publ Ital Assoc Nucl Med AIMN Int Assoc Radiopharmacol IAR Sect Soc Of. 2015 Mar;59(1):58–69.

80. Ambrosini V, Tomassetti P, Castellucci P, Campana D, Montini G, Rubello D, et al. Comparison between 68Ga-DOTA-NOC and 18F-DOPA PET for the detection of gastro-entero-pancreatic and lung neuro-endocrine tumours. Eur J Nucl Med Mol Imaging. 2008 Aug;35(8):1431–8.

81. Bodei L, Mueller-Brand J, Baum RP, Pavel ME, Hörsch D, O'Dorisio MS, et al. The joint IAEA, EANM, and SNMMI practical guidance on peptide receptor radionuclide therapy (PRRNT) in neuroendocrine tumours. Eur J Nucl Med Mol Imaging. 2013 May;40(5):800–16.

82. Reubi JC, Waser B, Mäcke H, Rivier J. Highly Increased 125I-JR11 Antagonist Binding In Vitro Reveals Novel Indications for sst2 Targeting in Human Cancers. J Nucl Med Off Publ Soc Nucl Med. 2017 Feb;58(2):300–6.

83. Wild D, Fani M, Fischer R, Del Pozzo L, Kaul F, Krebs S, et al. Comparison of somatostatin receptor agonist and antagonist for peptide receptor radionuclide therapy: a pilot study. J Nucl Med Off Publ Soc Nucl Med. 2014 Aug;55(8):1248–52.

84. Luo Y, Pan Q, Yao S, Yu M, Wu W, Xue H, et al. Glucagon-Like Peptide-1 Receptor PET/CT with 68Ga-NOTA-Exendin-4 for Detecting Localized Insulinoma: A Prospective Cohort Study. J Nucl Med Off Publ Soc Nucl Med. 2016 May;57(5):715–20.

85. Antwi K, Fani M, Nicolas G, Rottenburger C, Heye T, Reubi JC, et al. Localization of Hidden Insulinomas with ^{68}Ga-DOTA-Exendin-4 PET/CT: A Pilot Study. J Nucl Med Off Publ Soc Nucl Med. 2015 Jul;56(7):1075–8.

86. Metz DC, Choi J, Strosberg J, Heaney AP, Howden CW, Klimstra D, et al. A rationale for multidisciplinary care in treating neuroendocrine tumours. Curr Opin Endocrinol Diabetes Obes. 2012 Aug;19(4):306–13.

87. Magi L, Mazzuca F, Rinzivillo M, Arrivi G, Pilozzi E, Prosperi D, et al. Multidisciplinary Management of Neuroendocrine Neoplasia: A Real-World Experience from a Referral Center. J Clin Med. 2019 Jun 25;8(6).

88. Fazio N, Ungaro A, Spada F, Cella CA, Pisa E, Barberis M, et al. The role of multimodal treatment in patients with advanced lung neuroendocrine tumors. J Thorac Dis. 2017 Nov;9(Suppl 15):S1501–10.

89. Goretzki PE, Mogl MT, Akca A, Pratschke J. Curative and palliative surgery in patients with neuroendocrine tumors of the gastro-entero-pancreatic (GEP) tract. Rev Endocr Metab Disord. 2018 Jun;19(2):169–78.

90. Strosberg JR, Halfdanarson TR, Bellizzi AM, Chan JA, Dillon JS, Heaney AP, et al. The North American Neuroendocrine Tumor Society Consensus Guidelines for Surveillance and Medical Management of Midgut Neuroendocrine Tumors. Pancreas. 2017 Jul;46(6):707–14.

91. Howe JR, Cardona K, Fraker DL, Kebebew E, Untch BR, Wang Y-Z, et al. The Surgical Management of Small Bowel Neuroendocrine Tumors: Consensus Guidelines of the North American Neuroendocrine Tumor Society. Pancreas. 2017 Jul;46(6):715–31.

92. Caplin ME, Baudin E, Ferolla P, Filosso P, Garcia-Yuste M, Lim E, et al. Pulmonary neuroendocrine (carcinoid) tumors: European Neuroendocrine Tumor Society expert consensus and recommendations for best practice for typical and atypical pulmonary carcinoids. Ann Oncol Off J Eur Soc Med Oncol. 2015 Aug;26(8):1604–20.

93. Wood DE. National Comprehensive Cancer Network (NCCN) Clinical Practice Guidelines for Lung Cancer Screening. Thorac Surg Clin. 2015 May;25(2):185–97.

94. Heller DR, Jean RA, Luo J, Kurbatov V, Grisotti G, Jacobs D, et al. Practice Patterns and Guideline Non-Adherence in Surgical Management of Appendiceal Carcinoid Tumors. J Am Coll Surg. 2019 Jun;228(6):839–51.

95. Johnston ME, Carter MM, Wilson GC, Ahmad SA, Patel SH. Surgical management of primary pancreatic neuroendocrine tumors. J Gastrointest Oncol. 2020 Jun;11(3):578–89.

96. Brenner B, Tang LH, Shia J, Klimstra DS, Kelsen DP. Small cell carcinomas of the gastrointestinal tract: clinicopathological features and treatment approach. Semin Oncol. 2007 Feb;34(1):43–50.

97. Hellman P, Lundström T, Ohrvall U, Eriksson B, Skogseid B, Oberg K, et al. Effect of surgery on the outcome of midgut carcinoid disease with lymph node and liver metastases. World J Surg. 2002 Aug;26(8):991–7.

98. Norlén O, Stålberg P, Öberg K, Eriksson J, Hedberg J, Hessman O, et al. Long-term results of surgery for small intestinal neuroendocrine tumors at a tertiary referral center. World J Surg. 2012 Jun;36(6):1419–31.

99. Le Roux C, Lombard-Bohas C, Delmas C, Dominguez-Tinajero S, Ruszniewski P, Samalin E, et al. Relapse factors for ileal neuroendocrine tumours after curative surgery: a retrospective French multicentre study. Dig Liver Dis Off J Ital Soc Gastroenterol Ital Assoc Study Liver. 2011 Oct;43(10):828–33.

100. Mayo SC, de Jong MC, Pulitano C, Clary BM, Reddy SK, Gamblin TC, et al. Surgical management of hepatic neuroendocrine tumor metastasis: results from an international multi-institutional analysis. Ann Surg Oncol. 2010 Dec;17(12):3129–36.

101. Karppinen N, Lindén R, Sintonen H, Tarkkanen M, Roine R, Heiskanen I, et al. Health-Related Quality of Life in Patients with Small Intestine Neuroendocrine Tumors. Neuroendocrinology. 2018;107(4):366–74.

102. Milanetto AC, Nordenström E, Sundlöv A, Almquist M. Health-Related Quality of Life After Surgery for Small Intestinal Neuroendocrine Tumours. World J Surg. 2018 Oct;42(10):3231–9.

103. Ahmed A, Turner G, King B, Jones L, Culliford D, McCance D, et al. Midgut neuroendocrine tumours with liver metastases: results of the UKINETS study. Endocr Relat Cancer. 2009 Sep;16(3):885–94.

104. Givi B, Pommier SJ, Thompson AK, Diggs BS, Pommier RF. Operative resection of primary carcinoid neoplasms in patients with liver metastases yields significantly better survival. Surgery. 2006 Dec;140(6):891–7; discussion 897-898.

105. Daskalakis K, Karakatsanis A, Hessman O, Stuart HC, Welin S, Tiensuu Janson E, et al. Association of a Prophylactic Surgical Approach to Stage IV Small Intestinal Neuroendocrine Tumors With Survival. JAMA Oncol. 2018 Feb 1;4(2):183–9.

106. Gluckman CR, Metz DC. Gastric Neuroendocrine Tumors (Carcinoids). Curr Gastroenterol Rep. 2019 Mar 12;21(4):13.

107. Kunz PL, Reidy-Lagunes D, Anthony LB, Bertino EM, Brendtro K, Chan JA, et al. Consensus guidelines for the management and treatment of neuroendocrine tumors. Pancreas. 2013 May;42(4):557–77.

108. Pape U-F, Niederle B, Costa F, Gross D, Kelestimur F, Kianmanesh R, et al. ENETS Consensus Guidelines for Neuroendocrine Neoplasms of the Appendix (Excluding Goblet Cell Carcinomas). Neuroendocrinology. 2016;103(2):144–52.

109. Toumpanakis C, Fazio N, Tiensuu Janson E, Hörsch D, Pascher A, Reed N, et al. Unmet Needs in Appendiceal Neuroendocrine Neoplasms. Neuroendocrinology. 2019;108(1):37–44.

110. Mullen JT, Savarese DMF. Carcinoid tumors of the appendix: a population-based study. J Surg Oncol. 2011 Jul 1;104(1):41–4.

111. Clancy TE. Surgical Management of Pancreatic Neuroendocrine Tumors. Hematol Oncol Clin North Am. 2016 Feb;30(1):103–18.

112. Mehrabi A, Fischer L, Hafezi M, Dirlewanger A, Grenacher L, Diener MK, et al. A systematic review of localization, surgical treatment options, and outcome of insulinoma. Pancreas. 2014 Jul;43(5):675–86.

113. Fischer L, Kleeff J, Esposito I, Hinz U, Zimmermann A, Friess H, et al. Clinical outcome and long-term survival in 118 consecutive patients with neuroendocrine tumours of the pancreas. Br J Surg. 2008 May;95(5):627–35.

114. Kleine M, Schrem H, Vondran FWR, Krech T, Klempnauer J, Bektas H. Extended surgery for advanced pancreatic endocrine tumours. Br J Surg. 2012 Jan;99(1):88–94.

115. de Mestier L, Gaujoux S, Cros J, Hentic O, Vullierme M-P, Couvelard A, et al. Long-term Prognosis of Resected Pancreatic Neuroendocrine Tumors in von Hippel-Lindau Disease Is Favorable and Not Influenced by Small Tumors Left in Place. Ann Surg. 2015 Aug;262(2):384–8.

116. Gaujoux S, Gonen M, Tang L, Klimstra D, Brennan MF, D'Angelica M, et al. Synchronous resection of primary and liver metastases for neuroendocrine tumors. Ann Surg Oncol. 2012 Dec;19(13):4270–7.

117. Cheema A, Weber J, Strosberg JR. Incidental detection of pancreatic neuroendocrine tumors: an analysis of incidence and outcomes. Ann Surg Oncol. 2012 Sep;19(9):2932–6.

118. Gaujoux S, Partelli S, Maire F, D'Onofrio M, Larroque B, Tamburrino D, et al. Observational study of natural history of small sporadic nonfunctioning pancreatic neuroendocrine tumors. J Clin Endocrinol Metab. 2013 Dec;98(12):4784–9.

119. de Mestier L, Lorenzo D, Fine C, Cros J, Hentic O, Walter T, et al. Endoscopic, transanal, laparoscopic, and transabdominal management of rectal neuroendocrine tumors. Best Pract Res Clin Endocrinol Metab. 2019 Oct;33(5):101293.

120. Kwaan MR, Goldberg JE, Bleday R. Rectal carcinoid tumors: review of results after endoscopic and surgical therapy. Arch Surg Chic Ill 1960. 2008 May;143(5):471–5.

121. Bertani E, Ravizza D, Milione M, Massironi S, Grana CM, Zerini D, et al. Neuroendocrine neoplasms of rectum: A management update. Cancer Treat Rev. 2018 May;66:45–55.

122. Matsuhashi N, Takahashi T, Tomita H, Araki H, Ibuka T, Tanaka K, et al. Evaluation of treatment for rectal neuroendocrine tumors sized under 20 mm in comparison with the WHO 2010 guidelines. Mol Clin Oncol. 2017 Sep;7(3):476–80.

123. Scherübl H, Jensen RT, Cadiot G, Stölzel U, Klöppel G. Management of early gastrointestinal neuroendocrine neoplasms. World J Gastrointest Endosc. 2011 Jul 16;3(7):133–9.

124. Soga J. Early-stage carcinoids of the gastrointestinal tract: an analysis of 1914 reported cases. Cancer. 2005 Apr 15;103(8):1587–95.

125. Anthony LB, Strosberg JR, Klimstra DS, Maples WJ, O'Dorisio TM, Warner RRP, et al. The NANETS consensus guidelines for the diagnosis and management of gastrointestinal neuroendocrine tumors (nets): well-differentiated nets of the distal colon and rectum. Pancreas. 2010 Aug;39(6):767–74.

126. Steinmüller T, Kianmanesh R, Falconi M, Scarpa A, Taal B, Kwekkeboom DJ, et al. Consensus guidelines for the management of patients with liver metastases from digestive (neuro)endocrine tumors: foregut, midgut, hindgut, and unknown primary. Neuroendocrinology. 2008;87(1):47–62.

127. Kennedy A, Bester L, Salem R, Sharma RA, Parks RW, Ruszniewski P, et al. Role of hepatic intra-arterial therapies in metastatic neuroendocrine tumours (NET): guidelines from the NET-Liver-Metastases Consensus Conference. HPB. 2015 Jan;17(1):29–37.

128. Bertani E, Fazio N, Botteri E, Chiappa A, Falconi M, Grana C, et al. Resection of the primary pancreatic neuroendocrine tumor in patients with unresectable liver metastases: possible indications for a multimodal approach. Surgery. 2014 Apr;155(4):607–14.

129. Capurso G, Rinzivillo M, Bettini R, Boninsegna L, Delle Fave G, Falconi M. Systematic review of resection of primary midgut carcinoid tumour in patients with unresectable liver metastases. Br J Surg. 2012 Nov;99(11):1480–6.

130. Gupta S, Yao JC, Ahrar K, Wallace MJ, Morello FA, Madoff DC, et al. Hepatic artery embolization and chemoembolization for treatment of patients with

metastatic carcinoid tumors: the M.D. Anderson experience. Cancer J Sudbury Mass. 2003 Aug;9(4):261–7.

131. Osborne DA, Zervos EE, Strosberg J, Strosberg J, Boe BA, Malafa M, et al. Improved outcome with cytoreduction versus embolization for symptomatic hepatic metastases of carcinoid and neuroendocrine tumors. Ann Surg Oncol. 2006 Apr;13(4):572–81.

132. King J, Quinn R, Glenn DM, Janssen J, Tong D, Liaw W, et al. Radioembolization with selective internal radiation microspheres for neuroendocrine liver metastases. Cancer. 2008 Sep 1;113(5):921–9.

133. Dawod Q, Shah SL, Fahey TJ, Sharaiha RZ. EUS-guided radiofrequency ablation of a pancreatic neuroendocrine tumor. VideoGIE Off Video J Am Soc Gastrointest Endosc. 2020 May;5(5):203–4.

134. Dogliotti L, Tampellini M, Stivanello M, Gorzegno G, Fabiani L. The clinical management of neuroendocrine tumors with long-acting repeatable (LAR) octreotide: comparison with standard subcutaneous octreotide therapy. Ann Oncol Off J Eur Soc Med Oncol. 2001;12 Suppl 2:S105-109.

135. Pavel M, O'Toole D, Costa F, Capdevila J, Gross D, Kianmanesh R, et al. ENETS Consensus Guidelines Update for the Management of Distant Metastatic Disease of Intestinal, Pancreatic, Bronchial Neuroendocrine Neoplasms (NEN) and NEN of Unknown Primary Site. Neuroendocrinology. 2016;103(2):172–85.

136. Ruszniewski P, Ish-Shalom S, Wymenga M, O'Toole D, Arnold R, Tomassetti P, et al. Rapid and sustained relief from the symptoms of carcinoid syndrome: results from an open 6-month study of the 28-day prolonged-release formulation of lanreotide. Neuroendocrinology. 2004;80(4):244–51.

137. Bajetta E, Procopio G, Catena L, Martinetti A, De Dosso S, Ricci S, et al. Lanreotide autogel every 6 weeks compared with Lanreotide microparticles every 3 weeks in patients with well differentiated neuroendocrine tumors: a Phase III Study. Cancer. 2006 Nov 15;107(10):2474–81.

138. Vinik AI, Wolin EM, Liyanage N, Gomez-Panzani E, Fisher GA, ELECT Study Group *. EVALUATION OF LANREOTIDE DEPOT/AUTOGEL EFFICACY AND SAFETY AS A CARCINOID SYNDROME TREATMENT (ELECT): A RANDOMIZED, DOUBLE-BLIND, PLACEBO-CONTROLLED TRIAL. Endocr Pract Off J Am Coll Endocrinol Am Assoc Clin Endocrinol. 2016 Sep;22(9):1068–80.

139. Fisher GA, Wolin EM, Liyanage N, Pitman Lowenthal S, Mirakhur B, Pommier RF, et al. Patient-Reported Symptom Control of Diarrhea and Flushing in Patients with Neuroendocrine Tumors Treated with Lanreotide Depot/Autogel: Results from a Randomized, Placebo-Controlled, Double-Blind and 32-Week Open-Label Study. The Oncologist. 2018 Jan;23(1):16–24.

140. Modlin IM, Pavel M, Kidd M, Gustafsson BI. Review article: somatostatin analogues in the treatment of gastroenteropancreatic neuroendocrine (carcinoid) tumours. Aliment Pharmacol Ther. 2010 Jan 15;31(2):169–88.

141. Hofland J, Herrera-Martínez AD, Zandee WT, de Herder WW. Management of carcinoid syndrome: a systematic review and meta-analysis. Endocr Relat Cancer. 2019 Mar;26(3):R145–56.

142. Rinke A, Müller H-H, Schade-Brittinger C, Klose K-J, Barth P, Wied M, et al. Placebo-controlled, double-blind, prospective, randomized study on the effect of octreotide LAR in the control of tumor growth in patients with metastatic neuroendocrine midgut tumors: a report from the PROMID Study Group. J Clin Oncol Off J Am Soc Clin Oncol. 2009 Oct 1;27(28):4656–63.

143. Caplin ME, Pavel M, Ruszniewski P. Lanreotide in metastatic enteropancreatic neuroendocrine tumors. N Engl J Med. 2014 Oct 16;371(16):1556–7.

144. Bodei L, Kidd M, Prasad V, Modlin IM. Peptide Receptor Radionuclide Therapy of Neuroendocrine Tumors. Front Horm Res. 2015;44:198–215.

145. Cives M, Strosberg J. Radionuclide Therapy for Neuroendocrine Tumors. Curr Oncol Rep. 2017 Feb;19(2):9.

146. Bodei L, Kidd M, Paganelli G, Grana CM, Drozdov I, Cremonesi M, et al. Long-term tolerability of PRRT in 807 patients with neuroendocrine tumours: the value and limitations of clinical factors. Eur J Nucl Med Mol Imaging. 2015 Jan;42(1):5–19.

147. Sansovini M, Severi S, Ambrosetti A, Monti M, Nanni O, Sarnelli A, et al. Treatment with the radiolabelled somatostatin analog Lu-DOTATATE for advanced pancreatic neuroendocrine tumors. Neuroendocrinology. 2013;97(4):347–54.

148. Sundlöv A, Sjögreen-Gleisner K, Svensson J, Ljungberg M, Olsson T, Bernhardt P, et al. Individualised 177Lu-DOTATATE treatment of neuroendocrine tumours based on kidney dosimetry. Eur J Nucl Med Mol Imaging. 2017 Aug;44(9):1480–9.

149. Krenning EP, Kwekkeboom DJ, Oei HY, Reubi JC, van Hagen PM, Kooij PP, et al. Somatostatin receptor imaging of endocrine gastrointestinal tumors. Schweiz Med Wochenschr. 1992 Apr 25;122(17):634–7.

150. Jonathan R. Strosberg, Martyn E Caplin, Pamela L. Kunz, Philippe B Ruszniewski, Lisa Bodei, Andrew Eugene Hendifar, Erik Mittra, Edward M. Wolin, James C. Yao, Marianne E Pavel, Enrique Grande, Eric Van Cutsem, Ettore Seregni, Hugo Duarte, Germo Gericke, Amy Bartalotta, Arnaud Demange, Sakir Mutevelic, Eric Krenning, and on behalf of the NETTER-1 study group. Final overall survival in the phase 3 NETTER-1 study of lutetium-177-DOTATATE in patients with midgut neuroendocrine tumors. Journal of Clinical Oncology 2021 39:15_suppl, 4112-4112.

151. Yao JC, Shah MH, Ito T, Bohas CL, Wolin EM, Van Cutsem E, et al. Everolimus for advanced pancreatic neuroendocrine tumors. N Engl J Med. 2011 Feb 10;364(6):514–23.

152. Yao JC, Fazio N, Singh S, Buzzoni R, Carnaghi C, Wolin E, et al. Everolimus for the treatment of advanced, non-functional neuroendocrine tumours of the lung or gastrointestinal tract (RADIANT-4): a randomised, placebo-controlled, phase 3 study. Lancet Lond Engl. 2016 Mar 5;387(10022):968–77.

153. Fazio N, Buzzoni R, Delle Fave G, Tesselaar ME, Wolin E, Van Cutsem E, et al. Everolimus in advanced, progressive, well-differentiated, non-functional neuroendocrine tumors: RADIANT-4 lung subgroup analysis. Cancer Sci. 2018 Jan;109(1):174–81.

154. Raymond E, Dahan L, Raoul J-L, Bang Y-J, Borbath I, Lombard-Bohas C, et al. Sunitinib malate for the treatment of pancreatic neuroendocrine tumors. N Engl J Med. 2011 Feb 10;364(6):501–13.

155. Faivre S, Niccoli P, Castellano D, Valle JW, Hammel P, Raoul J-L, et al. Sunitinib in pancreatic neuroendocrine tumors: updated progression-free survival and final overall survival from a phase III randomized study. Ann Oncol Off J Eur Soc Med Oncol. 2017 Feb 1;28(2):339–43.

156. Xu J, Shen L, Zhou Z, Li J, Bai C, Chi Y, et al. Surufatinib in advanced extrapancreatic neuroendocrine tumours (SANET-ep): a randomised, double-blind, placebo-controlled, phase 3 study. Lancet Oncol. 2020 Nov;21(11):1500–12.

157. Xu J, Shen L, Bai C, Wang W, Li J, Yu X, et al. Surufatinib in advanced pancreatic neuroendocrine tumours (SANET-p): a randomised, double-blind, placebo-controlled, phase 3 study. Lancet Oncol. 2020 Nov;21(11):1489–99.

158. Espinosa-Olarte P, La Salvia A, Riesco-Martinez MC, Anton-Pascual B, Garcia-Carbonero R. Chemotherapy in NEN: still has a role? Rev Endocr Metab Disord. 2021 Apr 11;

159. Moertel CG, Hanley JA, Johnson LA. Streptozocin alone compared with streptozocin plus fluorouracil in the treatment of advanced islet-cell carcinoma. N Engl J Med. 1980 Nov 20;303(21):1189–94.

160. Moertel CG, Lefkopoulo M, Lipsitz S, Hahn RG, Klaassen D. Streptozocin-doxorubicin, streptozocin-fluorouracil or chlorozotocin in the treatment of advanced islet-cell carcinoma. N Engl J Med. 1992 Feb 20;326(8):519–23.

161. Alexandraki KI, Karapanagioti A, Karoumpalis I, Boutzios G, Kaltsas GA. Advances and Current Concepts in the Medical Management of Gastroenteropancreatic Neuroendocrine Neoplasms. BioMed Res Int. 2017;2017:9856140.

162. Chan JA, Kulke MH. New treatment options for patients with advanced neuroendocrine tumors. Curr Treat Options Oncol. 2011 Jun;12(2):136–48.

163. Lamarca A, Elliott E, Barriuso J, Backen A, McNamara MG, Hubner R, et al. Chemotherapy for advanced non-pancreatic well-differentiated neuroendocrine tumours of the gastrointestinal tract, a systematic review and meta-analysis: A lost cause? Cancer Treat Rev. 2016 Mar;44:26–41.

164. Kotteas EA, Syrigos KN, Saif MW. Profile of capecitabine/temozolomide combination in the treatment of well-differentiated neuroendocrine tumors. OncoTargets Ther. 2016;9:699–704.

165. Strosberg JR, Fine RL, Choi J, Nasir A, Coppola D, Chen D-T, et al. First-line chemotherapy with capecitabine and temozolomide in patients with metastatic pancreatic endocrine carcinomas. Cancer. 2011 Jan 15;117(2):268–75.

166. Moertel CG, Kvols LK, O'Connell MJ, Rubin J. Treatment of neuroendocrine carcinomas with combined etoposide and cisplatin. Evidence of major therapeutic activity in the anaplastic variants of these neoplasms. Cancer. 1991 Jul 15;68(2):227–32.

167. Assarzadegan N, Montgomery E. What is New in 2019 World Health Organization (WHO) Classification of Tumors of the Digestive System: Review of Selected Updates on Neuroendocrine Neoplasms, Appendiceal Tumors, and Molecular Testing. Arch Pathol Lab Med. 2020 Apr 1;

168. Ferrarotto R, Testa L, Riechelmann RP, Sahade M, Siqueira LT, Costa FP, et al. Combination of Capecitabine and Oxaliplatin is an Effective Treatment Option for Advanced Neuroendocrine Tumors. Rare Tumors. 2013;5(3):e35.

169. Hadoux J, Malka D, Planchard D, Scoazec JY, Caramella C, Guigay J, et al. Post-first-line FOLFOX chemotherapy for grade 3 neuroendocrine carcinoma. Endocr Relat Cancer. 2015 Jun;22(3):289–98.

170. Hentic O, Hammel P, Couvelard A, Rebours V, Zappa M, Palazzo M, et al. FOLFIRI regimen: an effective second-line chemotherapy after failure of etoposide-platinum combination in patients with neuroendocrine carcinomas grade 3. Endocr Relat Cancer. 2012 Dec;19(6):751–7.

171. Welin S, Sorbye H, Sebjornsen S, Knappskog S, Busch C, Oberg K. Clinical effect of temozolomide-based chemotherapy in poorly differentiated endocrine carcinoma after progression on first-line chemotherapy. Cancer. 2011 Oct 15;117(20):4617–22.

172. Olsen IH, Sørensen JB, Federspiel B, Kjaer A, Hansen CP, Knigge U, et al. Temozolomide as second or third line treatment of patients with neuroendocrine carcinomas. ScientificWorldJournal. 2012;2012:170496.

173. Oronsky B, Ma PC, Morgensztern D, Carter CA. Nothing But NET: A Review of Neuroendocrine Tumors and Carcinomas. Neoplasia N Y N. 2017 Dec;19(12):991–1002.

174. McNamara MG, Frizziero M, Jacobs T, Lamarca A, Hubner RA, Valle JW, et al. Second-line treatment in patients with advanced extra-pulmonary poorly

differentiated neuroendocrine carcinoma: a systematic review and meta-analysis. Ther Adv Med Oncol. 2020;12:1758835920915299.

175. Lewis MA. Hereditary Syndromes in Neuroendocrine Tumors. Curr Treat Options Oncol. 2020 Apr 30;21(6):50.

176. Knudson AG. Mutation and cancer: statistical study of retinoblastoma. Proc Natl Acad Sci U S A. 1971 Apr;68(4):820–3.

177. Ramundo V, Milone F, Severino R, Savastano S, Di Somma C, Vuolo L, et al. Clinical and prognostic implications of the genetic diagnosis of hereditary NET syndromes in asymptomatic patients. Horm Metab Res Horm Stoffwechselforschung Horm Metab. 2011 Oct;43(11):794–800.

178. Faggiano A, Ferolla P, Grimaldi F, Campana D, Manzoni M, Davì MV, et al. Natural history of gastro-entero-pancreatic and thoracic neuroendocrine tumors. Data from a large prospective and retrospective Italian epidemiological study: the NET management study. J Endocrinol Invest. 2012 Oct;35(9):817–23.

179. Brandi ML, Agarwal SK, Perrier ND, Lines KE, Valk GD, Thakker RV. Multiple Endocrine Neoplasia Type 1: Latest Insights. Endocr Rev. 2021 Mar 15;42(2):133–70.

180. Thakker RV, Newey PJ, Walls GV, Bilezikian J, Dralle H, Ebeling PR, et al. Clinical practice guidelines for multiple endocrine neoplasia type 1 (MEN1). J Clin Endocrinol Metab. 2012 Sep;97(9):2990–3011.

181. Brandi ML, Gagel RF, Angeli A, Bilezikian JP, Beck-Peccoz P, Bordi C, et al. Guidelines for diagnosis and therapy of MEN type 1 and type 2. J Clin Endocrinol Metab. 2001 Dec;86(12):5658–71.

182. Agarwal SK. Multiple endocrine neoplasia type 1. Front Horm Res. 2013;41:1–15.

183. Falchetti A. Genetics of multiple endocrine neoplasia type 1 syndrome: what's new and what's old. F1000Research. 2017;6.

184. Machens A, Schaaf L, Karges W, Frank-Raue K, Bartsch DK, Rothmund M, et al. Age-related penetrance of endocrine tumours in multiple endocrine neoplasia type 1 (MEN1): a multicentre study of 258 gene carriers. Clin Endocrinol (Oxf). 2007 Oct;67(4):613–22.

185. Bassett JH, Forbes SA, Pannett AA, Lloyd SE, Christie PT, Wooding C, et al. Characterization of mutations in patients with multiple endocrine neoplasia type 1. Am J Hum Genet. 1998 Feb;62(2):232–44.

186. Goudet P, Dalac A, Le Bras M, Cardot-Bauters C, Niccoli P, Lévy-Bohbot N, et al. MEN1 disease occurring before 21 years old: a 160-patient cohort study from the Groupe d'étude des Tumeurs Endocrines. J Clin Endocrinol Metab. 2015 Apr;100(4):1568–77.

187. Lee M, Pellegata NS. Multiple endocrine neoplasia type 4. Front Horm Res. 2013;41:63–78.

188. Alrezk R, Hannah-Shmouni F, Stratakis CA. MEN4 and CDKN1B mutations: the latest of the MEN syndromes. Endocr Relat Cancer. 2017 Oct;24(10):T195–208.

189. Mulligan LM, Kwok JB, Healey CS, Elsdon MJ, Eng C, Gardner E, et al. Germ-line mutations of the RET proto-oncogene in multiple endocrine neoplasia type 2A. Nature. 1993 Jun 3;363(6428):458–60.

190. Hofstra RM, Landsvater RM, Ceccherini I, Stulp RP, Stelwagen T, Luo Y, et al. A mutation in the RET proto-oncogene associated with multiple endocrine neoplasia type 2B and sporadic medullary thyroid carcinoma. Nature. 1994 Jan 27;367(6461):375–6.

191. Wells SA, Pacini F, Robinson BG, Santoro M. Multiple endocrine neoplasia type 2 and familial medullary thyroid carcinoma: an update. J Clin Endocrinol Metab. 2013 Aug;98(8):3149–64.

192. Romei C, Pardi E, Cetani F, Elisei R. Genetic and clinical features of multiple endocrine neoplasia types 1 and 2. J Oncol. 2012;2012:705036.

193. Asari R, Scheuba C, Kaczirek K, Niederle B. Estimated risk of pheochromocytoma recurrence after adrenal-sparing surgery in patients with multiple endocrine neoplasia type 2A. Arch Surg Chic Ill 1960. 2006 Dec;141(12):1199–205; discussion 1205.

194. Howe JR, Norton JA, Wells SA. Prevalence of pheochromocytoma and hyperparathyroidism in multiple endocrine neoplasia type 2A: results of long-term follow-up. Surgery. 1993 Dec;114(6):1070–7.

195. Verdy M, Weber AM, Roy CC, Morin CL, Cadotte M, Brochu P. Hirschsprung's disease in a family with multiple endocrine neoplasia type 2. J Pediatr Gastroenterol Nutr. 1982;1(4):603–7.

196. Al-Salameh A, Baudry C, Cohen R. Update on multiple endocrine neoplasia Type 1 and 2. Presse Medicale Paris Fr 1983. 2018 Sep;47(9):722–31.

197. Lonser RR, Glenn GM, Walther M, Chew EY, Libutti SK, Linehan WM, et al. von Hippel-Lindau disease. Lancet Lond Engl. 2003 Jun 14;361(9374):2059–67.

198. Walther MM, Reiter R, Keiser HR, Choyke PL, Venzon D, Hurley K, et al. Clinical and genetic characterization of pheochromocytoma in von Hippel-Lindau families: comparison with sporadic pheochromocytoma gives insight into natural history of pheochromocytoma. J Urol. 1999 Sep;162(3 Pt 1):659–64.

199. Eisenhofer G, Walther MM, Huynh TT, Li ST, Bornstein SR, Vortmeyer A, et al. Pheochromocytomas in von Hippel-Lindau syndrome and multiple endocrine neoplasia type 2 display distinct biochemical and clinical phenotypes. J Clin Endocrinol Metab. 2001 May;86(5):1999–2008.

200. Keutgen XM, Hammel P, Choyke PL, Libutti SK, Jonasch E, Kebebew E. Evaluation and management of pancreatic lesions in patients with von Hippel-Lindau disease. Nat Rev Clin Oncol. 2016 Sep;13(9):537–49.

201. Chittiboina P, Lonser RR. Von Hippel-Lindau disease. Handb Clin Neurol. 2015;132:139–56.

202. Hirbe AC, Gutmann DH. Neurofibromatosis type 1: a multidisciplinary approach to care. Lancet Neurol. 2014 Aug;13(8):834–43.

203. Anderson JL, Gutmann DH. Neurofibromatosis type 1. Handb Clin Neurol. 2015;132:75–86.

204. Jiao Y, Shi C, Edil BH, de Wilde RF, Klimstra DS, Maitra A, et al. DAXX/ATRX, MEN1, and mTOR pathway genes are frequently altered in pancreatic neuroendocrine tumors. Science. 2011 Mar 4;331(6021):1199–203.

205. Scarpa A, Chang DK, Nones K, Corbo V, Patch A-M, Bailey P, et al. Whole-genome landscape of pancreatic neuroendocrine tumours. Nature. 2017 Mar 2;543(7643):65–71.

206. Speisky D, Duces A, Bièche I, Rebours V, Hammel P, Sauvanet A, et al. Molecular profiling of pancreatic neuroendocrine tumors in sporadic and Von Hippel-Lindau patients. Clin Cancer Res Off J Am Assoc Cancer Res. 2012 May 15;18(10):2838–49.

207. Banck MS, Kanwar R, Kulkarni AA, Boora GK, Metge F, Kipp BR, et al. The genomic landscape of small intestine neuroendocrine tumors. J Clin Invest. 2013 Jun;123(6):2502–8.

208. Simbolo M, Vicentini C, Mafficini A, Fassan M, Pedron S, Corbo V, et al. Mutational and copy number asset of primary sporadic neuroendocrine tumors of the small intestine. Virchows Arch Int J Pathol. 2018 Dec;473(6):709–17.

209. Francis JM, Kiezun A, Ramos AH, Serra S, Pedamallu CS, Qian ZR, et al. Somatic mutation of CDKN1B in small intestine neuroendocrine tumors. Nat Genet. 2013 Dec;45(12):1483–6.

210. Crona J, Gustavsson T, Norlén O, Edfeldt K, Åkerström T, Westin G, et al. Somatic Mutations and Genetic Heterogeneity at the CDKN1B Locus in Small Intestinal Neuroendocrine Tumors. Ann Surg Oncol. 2015 Dec;22 Suppl 3:S1428-1435.

211. Maxwell JE, Sherman SK, Li G, Choi AB, Bellizzi AM, O'Dorisio TM, et al. Somatic alterations of CDKN1B are associated with small bowel neuroendocrine tumors. Cancer Genet. 2015 Sep 15;

212. Fernandez-Cuesta L, Peifer M, Lu X, Sun R, Ozretić L, Seidal D, et al. Frequent mutations in chromatin-remodelling genes in pulmonary carcinoids. Nat Commun. 2014 Mar 27;5:3518.

213. Alcala N, Leblay N, Gabriel A a. G, Mangiante L, Hervas D, Giffon T, et al. Integrative and comparative genomic analyses identify clinically relevant pulmonary carcinoid groups and unveil the supra-carcinoids. Nat Commun. 2019 Aug 20;10(1):3407.

214. Gazdar AF, Bunn PA, Minna JD. Small-cell lung cancer: what we know, what we need to know and the path forward. Nat Rev Cancer. 2017 Dec;17(12):725–37.

215. Gara RK, Kumari S, Ganju A, Yallapu MM, Jaggi M, Chauhan SC. Slit/Robo pathway: a promising therapeutic target for cancer. Drug Discov Today. 2015 Jan;20(1):156–64.

216. George J, Lim JS, Jang SJ, Cun Y, Ozretić L, Kong G, et al. Comprehensive genomic profiles of small cell lung cancer. Nature. 2015 Aug 6;524(7563):47–53.

217. George J, Walter V, Peifer M, Alexandrov LB, Seidel D, Leenders F, et al. Integrative genomic profiling of large-cell neuroendocrine carcinomas reveals distinct subtypes of high-grade neuroendocrine lung tumors. Nat Commun. 2018 Mar 13;9(1):1048.

218. Jesinghaus M, Konukiewitz B, Keller G, Kloor M, Steiger K, Reiche M, et al. Colorectal mixed adenoneuroendocrine carcinomas and neuroendocrine carcinomas are genetically closely related to colorectal adenocarcinomas. Mod Pathol Off J U S Can Acad Pathol Inc. 2017 Apr;30(4):610–9.

219. Yachida S, Vakiani E, White CM, Zhong Y, Saunders T, Morgan R, et al. Small cell and large cell neuroendocrine carcinomas of the pancreas are genetically similar and distinct from well-differentiated pancreatic neuroendocrine tumors. Am J Surg Pathol. 2012 Feb;36(2):173–84.

220. Goyal B, Duncavage EJ, Martinez D, Lewis JS, Chernock RD. Next-generation sequencing of salivary high-grade neuroendocrine carcinomas identifies alterations in RB1 and the mTOR pathway. Exp Mol Pathol. 2014 Dec;97(3):572–8.

221. Chang MT, Penson A, Desai NB, Socci ND, Shen R, Seshan VE, et al. Small-Cell Carcinomas of the Bladder and Lung Are Characterized by a Convergent but Distinct Pathogenesis. Clin Cancer Res Off J Am Assoc Cancer Res. 2018 Apr 15;24(8):1965–73.

222. Xing D, Zheng G, Schoolmeester JK, Li Z, Pallavajjala A, Haley L, et al. Next-generation Sequencing Reveals Recurrent Somatic Mutations in Small Cell Neuroendocrine Carcinoma of the Uterine Cervix. Am J Surg Pathol. 2018 Jun;42(6):750–60.

223. Sinha N, Gaston D, Manders D, Goudie M, Matsuoka M, Xie T, et al. Characterization of genome-wide copy number aberrations in colonic mixed adenoneuroendocrine carcinoma and neuroendocrine carcinoma reveals recurrent amplification of PTGER4 and MYC genes. Hum Pathol. 2018 Mar;73:16–25.

224. Takizawa N, Ohishi Y, Hirahashi M, Takahashi S, Nakamura K, Tanaka M, et al. Molecular characteristics of colorectal neuroendocrine carcinoma; similarities with

adenocarcinoma rather than neuroendocrine tumor. Hum Pathol. 2015 Dec;46(12):1890–900.

225. Capdevila J, Arqués O, Hernández Mora JR, Matito J, Caratù G, Mancuso FM, et al. Epigenetic EGFR Gene Repression Confers Sensitivity to Therapeutic BRAFV600E Blockade in Colon Neuroendocrine Carcinomas. Clin Cancer Res Off J Am Assoc Cancer Res. 2020 Feb 15;26(4):902–9.

226. Arnold CN, Nagasaka T, Goel A, Scharf I, Grabowski P, Sosnowski A, et al. Molecular characteristics and predictors of survival in patients with malignant neuroendocrine tumors. Int J Cancer. 2008 Oct 1;123(7):1556–64.

227. Sahnane N, Furlan D, Monti M, Romualdi C, Vanoli A, Vicari E, et al. Microsatellite unstable gastrointestinal neuroendocrine carcinomas: a new clinicopathologic entity. Endocr Relat Cancer. 2015 Feb;22(1):35–45.

228. Frizziero M, Chakrabarty B, Nagy B, Lamarca A, Hubner RA, Valle JW, et al. Mixed Neuroendocrine Non-Neuroendocrine Neoplasms: A Systematic Review of a Controversial and Underestimated Diagnosis. J Clin Med. 2020 Jan 19;9(1).

229. Fiehn O. Combining genomics, metabolome analysis, and biochemical modelling to understand metabolic networks. Comp Funct Genomics. 2001;2(3):155–68.

230. Khakimov B, Rasmussen MA, Kannangara RM, Jespersen BM, Munck L, Engelsen SB. From metabolome to phenotype: GC-MS metabolomics of developing mutant barley seeds reveals effects of growth, temperature and genotype. Sci Rep. 2017 Aug 15;7(1):8195.

231. Ryan D, Robards K. Metabolomics: The greatest omics of them all? Anal Chem. 2006 Dec 1;78(23):7954–8.

232. Dunn WB, Bailey NJC, Johnson HE. Measuring the metabolome: current analytical technologies. The Analyst. 2005 May;130(5):606–25.

233. Roessner U, Luedemann A, Brust D, Fiehn O, Linke T, Willmitzer L, et al. Metabolic profiling allows comprehensive phenotyping of genetically or environmentally modified plant systems. Plant Cell. 2001 Jan;13(1):11–29.

234. Boros LG, Lerner MR, Morgan DL, Taylor SL, Smith BJ, Postier RG, et al. [1,2-13C2]-D-glucose profiles of the serum, liver, pancreas, and DMBA-induced pancreatic tumors of rats. Pancreas. 2005 Nov;31(4):337–43.

235. Beger RD, Dunn W, Schmidt MA, Gross SS, Kirwan JA, Cascante M, et al. Metabolomics enables precision medicine: 'A White Paper, Community Perspective'. Metabolomics Off J Metabolomic Soc. 2016;12(10):149.

236. Jacob M, Lopata AL, Dasouki M, Abdel Rahman AM. Metabolomics toward personalized medicine. Mass Spectrom Rev. 2019 May;38(3):221–38.

237. Junot C, Fenaille F, Colsch B, Bécher F. High resolution mass spectrometry based techniques at the crossroads of metabolic pathways. Mass Spectrom Rev. 2014 Dec;33(6):471–500.

238. Kohler I, Verhoeven A, Derks RJ, Giera M. Analytical pitfalls and challenges in clinical metabolomics. Bioanalysis. 2016 Jul;8(14):1509–32.

239. Duarte IF, Gil AM. Metabolic signatures of cancer unveiled by NMR spectroscopy of human biofluids. Prog Nucl Magn Reson Spectrosc. 2012 Apr;62:51–74.

240. Fan TW-M, Lane AN. Applications of NMR spectroscopy to systems biochemistry. Prog Nucl Magn Reson Spectrosc. 2016 Feb;92–93:18–53.

241. Ranjan R, Sinha N. Nuclear magnetic resonance (NMR)-based metabolomics for cancer research. NMR Biomed. 2019 Oct;32(10):e3916.

242. Fonslow BR, Yates JR. Capillary electrophoresis applied to proteomic analysis. J Sep Sci. 2009 Apr;32(8):1175–88.

243. Mischak H, Coon JJ, Novak J, Weissinger EM, Schanstra JP, Dominiczak AF. Capillary electrophoresis-mass spectrometry as a powerful tool in biomarker discovery and clinical diagnosis: an update of recent developments. Mass Spectrom Rev. 2009 Oct;28(5):703–24.

244. Ramautar R. Capillary Electrophoresis-Mass Spectrometry for Clinical Metabolomics. Adv Clin Chem. 2016;74:1–34.

245. Büscher JM, Czernik D, Ewald JC, Sauer U, Zamboni N. Cross-platform comparison of methods for quantitative metabolomics of primary metabolism. Anal Chem. 2009 Mar 15;81(6):2135–43.

246. DiBattista A, McIntosh N, Lamoureux M, Al-Dirbashi OY, Chakraborty P, Britz-McKibbin P. Metabolic Signatures of Cystic Fibrosis Identified in Dried Blood Spots For Newborn Screening Without Carrier Identification. J Proteome Res. 2019 Mar 1;18(3):841–54.

247. Pöhö P, Lipponen K, Bespalov MM, Sikanen T, Kotiaho T, Kostiainen R. Comparison of liquid chromatography-mass spectrometry and direct infusion microchip electrospray ionization mass spectrometry in global metabolomics of cell samples. Eur J Pharm Sci Off J Eur Fed Pharm Sci. 2019 Oct 1;138:104991.

248. Ambati CR, Vantaku V, Donepudi SR, Amara CS, Ravi SS, Mandalapu A, et al. Measurement of methylated metabolites using Liquid Chromatography-Mass Spectrometry and its biological application. Anal Methods Adv Methods Appl. 2019 Jan 7;11(1):49–57.

249. Begou O, Gika HG, Theodoridis GA, Wilson ID. Quality Control and Validation Issues in LC-MS Metabolomics. Methods Mol Biol Clifton NJ. 2018;1738:15–26.

250. Honour JW. Gas chromatography-mass spectrometry. Methods Mol Biol Clifton NJ. 2006;324:53–74.

251. Papadimitropoulos M-EP, Vasilopoulou CG, Maga-Nteve C, Klapa MI. Untargeted GC-MS Metabolomics. Methods Mol Biol Clifton NJ. 2018;1738:133–47.

252. Grimm F, Fets L, Anastasiou D. Gas Chromatography Coupled to Mass Spectrometry (GC-MS) to Study Metabolism in Cultured Cells. Adv Exp Med Biol. 2016;899:59–88.

253. Robles AI, Harris CC. Integration of multiple 'OMIC' biomarkers: A precision medicine strategy for lung cancer. Lung Cancer Amst Neth. 2017 May;107:50–8.

254. Tumas J, Kvederaviciute K, Petrulionis M, Kurlinkus B, Rimkus A, Sakalauskaite G, et al. Metabolomics in pancreatic cancer biomarkers research. Med Oncol Northwood Lond Engl. 2016 Dec;33(12):133.

255. Tian J, Xue W, Yin H, Zhang N, Zhou J, Long Z, et al. Differential Metabolic Alterations and Biomarkers Between Gastric Cancer and Colorectal Cancer: A Systematic Review and Meta-Analysis. OncoTargets Ther. 2020;13:6093–108.

256. Claudino WM, Quattrone A, Biganzoli L, Pestrin M, Bertini I, Di Leo A. Metabolomics: available results, current research projects in breast cancer, and future applications. J Clin Oncol Off J Am Soc Clin Oncol. 2007 Jul 1;25(19):2840–6.

257. DeFeo EM, Wu C-L, McDougal WS, Cheng LL. A decade in prostate cancer: from NMR to metabolomics. Nat Rev Urol. 2011 May 17;8(6):301–11.

258. Bayci AWL, Baker DA, Somerset AE, Turkoglu O, Hothem Z, Callahan RE, et al. Metabolomic identification of diagnostic serum-based biomarkers for advanced stage melanoma. Metabolomics Off J Metabolomic Soc. 2018 Aug 3;14(8):105.

259. Kim H-Y, Lee H, Kim S-H, Jin H, Bae J, Choi H-K. Discovery of potential biomarkers in human melanoma cells with different metastatic potential by metabolic and lipidomic profiling. Sci Rep. 2017 Aug 18;7(1):8864.

260. Miolo G, Di Gregorio E, Saorin A, Lombardi D, Scalone S, Buonadonna A, et al. Integration of Serum Metabolomics into Clinical Assessment to Improve Outcome Prediction of Metastatic Soft Tissue Sarcoma Patients Treated with Trabectedin. Cancers. 2020 Jul 21;12(7).

261. Mathé EA, Patterson AD, Haznadar M, Manna SK, Krausz KW, Bowman ED, et al. Noninvasive urinary metabolomic profiling identifies diagnostic and prognostic markers in lung cancer. Cancer Res. 2014 Jun 15;74(12):3259–70.

262. Mayers JR, Wu C, Clish CB, Kraft P, Torrence ME, Fiske BP, et al. Elevation of circulating branched-chain amino acids is an early event in human pancreatic adenocarcinoma development. Nat Med. 2014 Oct;20(10):1193–8.

263. Szpetnar M, Matras P, Boguszewska-Czubara A, Kiełczykowska M, Rudzki S, Musik I. Is additional enrichment of diet in branched-chain amino acids or glutamine beneficial for patients receiving total parenteral nutrition after

gastrointestinal cancer surgery? Adv Clin Exp Med Off Organ Wroclaw Med Univ. 2014 Jun;23(3):423–31.

264. Fukutake N, Ueno M, Hiraoka N, Shimada K, Shiraishi K, Saruki N, et al. A Novel Multivariate Index for Pancreatic Cancer Detection Based On the Plasma Free Amino Acid Profile. PloS One. 2015;10(7):e0132223.

265. Tan B, Qiu Y, Zou X, Chen T, Xie G, Cheng Y, et al. Metabonomics identifies serum metabolite markers of colorectal cancer. J Proteome Res. 2013 Jun 7;12(6):3000–9.

266. Leichtle AB, Nuoffer J-M, Ceglarek U, Kase J, Conrad T, Witzigmann H, et al. Serum amino acid profiles and their alterations in colorectal cancer. Metabolomics Off J Metabolomic Soc. 2012 Aug;8(4):643–53.

267. Tang Y, Li Z, Lazar L, Fang Z, Tang C, Zhao J. Metabolomics workflow for lung cancer: Discovery of biomarkers. Clin Chim Acta Int J Clin Chem. 2019 Aug;495:436–45.

268. Warburg O, Wind F, Negelein E. THE METABOLISM OF TUMORS IN THE BODY. J Gen Physiol. 1927 Mar 7;8(6):519–30.

269. Boroughs LK, DeBerardinis RJ. Metabolic pathways promoting cancer cell survival and growth. Nat Cell Biol. 2015 Apr;17(4):351–9.

270. Cairns RA, Harris IS, Mak TW. Regulation of cancer cell metabolism. Nat Rev Cancer. 2011 Feb;11(2):85–95.

271. Fan TWM, Kucia M, Jankowski K, Higashi RM, Ratajczak J, Ratajczak MZ, et al. Rhabdomyosarcoma cells show an energy producing anabolic metabolic phenotype compared with primary myocytes. Mol Cancer. 2008 Oct 21;7:79.

272. Mazurek S, Eigenbrodt E. The tumor metabolome. Anticancer Res. 2003 Apr;23(2A):1149–54.

273. Pavlova NN, Thompson CB. The Emerging Hallmarks of Cancer Metabolism. Cell Metab. 2016 Jan 12;23(1):27–47.

274. Vander Heiden MG, DeBerardinis RJ. Understanding the Intersections between Metabolism and Cancer Biology. Cell. 2017 Feb 9;168(4):657–69.

275. Osthus RC, Shim H, Kim S, Li Q, Reddy R, Mukherjee M, et al. Deregulation of glucose transporter 1 and glycolytic gene expression by c-Myc. J Biol Chem. 2000 Jul 21;275(29):21797–800.

276. Liang J, Cao R, Zhang Y, Xia Y, Zheng Y, Li X, et al. PKM2 dephosphorylation by Cdc25A promotes the Warburg effect and tumorigenesis. Nat Commun. 2016 Aug 3;7:12431.

277. Luo W, Chang R, Zhong J, Pandey A, Semenza GL. Histone demethylase JMJD2C is a coactivator for hypoxia-inducible factor 1 that is required for breast cancer progression. Proc Natl Acad Sci U S A. 2012 Dec 4;109(49):E3367-3376.

278. Yang W, Zheng Y, Xia Y, Ji H, Chen X, Guo F, et al. ERK1/2-dependent phosphorylation and nuclear translocation of PKM2 promotes the Warburg effect. Nat Cell Biol. 2012 Dec;14(12):1295–304.

279. Xian S, Shang D, Kong G, Tian Y. FOXJ1 promotes bladder cancer cell growth and regulates Warburg effect. Biochem Biophys Res Commun. 2018 Jan 1;495(1):988–94.

280. Nagdas S, Kashatus JA, Nascimento A, Hussain SS, Trainor RE, Pollock SR, et al. Drp1 Promotes KRas-Driven Metabolic Changes to Drive Pancreatic Tumor Growth. Cell Rep. 2019 Aug 13;28(7):1845-1859.e5.

281. Maddocks ODK, Berkers CR, Mason SM, Zheng L, Blyth K, Gottlieb E, et al. Serine starvation induces stress and p53-dependent metabolic remodelling in cancer cells. Nature. 2013 Jan 24;493(7433):542–6.

282. Dibble CC, Manning BD. Signal integration by mTORC1 coordinates nutrient input with biosynthetic output. Nat Cell Biol. 2013 Jun;15(6):555–64.

283. DeBerardinis RJ, Chandel NS. Fundamentals of cancer metabolism. Sci Adv. 2016 May;2(5):e1600200.

284. Griffin JL, Shockcor JP. Metabolic profiles of cancer cells. Nat Rev Cancer. 2004 Jul;4(7):551–61.

285. Chen R, Mias GI, Li-Pook-Than J, Jiang L, Lam HYK, Chen R, et al. Personal omics profiling reveals dynamic molecular and medical phenotypes. Cell. 2012 Mar 16;148(6):1293–307.

286. Spratlin JL, Serkova NJ, Eckhardt SG. Clinical applications of metabolomics in oncology: a review. Clin Cancer Res Off J Am Assoc Cancer Res. 2009 Jan 15;15(2):431–40.

287. Luengo A, Gui DY, Vander Heiden MG. Targeting Metabolism for Cancer Therapy. Cell Chem Biol. 2017 Sep 21;24(9):1161–80.

288. Li J, Eu JQ, Kong LR, Wang L, Lim YC, Goh BC, et al. Targeting Metabolism in Cancer Cells and the Tumour Microenvironment for Cancer Therapy. Mol Basel Switz. 2020 Oct 20;25(20).

289. Ni Y, Xie G, Jia W. Metabonomics of human colorectal cancer: new approaches for early diagnosis and biomarker discovery. J Proteome Res. 2014 Sep 5;13(9):3857–70.

290. Tanasova M, Begoyan VV, Weselinski LJ. Targeting Sugar Uptake and Metabolism for Cancer Identification and Therapy: An Overview. Curr Top Med Chem. 2018;18(6):467–83.

291. Zu XL, Guppy M. Cancer metabolism: facts, fantasy, and fiction. Biochem Biophys Res Commun. 2004 Jan 16;313(3):459–65.

292. Ippolito JE, Xu J, Jain S, Moulder K, Mennerick S, Crowley JR, et al. An integrated functional genomics and metabolomics approach for defining poor prognosis in human neuroendocrine cancers. Proc Natl Acad Sci U S A. 2005 Jul 12;102(28):9901–6.

293. Li W, Cohen A, Sun Y, Squires J, Braas D, Graeber TG, et al. The Role of CD44 in Glucose Metabolism in Prostatic Small Cell Neuroendocrine Carcinoma. Mol Cancer Res MCR. 2016 Apr;14(4):344–53.

294. Eisenhofer G, Pacak K, Huynh T-T, Qin N, Bratslavsky G, Linehan WM, et al. Catecholamine metabolomic and secretory phenotypes in phaeochromocytoma. Endocr Relat Cancer. 2011 Feb;18(1):97–111.

295. Petenuci J, Guimaraes AG, Fagundes GFC, Benedetti AFF, Afonso ACF, Pereira MAA, et al. Genetic and clinical aspects of paediatric pheochromocytomas and paragangliomas. Clin Endocrinol (Oxf). 2021 Mar 20;

296. de Cubas AA, Korpershoek E, Inglada-Pérez L, Letouzé E, Currás-Freixes M, Fernández AF, et al. DNA Methylation Profiling in Pheochromocytoma and Paraganglioma Reveals Diagnostic and Prognostic Markers. Clin Cancer Res Off J Am Assoc Cancer Res. 2015 Jul 1;21(13):3020–30.

297. Jochmanova I, Pacak K. Pheochromocytoma: The First Metabolic Endocrine Cancer. Clin Cancer Res Off J Am Assoc Cancer Res. 2016 Oct 15;22(20):5001–11.

298. Letouzé E, Martinelli C, Loriot C, Burnichon N, Abermil N, Ottolenghi C, et al. SDH mutations establish a hypermethylator phenotype in paraganglioma. Cancer Cell. 2013 Jun 10;23(6):739–52.

299. Wallace PW, Conrad C, Brückmann S, Pang Y, Caleiras E, Murakami M, et al. Metabolomics, machine learning and immunohistochemistry to predict succinate dehydrogenase mutational status in phaeochromocytomas and paragangliomas. J Pathol. 2020 Aug;251(4):378–87.

300. Dwight T, Kim E, Novos T, Clifton-Bligh RJ. Metabolomics in the Diagnosis of Pheochromocytoma and Paraganglioma. Horm Metab Res Horm Stoffwechselforschung Horm Metab. 2019 Jul;51(7):443–50.

301. Peitzsch M, Pelzel D, Glöckner S, Prejbisz A, Fassnacht M, Beuschlein F, et al. Simultaneous liquid chromatography tandem mass spectrometric determination of urinary free metanephrines and catecholamines, with comparisons of free and deconjugated metabolites. Clin Chim Acta Int J Clin Chem. 2013 Mar 15;418:50–8.

302. Richter S, Gieldon L, Pang Y, Peitzsch M, Huynh T, Leton R, et al. Metabolome-guided genomics to identify pathogenic variants in isocitrate dehydrogenase,

fumarate hydratase, and succinate dehydrogenase genes in pheochromocytoma and paraganglioma. Genet Med Off J Am Coll Med Genet. 2019 Mar;21(3):705–17.

303. Rao JU, Engelke UFH, Sweep FCGJ, Pacak K, Kusters B, Goudswaard AG, et al. Genotype-specific differences in the tumor metabolite profile of pheochromocytoma and paraganglioma using untargeted and targeted metabolomics. J Clin Endocrinol Metab. 2015 Feb;100(2):E214-222.

304. Imperiale A, Moussallieh F-M, Roche P, Battini S, Cicek AE, Sebag F, et al. Metabolome profiling by HRMAS NMR spectroscopy of pheochromocytomas and paragangliomas detects SDH deficiency: clinical and pathophysiological implications. Neoplasia N Y N. 2015 Jan;17(1):55–65.

305. Kinross JM, Drymousis P, Jiménez B, Frilling A. Metabonomic profiling: a novel approach in neuroendocrine neoplasias. Surgery. 2013 Dec;154(6):1185–92; discussion 1192-1193.

306. Sadanandam A, Wullschleger S, Lyssiotis CA, Grötzinger C, Barbi S, Bersani S, et al. A Cross-Species Analysis in Pancreatic Neuroendocrine Tumors Reveals Molecular Subtypes with Distinctive Clinical, Metastatic, Developmental, and Metabolic Characteristics. Cancer Discov. 2015 Dec;5(12):1296–313.

307. Imperiale A, Poncet G, Addeo P, Ruhland E, Roche C, Battini S, et al. Metabolomics of Small Intestine Neuroendocrine Tumors and Related Hepatic Metastases. Metabolites. 2019 Dec 11;9(12).

308. Godzien J, Kalaska B, Adamska-Patruno E, Siroka J, Ciborowski M, Kretowski A, et al. Oxidized glycerophosphatidylcholines in diabetes through non-targeted metabolomics: Their annotation and biological meaning. J Chromatogr B Analyt Technol Biomed Life Sci. 2019 Jul 1;1120:62–70.

309. Dudzik D, Zorawski M, Skotnicki M, Zarzycki W, Kozlowska G, Bibik-Malinowska K, et al. Metabolic fingerprint of Gestational Diabetes Mellitus. J Proteomics. 2014 May 30;103:57–71.

310. Naz S, Garcia A, Rusak M, Barbas C. Method development and validation for rat serum fingerprinting with CE-MS: application to ventilator-induced-lung-injury study. Anal Bioanal Chem. 2013 May;405(14):4849–58.

311. Gil-de-la-Fuente A, Godzien J, Saugar S, Garcia-Carmona R, Badran H, Wishart DS, et al. CEU Mass Mediator 3.0: A Metabolite Annotation Tool. J Proteome Res. 2019 Feb 1;18(2):797–802.

312. Pauling JK, Hermansson M, Hartler J, Christiansen K, Gallego SF, Peng B, et al. Proposal for a common nomenclature for fragment ions in mass spectra of lipids. PloS One. 2017;12(11):e0188394.

313. Das R, Pal TK. Method Development and Validation of Liquid Chromatography-Tandem Mass Spectrometry for Angiotensin-II in Human Plasma: Application to Study Interaction Between Atorvastatin & Olmesartan Drug Combination. Indian J Clin Biochem IJCB. 2015 Jul;30(3):334–44.

314. Mudarra Rubio A, Montes-Bayón M, Blanco-González E, Sanz-Medel A. Sample preparation strategies for quantitative analysis of catalase in red blood cells by elemental mass spectrometry. Met Integr Biometal Sci. 2010 Sep;2(9):638–45.

315. Choe S, Kim S, Choi H, Choi H, Chung H, Hwang B. Automated toxicological screening reports of modified Agilent MSD Chemstation combined with Microsoft Visual Basic application programs. Forensic Sci Int. 2010 Jun 15;199(1–3):50–7.

316. Choe S, Woo SH, Kim DW, Park Y, Choi H, Hwang BY, et al. Development of a target component extraction method from GC-MS data with an in-house program for metabolite profiling. Anal Biochem. 2012 Jul 15;426(2):94–102.

317. Chang S, Wang M, Tian Y, Qi J, Qiu Z. Systematic analysis and identification of the absorption and metabolic components of Zengye decoction in type 2 diabetic rats by HPLC-ESI-Q-TOF-MS/MS. Chin Med. 2020;15:50.

318. Vizcaino MI, Crawford JM. Secondary Metabolic Pathway-Targeted Metabolomics. Methods Mol Biol Clifton NJ. 2016;1401:175–95.

319. Triba MN, Le Moyec L, Amathieu R, Goossens C, Bouchemal N, Nahon P, et al. PLS/OPLS models in metabolomics: the impact of permutation of dataset rows on the K-fold cross-validation quality parameters. Mol Biosyst. 2015 Jan;11(1):13–9.

320. Gil de la Fuente A, Traldi F, Siroka J, Kretowski A, Ciborowski M, Otero A, et al. Characterization and annotation of oxidized glycerophosphocholines for non-targeted metabolomics with LC-QTOF-MS data. Anal Chim Acta. 2018 Dec 11;1037:358–68.

321. Montenegro-Burke JR, Guijas C, Siuzdak G. METLIN: A Tandem Mass Spectral Library of Standards. Methods Mol Biol Clifton NJ. 2020;2104:149–63.

322. Ruttkies C, Schymanski EL, Wolf S, Hollender J, Neumann S. MetFrag relaunched: incorporating strategies beyond in silico fragmentation. J Cheminformatics. 2016;8:3.

323. Jackson CH. flexsurv: A Platform for Parametric Survival Modeling in R. J Stat Softw. 2016 May 12;70.

324. Chong EY, Huang Y, Wu H, Ghasemzadeh N, Uppal K, Quyyumi AA, et al. Local false discovery rate estimation using feature reliability in LC/MS metabolomics data. Sci Rep. 2015 Nov 24;5:17221.

325. Aggarwal S, Yadav AK. False Discovery Rate Estimation in Proteomics. Methods Mol Biol Clifton NJ. 2016;1362:119–28.

326. Chong J, Soufan O, Li C, Caraus I, Li S, Bourque G, et al. MetaboAnalyst 4.0: towards more transparent and integrative metabolomics analysis. Nucleic Acids Res. 2018 Jul 2;46(W1):W486–94.

327. Chong J, Xia J. Using MetaboAnalyst 4.0 for Metabolomics Data Analysis, Interpretation, and Integration with Other Omics Data. Methods Mol Biol Clifton NJ. 2020;2104:337–60.

328. Gemperline DC, Scalf M, Smith LM, Vierstra RD. Morpheus Spectral Counter: A computational tool for label-free quantitative mass spectrometry using the Morpheus search engine. Proteomics. 2016 Mar;16(6):920–4.

329. López-López Á, Godzien J, Soldevilla B, Gradillas A, López-Gonzálvez Á, Lens-Pardo A, et al. Oxidized lipids in the metabolic profiling of neuroendocrine tumors - Analytical challenges and biological implications. J Chromatogr A. 2020 Aug 16;1625:461233.

330. Soldevilla B, López-López A, Lens-Pardo A, Carretero-Puche C, Lopez-Gonzalvez A, La Salvia A, et al. Comprehensive Plasma Metabolomic Profile of Patients with Advanced Neuroendocrine Tumors (NETs). Diagnostic and Biological Relevance. Cancers. 2021 May 27;13(11).

331. Suhre K, Shin S-Y, Petersen A-K, Mohney RP, Meredith D, Wägele B, et al. Human metabolic individuality in biomedical and pharmaceutical research. Nature. 2011 Aug 31;477(7362):54–60.

332. Sullivan LB, Gui DY, Vander Heiden MG. Altered metabolite levels in cancer: implications for tumour biology and cancer therapy. Nat Rev Cancer. 2016 Nov;16(11):680–93.

333. Newgard CB. Metabolomics and Metabolic Diseases: Where Do We Stand? Cell Metab. 2017 Jan 10;25(1):43–56.

334. Oakman C, Tenori L, Claudino WM, Cappadona S, Nepi S, Battaglia A, et al. Identification of a serum-detectable metabolomic fingerprint potentially correlated with the presence of micrometastatic disease in early breast cancer patients at varying risks of disease relapse by traditional prognostic methods. Ann Oncol Off J Eur Soc Med Oncol. 2011 Jun;22(6):1295–301.

335. Martín-Blázquez A, Díaz C, González-Flores E, Franco-Rivas D, Jiménez-Luna C, Melguizo C, et al. Untargeted LC-HRMS-based metabolomics to identify novel biomarkers of metastatic colorectal cancer. Sci Rep. 2019 Dec 27;9(1):20198.

336. Bertini I, Cacciatore S, Jensen BV, Schou JV, Johansen JS, Kruhøffer M, et al. Metabolomic NMR fingerprinting to identify and predict survival of patients with metastatic colorectal cancer. Cancer Res. 2012 Jan 1;72(1):356–64.

337. Deja S, Porebska I, Kowal A, Zabek A, Barg W, Pawelczyk K, et al. Metabolomics provide new insights on lung cancer staging and discrimination from chronic obstructive pulmonary disease. J Pharm Biomed Anal. 2014 Nov;100:369–80.

338. Corbet C, Feron O. Cancer cell metabolism and mitochondria: Nutrient plasticity for TCA cycle fueling. Biochim Biophys Acta Rev Cancer. 2017 Aug;1868(1):7–15.

339. Yang C, Ko B, Hensley CT, Jiang L, Wasti AT, Kim J, et al. Glutamine oxidation maintains the TCA cycle and cell survival during impaired mitochondrial pyruvate transport. Mol Cell. 2014 Nov 6;56(3):414–24.

340. Corbet C, Feron O. Metabolic and mind shifts: from glucose to glutamine and acetate addictions in cancer. Curr Opin Clin Nutr Metab Care. 2015 Jul;18(4):346–53.

341. Pollard PJ, Wortham NC, Tomlinson IPM. The TCA cycle and tumorigenesis: the examples of fumarate hydratase and succinate dehydrogenase. Ann Med. 2003;35(8):632–9.

342. Samudio I, Harmancey R, Fiegl M, Kantarjian H, Konopleva M, Korchin B, et al. Pharmacologic inhibition of fatty acid oxidation sensitizes human leukemia cells to apoptosis induction. J Clin Invest. 2010 Jan;120(1):142–56.

343. Santos CR, Schulze A. Lipid metabolism in cancer. FEBS J. 2012 Aug;279(15):2610–23.

344. Martín-Sierra C, Laranjeira P, Domingues MR, Paiva A. Lipoxidation and cancer immunity. Redox Biol. 2019 May;23:101103.

345. Carmeliet P, Jain RK. Angiogenesis in cancer and other diseases. Nature. 2000 Sep 14;407(6801):249–57.

346. La Rosa S, Uccella S, Finzi G, Albarello L, Sessa F, Capella C. Localization of vascular endothelial growth factor and its receptors in digestive endocrine tumors: correlation with microvessel density and clinicopathologic features. Hum Pathol. 2003 Jan;34(1):18–27.

347. Kamm A, Przychodzen P, Kuban-Jankowska A, Jacewicz D, Dabrowska AM, Nussberger S, et al. Nitric oxide and its derivatives in the cancer battlefield. Nitric Oxide Biol Chem. 2019 Dec 1;93:102–14.

348. Luu Hoang KN, Anstee JE, Arnold JN. The Diverse Roles of Heme Oxygenase-1 in Tumor Progression. Front Immunol. 2021;12:658315.

349. Jazwa A, Loboda A, Golda S, Cisowski J, Szelag M, Zagorska A, et al. Effect of heme and heme oxygenase-1 on vascular endothelial growth factor synthesis and angiogenic potency of human keratinocytes. Free Radic Biol Med. 2006 Apr 1;40(7):1250–63.

350. Tsolekile N, Nelana S, Oluwafemi OS. Porphyrin as Diagnostic and Therapeutic Agent. Mol Basel Switz. 2019 Jul 23;24(14).

351. Batlle AM. Porphyrins, porphyrias, cancer and photodynamic therapy--a model for carcinogenesis. J Photochem Photobiol B. 1993 Sep;20(1):5–22.

352. Udagawa M, Horie Y, Hirayama C. Aberrant porphyrin metabolism in hepatocellular carcinoma. Biochem Med. 1984 Apr;31(2):131–9.

353. el-Sharabasy MM, el-Waseef AM, Hafez MM, Salim SA. Porphyrin metabolism in some malignant diseases. Br J Cancer. 1992 Mar;65(3):409–12.

354. Brun A, Sandberg S. Mechanisms of photosensitivity in porphyric patients with special emphasis on erythropoietic protoporphyria. J Photochem Photobiol B. 1991 Sep;10(4):285–302.

355. Girotti AW. Photosensitized oxidation of membrane lipids: reaction pathways, cytotoxic effects, and cytoprotective mechanisms. J Photochem Photobiol B. 2001 Oct;63(1–3):103–13.

356. Golding JP, Wardhaugh T, Patrick L, Turner M, Phillips JB, Bruce JI, et al. Targeting tumour energy metabolism potentiates the cytotoxicity of 5-aminolevulinic acid photodynamic therapy. Br J Cancer. 2013 Aug 20;109(4):976–82.

357. Haeubl M, Schuerz S, Svejda B, Reith LM, Gruber B, Pfragner R, et al. Asymmetrically substituted cationic indole- and fluorene porphyrins inhibit tumor proliferation in small intestinal neuroendocrine tumors and medullary thyroid carcinomas. Eur J Med Chem. 2010 Feb;45(2):760–73.

358. Schwach G, Thamyongkit P, Reith LM, Svejda B, Knör G, Pfragner R, et al. A water soluble tri-cationic porphyrin-EDTA conjugate induces apoptosis in human neuroendocrine tumor cell lines. Bioorganic Chem. 2012 Feb;40(1):108–13.

359. Bonkovsky HL, Guo J-T, Hou W, Li T, Narang T, Thapar M. Porphyrin and heme metabolism and the porphyrias. Compr Physiol. 2013 Jan;3(1):365–401.

360. Sedlak TW, Snyder SH. Bilirubin benefits: cellular protection by a biliverdin reductase antioxidant cycle. Pediatrics. 2004 Jun;113(6):1776–82.

361. Kapitulnik J, Maines MD. Pleiotropic functions of biliverdin reductase: cellular signaling and generation of cytoprotective and cytotoxic bilirubin. Trends Pharmacol Sci. 2009 Mar;30(3):129–37.

362. Jansen T, Hortmann M, Oelze M, Opitz B, Steven S, Schell R, et al. Conversion of biliverdin to bilirubin by biliverdin reductase contributes to endothelial cell protection by heme oxygenase-1-evidence for direct and indirect antioxidant actions of bilirubin. J Mol Cell Cardiol. 2010 Aug;49(2):186–95.

363. Cavuoto P, Fenech MF. A review of methionine dependency and the role of methionine restriction in cancer growth control and life-span extension. Cancer Treat Rev. 2012 Oct;38(6):726–36.

364. De Luca A, Sanna F, Sallese M, Ruggiero C, Grossi M, Sacchetta P, et al. Methionine sulfoxide reductase A down-regulation in human breast cancer cells results in a more aggressive phenotype. Proc Natl Acad Sci U S A. 2010 Oct 26;107(43):18628–33.

365. Martínez Y, Li X, Liu G, Bin P, Yan W, Más D, et al. The role of methionine on metabolism, oxidative stress, and diseases. Amino Acids. 2017 Dec;49(12):2091–8.

366. Kim JI, Noh MR, Kim KY, Jang H-S, Kim H-Y, Park KM. Methionine sulfoxide reductase A deficiency exacerbates progression of kidney fibrosis induced by unilateral ureteral obstruction. Free Radic Biol Med. 2015 Dec;89:201–8.

367. Singh MP, Kim KY, Kim H-Y. Methionine sulfoxide reductase A deficiency exacerbates acute liver injury induced by acetaminophen. Biochem Biophys Res Commun. 2017 Feb 26;484(1):189–94.

368. Hansel A, Heinemann SH, Hoshi T. Heterogeneity and function of mammalian MSRs: enzymes for repair, protection and regulation. Biochim Biophys Acta. 2005 Jan 17;1703(2):239–47.

369. Xu Y-Y, Du F, Meng B, Xie G-H, Cao J, Fan D, et al. Hepatic overexpression of methionine sulfoxide reductase A reduces atherosclerosis in apolipoprotein E-deficient mice. J Lipid Res. 2015 Oct;56(10):1891–900.

370. Picot CR, Perichon M, Lundberg KC, Friguet B, Szweda LI, Petropoulos I. Alterations in mitochondrial and cytosolic methionine sulfoxide reductase activity during cardiac ischemia and reperfusion. Exp Gerontol. 2006 Jul;41(7):663–7.

371. Sanderson SM, Gao X, Dai Z, Locasale JW. Methionine metabolism in health and cancer: a nexus of diet and precision medicine. Nat Rev Cancer. 2019 Nov;19(11):625–37.

372. Wanders D, Hobson K, Ji X. Methionine Restriction and Cancer Biology. Nutrients. 2020 Mar 3;12(3).

373. Platten M, Nollen EAA, Röhrig UF, Fallarino F, Opitz CA. Tryptophan metabolism as a common therapeutic target in cancer, neurodegeneration and beyond. Nat Rev Drug Discov. 2019 May;18(5):379–401.

374. Zhai L, Spranger S, Binder DC, Gritsina G, Lauing KL, Giles FJ, et al. Molecular Pathways: Targeting IDO1 and Other Tryptophan Dioxygenases for Cancer Immunotherapy. Clin Cancer Res Off J Am Assoc Cancer Res. 2015 Dec 15;21(24):5427–33.

375. Opitz CA, Somarribas Patterson LF, Mohapatra SR, Dewi DL, Sadik A, Platten M, et al. The therapeutic potential of targeting tryptophan catabolism in cancer. Br J Cancer. 2020 Jan;122(1):30–44.

376. Amobi A, Qian F, Lugade AA, Odunsi K. Tryptophan Catabolism and Cancer Immunotherapy Targeting IDO Mediated Immune Suppression. Adv Exp Med Biol. 2017;1036:129–44.

377. Santhanam S, Alvarado DM, Ciorba MA. Therapeutic targeting of inflammation and tryptophan metabolism in colon and gastrointestinal cancer. Transl Res J Lab Clin Med. 2016 Jan;167(1):67–79.

378. Romas NA, Ionascu L, Ionescu G, Wechsler M, Tannenbaum M, Veenema RJ. Anergy and tryptophan metabolism in bladder cancer. J Urol. 1976 Apr;115(4):387–9.

379. Wettersten HI, Aboud OA, Lara PN, Weiss RH. Metabolic reprogramming in clear cell renal cell carcinoma. Nat Rev Nephrol. 2017 Jul;13(7):410–9.

380. Schroecksnadel K, Winkler C, Fuith LC, Fuchs D. Tryptophan degradation in patients with gynecological cancer correlates with immune activation. Cancer Lett. 2005 Jun 8;223(2):323–9.

381. Swami T, Weber HC. Updates on the biology of serotonin and tryptophan hydroxylase. Curr Opin Endocrinol Diabetes Obes. 2018 Feb;25(1):12–21.

382. Kvols LK. Metastatic carcinoid tumors and the malignant carcinoid syndrome. Ann N Y Acad Sci. 1994 Sep 15;733:464–70.

383. Chan DL, Clarke SJ, Diakos CI, Roach PJ, Bailey DL, Singh S, et al. Prognostic and predictive biomarkers in neuroendocrine tumours. Crit Rev Oncol Hematol. 2017 May;113:268–82.

384. Tirosh A, Nilubol N, Patel D, Kebebew E. Prognostic Utility of 24-Hour Urinary 5-HIAA Doubling Time in Patients With Neuroendocrine Tumors. Endocr Pract Off J Am Coll Endocrinol Am Assoc Clin Endocrinol. 2018 Aug;24(8):710–7.

385. Turner GB, Johnston BT, McCance DR, McGinty A, Watson RGP, Patterson CC, et al. Circulating markers of prognosis and response to treatment in patients with midgut carcinoid tumours. Gut. 2006 Nov;55(11):1586–91.

386. Suzawa S, Takahashi K, Shimada T, Ohta T. Carbonyl stress-induced 5-hydroxytriptamine secretion from RIN-14B, rat pancreatic islet tumor cells, via the activation of transient receptor potential ankyrin 1. Brain Res Bull. 2016 Jul;125:181–6.

387. Eleftheriadis T, Pissas G, Sounidaki M, Tsogka K, Antoniadis N, Antoniadi G, et al. Indoleamine 2,3-dioxygenase, by degrading L-tryptophan, enhances carnitine palmitoyltransferase I activity and fatty acid oxidation, and exerts fatty acid-dependent effects in human alloreactive CD4+ T-cells. Int J Mol Med. 2016 Nov;38(5):1605–13.

388. Reuter SE, Evans AM. Carnitine and acylcarnitines: pharmacokinetic, pharmacological and clinical aspects. Clin Pharmacokinet. 2012 Sep 1;51(9):553–72.

389. Gao B, Lue H-W, Podolak J, Fan S, Zhang Y, Serawat A, et al. Multi-Omics Analyses Detail Metabolic Reprogramming in Lipids, Carnitines, and Use of Glycolytic Intermediates between Prostate Small Cell Neuroendocrine Carcinoma and Prostate Adenocarcinoma. Metabolites. 2019 Apr 26;9(5).

9. SUPPLEMENTARY MATERIALS

Table 1. List of statistically significant annotated metabolites discriminating between the plasma profiles of NET patients (N=77) and controls (N=68) with their statistical characteristics after UVDA and MVDA (percentage of change, p-value, p(corr) and VIP) and analytical descriptors (measured mass and its deviation from the theoretical one, experimental retention time, analytical platform on which it has been detected, identification source where DB corresponds to database result, confidence level for identification according to the metabolomics standards initiative and its corresponding Human Metabolome Database (HMDB) code (http://www.hmdb.ca/)). (* = Multiple identification options)

Compound	Formula	Mass (Da)	RT (min)	% change	*P*- value	p(corr)	VIP	Mass error (ppm)	Analytical platform	Identification source	Confidence level	HMDB Code
Amines												
Triethylamine	$C_6H_{15}N$	101.1204	10.28	-53	0.0009			0	CE-MS	DB	3	HMDB0032539
Amino acids, peptides, and analogues												
Arginine	$C_6H_{14}N_4O_2$	174.1131	9.98	243	4.58E-35	-0.80	2.33	15	CE-MS LC-MS(+)	DB	2	HMDB0000517
Arg-Val	$C_{11}H_{23}N_5O_3$	273.1822	9.95	66	0.0004			8	CE-MS	DB	3	HMDB0028722
Aspartate	$C_4H_7NO_4$	133.0375	13.80	-32	4.98E-13			2	CE-MS	DB	2	HMDB0000191
Cys-Gly	$C_5H_{10}N_2O_3S$	178.0412	12.19	-29	8.00E-09			0	CE-MS	DB	3	HMDB0000078
Cys-Gly disulfide	$C_8H_{15}N_3O_5S_2$	297.0455	12.19	-41	1.39E-08	0.49	1.63	1	CE-MS	DB	3	HMDB0000709
Cysteineglutathione disulfide	$C_{13}H_{22}N_4O_8S_2$	426.0912	13.95	-37	7.40E-06			8	CE-MS	DB	3	HMDB0000656
Dimethyl-Arginine (symmetric)	$C_8H_{18}N_4O_2$	202.1428	10.67	25	0.0006			1	CE-MS	DB	2	HMDB0003334
GalactosylhydroxyLys	$C_{12}H_{24}N_2O_8$	324.1558	11.49	42	0.0014			8	CE-MS	DB	3	HMDB0000600
gamma-Glu-orn *	$C_{10}H_{19}N_3O_5$	261.1335	11.30	34	0.0103			4	CE-MS	DB	3	HMDB0002248
Glu-Ala*	$C_8H_{14}N_2O_5$	218.0904	14.40	135	4.38E-14			1	CE-MS	DB	3	HMDB0006248
Glu-Arg	$C_{11}H_{21}N_5O_5$	303.1554	11.49	87	6.28E-14	-0.52	1.55	4	CE-MS	DB	3	HMDB0028813
Glu-Asp	$C_9H_{14}N_2O_7$	262.0801	3.78	54	0.0036			7	LC-MS(-)	MSMS	2	HMDB0030419
Glu-hyp	$C_{10}H_{16}N_2O_6$	260.0993	12.98	37	5.12E-07			6	CE-MS	DB	3	HMDB0011161
Glu-Lys/Ɛ-Glu-Lys	$C_{11}H_{21}N_3O_5$	275.1481	12.32	67	1.20E-09			2	CE-MS	DB	3	HMDB0029154
Glu-Lys/Ɛ-Glu-Lys	$C_{11}H_{21}N_3O_5$	275.1481	11.37	58	1.55E-07			2	CE-MS	DB	3	HMDB0029155
Glutamine	$C_5H_{10}N_2O_3$	146.0691	1.34	69	0.0006			1	LC-MS(+) LC-MS(-)	MSMS	2	HMDB0000641

Compound	Formula	Mass (Da)	RT (min)	% change	*P*- value	p(corr)	VIP	Mass error (ppm)	Analytical platform	Identification source	Confidence level	HMDB Code
Glu-Val	$C_{10}H_{18}N_2O_5$	246.1217	14.68	48	0.0009			1	CE-MS LC-MS(+)	DB	3	HMDB0028832
Glycine	$C_2H_5NO_2$	75.0320	9.75	32	0.0202			-	GC-MS	Fiehn	2	HMDB0000123
Gly-Pro	$C_7H_{12}N_2O_3$	172.0831	15.89	-20	0.0275			10	CE-MS	DB	3	HMDB0000721
Homocitrulline	$C_7H_{15}N_3O_3$	189.1118	13.52	44	0.0027			3	CE-MS	DB	3	HMDB0000679
Iminodiacetic acid	$C_4H_7NO_4$	133.0375	12.87	-37	0.0158			-	GC-MS CE-MS	Fiehn	2	HMDB0011753
Indoleacetyl glutamine	$C_{15}H_{17}N_3O_4$	303.1219	1.70	203	1.43E-06	-0.58	2.05	2	LC-MS(-) LC-MS(+)	DB	3	HMDB0013240
Leu-hyp	$C_{11}H_{20}N_2O_4$	244.1423	2.00	87	0.0018			2	LC-MS(-)	DB	3	HMDB0028867
Leu-Phe	$C_{15}H_{22}N_2O_3$	278.1630	2.14	Presented in cancer group	3.54E-05	-0.60	2.45	0	LC-MS(-)	DB	3	HMDB0013243
Lys-Asp*	$C_{10}H_{19}N_3O_5$	261.1335	11.30	34	0.0103			4	CE-MS	DB	3	HMDB0028947
Methionine S-oxide	$C_5H_{11}NO_3S$	165.0478	14.06	110	3.30E-09			11	CE-MS	DB	2	HMDB0002005
N2-Methyl-lysine	$C_7H_{16}N_2O_2$	160.1208	10.67	-77	6.97E-09			2	CE-MS	DB	2	HMDB0002038
N2-Methylproline	$C_6H_{11}NO_2$	129.0791	14.59	-43	0.0031			1	CE-MS	DB	2	HMDB0059649
N6-Acetyl-hydroxy-lysine*	$C_8H_{16}N_2O_4$	204.1103	12.78	-55	0.0002			3	CE-MS	DB	3	HMDB0033891
N-acetyl-lysine	$C_8H_{16}N_2O_3$	188.1155	13.70	20	0.0002			3	CE-MS	DB	2	HMDB0000206
Ornithine	$C_5H_{12}N_2O_2$	132.0906	9.66	-39	5.58E-19	0.65	1.65	6	CE-MS	DB	2	HMDB0000214
Phenylalanine	$C_9H_{11}NO_2$	165.0770	13.88	-58	0.0050			12	CE-MS GC-MS	DB	2	HMDB0000159
Pipecolic acid	$C_6H_{11}NO_2$	129.0790	10.14	49	0.0307			-	GC-MS	Fiehn	2	HMDB0000716
Pyroglutamine	$C_5H_8N_2O_2$	128.0583	11.48	68	1.41E-05			2	CE-MS	DB	3	HMDB0062558
Ser-Ala*	$C_6H_{12}N_2O_4$	176.0789	13.07	-38	1.37E-08			4	CE-MS	DB	3	HMDB0029032
Ser-hyp*	$C_8H_{14}N_2O_5$	218.0904	14.40	135	4.38E-14			1	CE-MS	DB	3	HMDB0029040
Ser-Val*	$C_8H_{16}N_2O_4$	204.1103	12.78	-55	0.0002			3	CE-MS	DB	3	HMDB0029052
Stearoyl-tyrosine*	$C_{27}H_{45}NO_4$	447.3349	5.15	-66	9.67E-17	0.75	3.74	1	LC-MS(+)	DB	3	HMDB0062343
Suberylglycine	$C_{10}H_{17}NO_5$	231.1106	1.19	Presented in cancer group	0.0001	-0.73	3.82	1	LC-MS(-)	DB	3	HMDB0000953

Compound	Formula	Mass (Da)	RT (min)	% change	*P*- value	p(corr)	VIP	Mass error (ppm)	Analytical platform	Identification source	Confidence level	HMDB Code
Thr-Ala	$C_7H_{14}N_2O_4$	190.0954	13.83	90	5.09E-11			0	CE-MS	DB	3	HMDB0029054
Thr-Gly*	$C_6H_{12}N_2O_4$	176.0789	13.07	-38	1.37E-08			4	CE-MS	DB	3	HMDB0029061
Trp-Phe	$C_{20}H_{21}N_3O_3$	351.1582	2.32	74	3.73E-11	-0.63	1.56	1	LC-MS(-)	DB	3	HMDB0029090
Val-Leu	$C_{11}H_{22}N_2O_3$	230.1616	12.83	51	0.0012			6	CE-MS	DB	3	HMDB0029131
Benzene and substituted derivatives												
Mandelic acid	$C_8H_8O_3$	152.0473	2.28	335	0.0037			3	LC-MS(-)	DB	3	HMDB0000703
3-phenylprop-2-en-1-yloxysulfonic acid	$C_9H_{10}O_4S$	214.0299	2.77	118	0.0005			2	LC-MS(-)	DB	3	HMDB0135284
Carbohydrates and carbohydrate conjugates												
Allose	$C_6H_{12}O_6$	180.0633	17.10	139	1.32E-14	0.62	1.44	-	GC-MS	Fiehn	2	HMDB0001151
Glucose	$C_6H_{12}O_6$	180.0633	17.45	174	1.98E-15	0.62	1.64	-	GC-MS	Fiehn	2	HMDB0000122
Glycerol	$C_3H_8O_3$	92.0473	9.28	45	0.0000			-	GC-MS	Fiehn	2	HMDB0000131
Mannitol	$C_6H_{14}O_6$	182.0790	17.59	196	0.0017			-	GC-MS	Fiehn	2	HMDB0000765
Phenylglucuronide	$C_{12}H_{14}O_7$	270.0739	0.93	308	0.0052	-0.52	2.37	2	LC-MS(-)	DB	3	HMDB0060014
PYRANOSE (glucose/altrose /galactose /talose)	$C_6H_{12}O_6$	180.0633	17.24	194	1.61E-16	0.63	1.71	-	GC-MS	Fiehn	2	
Carboximidic acids and derivatives												
Acetylspermidine	$C_9H_{21}N_3O$	187.1671	9.15	38	6.27E-06			7	CE-MS	DB	3	HMDB0001276
Carboxylic acids and derivatives												
1-Aminocyclohexanecarboxylic acid	$C_7H_{13}NO_2$	143.0944	13.89	-32	0.0366			1	CE-MS	DB	3	HMDB0038249
di-Hydroxymelatonin*	$C_{13}H_{16}N_2O_4$	264.1110	1.34	46	0.0268			2	LC-MS(-)	DB	3	HMDB0061136
Edetic Acid	$C_{10}H_{16}N_2O_8$	292.0906	0.24	35	0.0001			1	LC-MS(+)	DB	3	HMDB0015109
Isocitric acid Citric acid	$C_6H_8O_7$	192.0270	0.23	64	5.83E-05			0	LC-MS(-)	MSMS	2	HMDB0000193 HMDB0000094
Diazines/ Pyrimidines and pyrimidine derivatives												
5,6-Dihydrothymine	$C_5H_8N_2O_2$	128.0570	12.22	56	0.0169			12	CE-MS	DB	3	HMDB0000079
Fatty Acyls												
3-carboxy-4-methyl-5-propyl-2-furanpropanoic acid (CMPF)	$C_{12}H_{16}O_5$	240.0998	3.78	69	0.004			2	LC-MS(+)	MSMS	2	HMDB0061112

Compound	Formula	Mass (Da)	RT (min)	% change	*P*- value	p(corr)	VIP	Mass error (ppm)	Analytical platform	Identification source	Confidence level	HMDB Code
8-amino-7-oxo-nonanoic acid*	$C_9H_{17}NO_3$	187.1208	2.06	418	0.0220			2	LC-MS(-)	DB	3	
Arachidonic acid	$C_{20}H_{32}O_2$	304.2402	7.13	62	1.59E-05			1	LC-MS(-)	MSMS	2	HMDB0001043
beta-Phenylalanoyl-CoA*	$C_{30}H_{45}N_8O_{17}P_3S$	914.1836	2.83	73	7.07E-03			1	LC-MS(-)	DB	3	
beta-Phenylalanoyl-CoA*	$C_{30}H_{45}N_8O_{17}P_3S$	914.1836	3.62	65	8.78E-03			0	LC-MS(-)	DB	3	
DG(31:0)	$C_{34}H_{66}O_5$	554.4910	8.18	-37	0.0008			0	LC-MS(+)	DB	3	HMDB0093505
Docosapentaenoic acid	$C_{22}H_{34}O_2$	330.2558	7.25	75	6.87E-09	-0.55	1.51	1	LC-MS(-)	DB	3	HMDB0006528
Dodecenedioic acid	$C_{12}H_{20}O_4$	228.1362	3.50	191	9.87E-08	-0.60	2.24	2	LC-MS(-)	DB	3	HMDB0000933
Eicosapentaenoic acid	$C_{20}H_{30}O_2$	302.2246	6.77	65	3.88E-04			2	LC-MS(-)	DB	3	HMDB0001999
Eicosatrienoic acid	$C_{20}H_{34}O_2$	306.2558	7.39	82	1.85E-10			1	LC-MS(-)	DB	3	HMDB0010378
Eicosenoic acid	$C_{20}H_{38}O_2$	310.2871	8.34	79	2.75E-10	-0.51	1.50	1	LC-MS(-)	DB	3	HMDB0002231
Glucosylgalactosylhydroxylysine	$C_{18}H_{34}N_2O_{13}$	486.2093	12.38	46	1.73E-05			7	CE-MS	DB	3	HMDB0000585
HETE	$C_{20}H_{32}O_3$	320.2351	5.92	Presented in cancer group	1.24E-05	-0.63	2.64	0	LC-MS(-)	MSMS	2	HMDB0060101
MG(18:2)	$C_{21}H_{38}O_4$	354.2770	6.81	116	0.0007			2	LC-MS(+)	MSMS	2	HMDB0011538
MG(20:0)	$C_{23}H_{46}O_4$	386.3396	7.79	-86	1.30E-12			5	LC-MS(+)	DB	3	HMDB0072859
N-palmitoyl glutamic acid*	$C_{21}H_{39}NO_5$	385.2828	4.13	62	0.004			0	LC-MS(+)	DB	3	
Oleic acid	$C_{18}H_{34}O_2$	282.2559	20.47	67	0.0013			-	GC-MS LC-MS(+)	Fiehn	2	HMDB0000207
Vaccenic acid	$C_{18}H_{34}O_2$	282.2559	20.56	23	0.0158			-	GC-MS	Fiehn	2	HMDB0041480
3-hydroxy-5-octenoylcarnitine	$C_{15}H_{27}NO_5$	301.1889	4.23	Presented in cancer group	3.57E-02	-0.72	3.96	3	LC-MS(-)	DB	3	
3-Hydroxy-5-tetradecenoylcarnitine*	$C_{21}H_{39}NO_5$	385.2828	4.13	62	0.004			0	LC-MS(+)	DB	3	HMDB0013330
9-Decenoylcarnitine	$C_{17}H_{31}NO_4$	313.2232	12.99	-15	0.0325			7	CE-MS	DB	3	HMDB0013205
Arachidonoylcarnitine*	$C_{27}H_{45}NO_4$	447.3349	5.15	-66	9.67E-17	0.75	3.74	1	LC-MS(+)	DB	3	HMDB0062343
α-Linolenyl carnitine	$C_{25}H_{43}NO_4$	421.3192	4.91	-41	1.79E-08	0.53	2.26	0	LC-MS(+)	DB	3	HMDB0006319
Linoleyl carnitine	$C_{25}H_{45}NO_4$	423.3349	5.14	-59	4.03E-16	0.73	3.40	0	LC-MS(+)	DB	3	HMDB0006469

Compound	Formula	Mass (Da)	RT (min)	% change	*P*- value	p(corr)	VIP	Mass error (ppm)	Analytical platform	Identification source	Confidence level	HMDB Code
Vaccenylcarnitine Elaidic carnitine	$C_{25}H_{47}NO_4$	425.3504	5.43	-41	1.41E-08	0.51	2.40	1	LC-MS(+)	MSMS	2	HMDB0006351 HMDB0006464
Flavonoids												
Anthraniloyl-CoA	$C_{28}H_{41}N_8O_{17}P_3S$	886.1523	0.23	186	3.47E-21	-0.69	2.39	3	LC-MS(-)	DB	3	
Glycerolipids												
11-Oxo-androsterone glucuronide	$C_{25}H_{36}O_9$	480.2359	3.43	-45	8.06E-06	0.53	2.06	1	LC-MS(-)	DB	3	HMDB0010338
Glycerophospholipids												
LPC(16:0)-OH	$C_{24}H_{50}NO_8P$	511.3274	4.12	25	0.008			0	LC-MS(+) LC-MS(-)	MSMS	2	
LPC(16:0)-OH	$C_{24}H_{50}NO_8P$	511.3274	4.21	37	0.0005			0	LC-MS(+) LC-MS(-)	MSMS	2	
LPC(18:0)-OH	$C_{26}H_{54}NO_8P$	539.3587	4.71	27	0.0100			0	LC-MS(+) LC-MS(-)	MSMS	2	
LPC(18:2)-OH	$C_{26}H_{50}NO_8P$	535.3274	4.41	Presented in cancer group	2.19E-06			0	LC-MS(+) LC-MS(-)	MSMS	2	
LPA(13:0)	$C_{16}H_{33}O_7P$	368.1963	5.23	-57	4.95E-03	0.56	2.29	7	LC-MS(-)	DB	3	HMDB0114760
LPC(22:1)	$C_{30}H_{60}NO_7P$	577.4107	6.99	66	2.14E-05			2	LC-MS(-)	MSMS	2	HMDB0010399
LPE(16:0)	$C_{21}H_{44}NO_7P$	453.2855	5.65	25	0.008			0	LC-MS(+)	MSMS	2	HMDB0011473
LPE(20:5)	$C_{25}H_{42}NO_7P$	499.2699	5.08	179	2.80E-06			0	LC-MS(+)	MSMS	2	HMDB0011489
LPE(20:5)	$C_{25}H_{42}NO_7P$	499.2699	5.16	55	0.001			0	LC-MS(+) LC-MS(-)	MSMS	2	HMDB0011489
LPE(22:6)	$C_{27}H_{44}NO_7P$	525.2855	5.37	28	0.001			0	LC-MS(+)	MSMS	2	HMDB0011526
LPE(22:6)	$C_{27}H_{44}NO_7P$	525.2855	5.45	39	0.0005			0	LC-MS(+)	MSMS	2	HMDB0011496
LPE(P-16:0)	$C_{21}H_{44}NO_6P$	437.2906	5.83	36	0.002			0	LC-MS(+)	DB	3	HMDB0011152
LPI(16:1)	$C_{25}H_{47}O_{12}P$	570.2805	5.51	97	2.63E-03			1	LC-MS(-)	MSMS	2	
LPS(18:0)	$C_{24}H_{48}NO_9P$	525.3066	6.71	104	9.62E-06			2	LC-MS(-)	MSMS	2	
PC(32:0)	$C_{40}H_{80}NO_8P$	733.5622	10.47	51	3.91E-07			2	LC-MS(+)	DB	3	HMDB0007871
PC(38:2)	$C_{46}H_{88}NO_8P$	813.6247	11.94	39	0.0004			0	LC-MS(+)	MSMS	2	HMDB0007987
PC(38:5)	$C_{46}H_{82}NO_8P$	807.5778	9.82	-28	5.05E-05			2	LC-MS(+)	MSMS	2	HMDB0008156

Compound	Formula	Mass (Da)	RT (min)	% change	*P*- value	p(corr)	VIP	Mass error (ppm)	Analytical platform	Identification source	Confidence level	HMDB Code
PE(34:2) PE(O-34:3)	$C_{39}H_{74}NO_7P$	699.5203	10.25	-33	0.001			1	LC-MS(+)	MSMS	2	HMDB0011343
PE(38:6)	$C_{43}H_{74}NO_8P$	763.5151	9.31	-31	0.0087			1	LC-MS(+)	MSMS	2	HMDB0009294
PG(20:2)	$C_{26}H_{49}O_9P$	536.3114	7.41	-58	3.44E-11	0.59	2.33	4	LC-MS(-)	DB	3	
PG(28:0)	$C_{34}H_{67}O_{10}P$	666.4471	7.64	115	8.69E-15	-0.61	2.75	5	LC-MS(+)	DB	3	HMDB0116681
PS(39:5)	$C_{45}H_{78}NO_{10}P$	823.5363	10.46	25	1.60E-07			5	LC-MS(+)	DB	3	
Hydroxy acids and derivatives												
3-Hydroxydodecanedioic acid	$C_{12}H_{22}O_5$	246.1467	2.79	Presented in cancer group	2.42E-06	-0.68	2.97	0	LC-MS(-)	MSMS	2	HMDB0000413
3-Hydroxydodecanoic acid	$C_{12}H_{24}O_3$	216.1725	4.62	Presented in cancer group	2.32E-11	-0.72	2.79	2	LC-MS(-)	MSMS	2	HMDB0000387
Imidazoles												
Methylimidazole	$C_4H_6N_2$	82.0538	11.48	64	6.41E-06			9	CE-MS	DB	3	
Urocanate Nicotinamide N-oxide	$C_6H_6N_2O_2$	138.0435	11.02	24	0.001			4	CE-MS	DB	3	HMDB0034174 HMDB0002730
Imidazopyrimidines / Purines and purine derivatives												
Hypoxanthine	$C_5H_4N_4O$	136.0402	14.19	-34	8.20E-06			13	CE-MS	DB	2	HMDB0000157
Indoles and derivatives												
3-Indoleacetic acid	$C_{10}H_9NO_2$	175.0633	17.94	131	2.62E-07			-	GC-MS	Fiehn	2	HMDB0000197
5-Hydroxyindole	C_8H_7NO	133.0527	0.76	37	3.82E-02			1	LC-MS(-)	DB	3	HMDB0059805
5-Hydroxyindoleacetaldehyde	$C_{10}H_9NO_2$	175.0633	2.51	150	2.63E-05	-0.51	2.55	1	LC-MS(+)	MSMS	2	HMDB0004073
5-Hydroxyindoleacetic acid	$C_{10}H_9NO_3$	191.0582	0.80	Presented in cancer group	3.28E-08			0	LC-MS(+)	MSMS	2	HMDB0000763
Lactones												
N-(4-Coumaroyl)-homoserine lactone	$C_{13}H_{13}NO_4$	247.0845	1.34	55	0.0006			2	LC-MS(+)	DB	3	
Organic acids and derivatives												
(Homo)2-aconitate*	$C_8H_{10}O_6$	202.0477	0.26	-75	7.87E-59	0.84	2.98	11	LC-MS(-)	DB	3	
Lactic acid	$C_3H_6O_3$	90.0317	6.06	-77	4.72E-36	-0.92	2.58	-	GC-MS	Fiehn	2	HMDB0001311

Compound	Formula	Mass (Da)	RT (min)	% change	*P*- value	p(corr)	VIP	Mass error (ppm)	Analytical platform	Identification source	Confidence level	HMDB Code
Pyruvic acid	$C_3H_4O_3$	88.0160	5.89	-58	1.06E-14	-0.69	1.78	-	GC-MS	Fiehn	2	HMDB0000243
Succinylacetoacetate*	$C_8H_{10}O_6$	202.0477	0.26	-75	7.87E-59	0.84	2.98	11	LC-MS(-)	DB	3	HMDB0240258
Organic sulfuric acids and derivatives												
Indoxylsulfuric acid	$C_8H_7NO_4S$	213.0095	1.00	42	3.47E-02			1	LC-MS(-)	MSMS	2	HMDB0000682
p-Phenolsulfonic acid	$C_6H_6O_4S$	173.9986	0.65	174	3.45E-03			1	LC-MS(-)	MSMS	2	HMDB0060015
Organonitrogen compounds												
Phosphocholine	$C_5H_{14}NO_4P$	183.0660	5.37	32	0.003			1	LC-MS(+)	MSMS	2	
Organooxygen compounds												
4-Hydroxycyclohexylcarboxylic acid	$C_7H_{12}O_3$	144.0786	0.76	789	5.08E-10	-0.71	2.99	1	LC-MS(-)	DB	3	HMDB0001988
Acetyl-N-formyl-5-methoxykynurenamine (AFMK)*	$C_{13}H_{16}N_2O_4$	264.1110	1.34	46	0.0268			2	LC-MS(-)	DB	3	HMDB0004259
Phenols												
4-Methylcatechol	$C_7H_8O_2$	124.0524	1.23	-43	1.68E-02			2	LC-MS(-)	DB	3	HMDB0000873
Prenol lipids												
Retinol	$C_{20}H_{30}O$	286.2296	7.04	34	0.0003			2	LC-MS(+)	MSMS	2	HMDB0000305
Purine nucleosides												
1-Methyladenosine	$C_{11}H_{15}N_5O_4$	281.1132	12.49	41	3.68E-16	-0.58	1.20	3	CE-MS	DB	2	HMDB0003331
Pyridines and derivatives												
Norcotinine	$C_9H_{10}N_2O$	162.0790	11.48	34	0.0039			2	CE-MS	DB	3	HMDB0001297
Piperideine	C_5H_9N	83.0739	13.77	28	0.0239			5	CE-MS	DB	3	
Serotonine	$C_{10}H_{12}N_2O$	176.0954	11.40	228	0.0007			3	CE-MS	DB	2	HMDB0001046
Quinolines and derivatives												
8-Hydroxycarteolol	$C_{16}H_{24}N_2O_4$	308.1732	13.90	-31	0.0246			1	CE-MS	DB	3	HMDB0060990
Quinoline	C_9H_7N	129.0578	2.51	99	0.0008			1	LC-MS(+)	DB	3	HMDB0033731
Sphingolipids												
Cer(35:0)	$C_{35}H_{69}NO_3$	551.5277	11.39	58	4.24E-08			3	LC-MS(-)	DB	3	
Cer(36:1)	$C_{36}H_{71}NO_3$	565.5434	11.74	42	0.0003			1	LC-MS(+)	DB	3	HMDB0004950

Compound	Formula	Mass (Da)	RT (min)	% change	*P*- value	p(corr)	VIP	Mass error (ppm)	Analytical platform	Identification source	Confidence level	HMDB Code
SM(36:0)	$C_{41}H_{85}N_2O_6P$	732.6145	10.14	41	0.0014			1	LC-MS(+)	MSMS	2	HMDB0012087
Sphingosine-1-phosphate	$C_{18}H_{38}NO_5P$	379.2488	5.02	-30	2.17E-08	0.50	2.06	0	LC-MS(+)	MSMS	2	HMDB0000277
Steroids and steroid derivatives												
12a-Hydroxy-3-oxocholadienic acid	$C_{24}H_{34}O_4$	386.2457	4.27	144	3.66E-06	-0.54	2.12	0	LC-MS(-)	MSMS	2	HMDB0000385
Biliverdin	$C_{33}H_{34}N_4O_6$	582.2478	4.73	300	1.47E-16	-0.72	2.62	0	LC-MS(-)	DB	3	HMDB0001008
Hydroxy-3-oxo-4-cholestenoate	$C_{27}H_{42}O_4$	430.3083	5.53	54	2.78E-06				LC-MS(+) LC-MS(-)	MSMS	2	
Calcitroic acid	$C_{23}H_{34}O_4$	374.2457	7.39	84	6.25E-11	-0.54	1.76	6	LC-MS(-)	DB	3	HMDB0006472
Chenodeoxycholic acid 3-glucuronide*	$C_{30}H_{48}O_{10}$	568.3248	4.33	94	2.10E-03			1	LC-MS(-)	DB	3	
Cholestane-3,7,12,24,25-pentol	$C_{27}H_{48}O_5$	452.3501	7.77	-56	3.81E-10	0.56	2.03	2	LC-MS(-)	DB	3	HMDB0000483
Cholestane-3,7,12,25-tetrol-3-glucuronide	$C_{33}H_{56}O_{10}$	612.3873	4.71	97	4.89E-05			0	LC-MS(-)	DB	3	HMDB0010355
Cortisone acetate	$C_{23}H_{30}O_6$	402.2042	3.86	63	5.89E-04			9	LC-MS(-)	DB	3	HMDB0015459
Dehydroepiandrosterone 3-glucuronide Dehydroisoandrosterone 3-glucuronide	$C_{25}H_{36}O_8$	464.2410	3.91	-51	1.01E-05			2	LC-MS(-)	DB	3	HMDB0010348 HMDB0010327
Deoxycholic acid 3-glucuronide*	$C_{30}H_{48}O_{10}$	568.3248	4.33	94	2.10E-03			1	LC-MS(-)	DB	3	HMDB0002596
ecdysone 25-O-D-glucopyranoside	$C_{33}H_{54}O_{11}$	626.3666	4.41	88	1.02E-04			1	LC-MS(-)	DB	3	
Pregnanediol	$C_{21}H_{36}O_2$	320.2715	6.35	-51	4.21E-05			0	LC-MS(-)	DB	3	HMDB0004025
Pregnanolone sulfate	$C_{21}H_{34}O_5S$	398.2127	3.64	55	5.27E-03			0	LC-MS(-)	DB	3	HMDB0240591
Ursodeoxycholic acid	$C_{24}H_{40}O_4$	392.2927	4.34	188	3.93E-02	-0.51	2.35	1	LC-MS(-)	MSMS	2	HMDB0000946
Ursodeoxycholic acid 3-sulfate	$C_{24}H_{40}O_7S$	472.2494	3.75	130	4.38E-03	-0.54	2.36	1	LC-MS(-)	DB	3	HMDB0002642
Sterol Lipids												
24-Hydroxygeminivitamin D3	$C_{32}H_{54}O_5$	518.3971	6.79	-37	2.82E-07			1	LC-MS(+)	DB	3	
Tetrapyrroles and derivatives												
Bilirubin	$C_{33}H_{36}N_4O_6$	584.2635	3.85	674	3.79E-08	-0.68	2.63	4	LC-MS(-) LC-MS(+)	MSMS	2	HMDB0000054

Table 2. List of the 34 annotated metabolites significantly associated with NET patients prognosis (N=77) with their statistical characteristics after UVDA and MVDA (percentage of change, p-value, p(corr) and VIP) and analytical descriptors (measured mass and its deviation from the theoretical one, experimental retention time, analytical platform on which it has been detected, identification source where DB corresponds to database result, confidence level for identification according to the metabolomics standards initiative and its corresponding Human Metabolome Database (HMDB) code (http://www.hmdb.ca/)). (* = Multiple identification options)

Compound	Formula	Mass (Da)	RT (min)	% change	*P*- value	p(corr)	VIP	Mass error (ppm)	Analytical platform	Identification source	Confidence level	HMDB Code
Amino acids, peptides, and analogues												
Cys-Gly disulphide	$C_8H_{15}N_3O_5S_2$	297.0455	12.19	-41	1.39E-08	0.49	1.63	1	CE-MS	DB	3	HMDB0000709
Dimethyl-Arginine (symmetric)	$C_8H_{18}N_4O_2$	202.1428	10.67	25	0.0006			1	CE-MS	DB	2	HMDB0003334
Glu-hyp	$C_{10}H_{16}N_2O_6$	260.0993	12.98	37	5.12E-07			6	CE-MS	DB	3	HMDB0011161
Glu-Lys/Ɛ-Glu-Lys	$C_{11}H_{21}N_3O_5$	275.1481	12.32	67	1.20E-09			2	CE-MS	DB	3	HMDB0029154
Glu-Lys/Ɛ-Glu-Lys	$C_{11}H_{21}N_3O_5$	275.1481	11.37	58	1.55E-07			2	CE-MS	DB	3	HMDB0029155
Methionine S-oxide	$C_5H_{11}NO_3S$	165.0478	14.06	110	3.30E-09			11	CE-MS	DB	2	HMDB0002005
Pyroglutamine	$C_5H_8N_2O_2$	128.0583	11.48	68	1.41E-05			2	CE-MS	DB	3	HMDB0062558
Ser-Ala*	$C_6H_{12}N_2O_4$	176.0789	13.07	-38	1.37E-08			4	CE-MS	DB	3	HMDB0029032
Suberylglycine	$C_{10}H_{17}NO_5$	231.1106	1.19	Presented in cancer group	0.0001	-0.73	3.82	1	LC-MS(-)	DB	3	HMDB0000953
Thr-Gly*	$C_6H_{12}N_2O_4$	176.0789	13.07	-38	1.37E-08			4	CE-MS	DB	3	HMDB0029061
Carbohydrates and carbohydrate conjugates												
PYRANOSE (glucose/altrose /galactose /talose)	$C_6H_{12}O_6$	180.0633	17.24	194	1.61E-16	0.63	1.71	-	GC-MS	Fiehn	2	
Fatty Acyds												
Eicosapentaenoic acid	$C_{20}H_{30}O_2$	302.2246	6.77	65	3.88E-04			2	LC-MS(-)	DB	3	HMDB0001999
MG(20:0)	$C_{23}H_{46}O_4$	386.3396	7.79	-86	1.30E-12			5	LC-MS(+)	DB	3	HMDB0072859
N-palmitoyl glutamic acid*	$C_{21}H_{39}NO_5$	385.2828	4.13	62	0.004			0	LC-MS(+)	DB	3	
3-hydroxy-5-octenoylcarnitine	$C_{15}H_{27}NO_5$	301.1889	4.23	Presented in cancer group	3.57E-02	-0.72	3.96	3	LC-MS(-)	DB	3	

Compound	Formula	Mass (Da)	RT (min)	% change	*P*- value	p(corr)	VIP	Mass error (ppm)	Analytical platform	Identification source	Confidence level	HMDB Code
3-Hydroxy-5-tetradecenoylcarnitine*	$C_{21}H_{39}NO_5$	385.2828	4.13	62	0.004			0	LC-MS(+)	DB	3	HMDB0013330
Linoleyl carnitine	$C_{25}H_{45}NO_4$	423.3349	5.14	-59	4.03E-16	0.73	3.40	0	LC-MS(+)	DB	3	HMDB0006469
Glycerophospholipids												
LPC(16:0)-OH	$C_{24}H_{50}NO_8P$	511.3274	4.12	25	0.008			0	LC-MS(+) LC-MS(-)	MSMS	2	
LPA(13:0)	$C_{16}H_{33}O_7P$	368.1963	5.23	-57	4.95E-03	0.56	2.29	7	LC-MS(-)	DB	3	HMDB0114760
LPC(22:1)	$C_{30}H_{60}NO_7P$	577.4107	6.99	66	2.14E-05			2	LC-MS(-)	MSMS	2	HMDB0010399
LPE(22:6)	$C_{27}H_{44}NO_7P$	525.2855	5.37	28	0.001			0	LC-MS(+)	MSMS	2	HMDB0011526
PG(28:0)	$C_{34}H_{67}O_{10}P$	666.4471	7.64	115	8.69E-15	-0.61	2.75	5	LC-MS(+)	DB	3	HMDB0116681
Hydroxy acids and derivatives												
3-Hydroxydodecanoic acid	$C_{12}H_{24}O_3$	216.1725	4.62	Presented in cancer group	2.32E-11	-0.72	2.79	2	LC-MS(-)	MSMS	2	HMDB0000387
Imidazoles												
Methylimidazole	$C_4H_6N_2$	82.0538	11.48	64	6.41E-06			9	CE-MS	DB	3	
Urocanate Nicotinamide N-oxide	$C_6H_6N_2O_2$	138.0435	11.02	24	0.001			4	CE-MS	DB	3	HMDB0034174 HMDB0002730
Indoles and derivatives												
5-Hydroxyindoleacetic acid	$C_{10}H_9NO_3$	191.0582	0.80	Presented in cancer group	3.28E-08			0	LC-MS(+)	MSMS	2	HMDB0000763
Lactones												
N-(4-Coumaroyl)-homoserine lactone	$C_{13}H_{13}NO_4$	247.0845	1.34	55	0.0006			2	LC-MS(+)	DB	3	
Phenols												
4-Methylcatechol	$C_7H_8O_2$	124.0524	1.23	-43	1.68E-02			2	LC-MS(-)	DB	3	HMDB0000873
Purine nucleosides												
1-Methyladenosine	$C_{11}H_{15}N_5O_4$	281.1132	12.49	41	3.68E-16	-0.58	1.20	3	CE-MS	DB	2	HMDB0003331
Sphingolipids												
SM(36:0)	$C_{41}H_{85}N_2O_6P$	732.6145	10.14	41	0.0014			1	LC-MS(+)	MSMS	2	HMDB0012087

Compound	Formula	Mass (Da)	RT (min)	% change	*P*- value	p(corr)	VIP	Mass error (ppm)	Analytical platform	Identification source	Confidence level	HMDB Code
Steroids and steroid derivatives												
Biliverdin	$C_{33}H_{34}N_4O_6$	582.2478	4.73	300	1.47E-16	-0.72	2.62	0	LC-MS(-)	DB	3	HMDB0001008
Cholestane-3,7,12,24,25-pentol	$C_{27}H_{48}O_5$	452.3501	7.77	-56	3.81E-10	0.56	2.03	2	LC-MS(-)	DB	3	HMDB0000483
Cortisone acetate	$C_{23}H_{30}O_6$	402.2042	3.86	63	5.89E-04			9	LC-MS(-)	DB	3	HMDB0015459
ecdysone 25-O-D-glucopyranoside	$C_{33}H_{54}O_{11}$	626.3666	4.41	88	1.02E-04			1	LC-MS(-)	DB	3	

10. ANNEX: PUBLICATIONS

PUBLICATIONS

1. **La Salvia A**, Espinosa-Olarte P, Riesco-Martinez MDC, Anton-Pascual B, Garcia-Carbonero R. Targeted Cancer Therapy: What's New in the Field of Neuroendocrine Neoplasms? Cancers. 2021, 13, 1701. https://doi.org/10.3390/cancers13071701. **IF 6.126 Q1.**

2. Fazio N, Gervaso L, Halfdanarson TR, **La Salvia A**, Hofland J, Hernando J, Sonbol MB, Garcia-Carbonero R, Capdevila J, de Herder WW, Koumarianou A, Kaltsas G, Rossi M, Grozinsky-Glasberg S, Oleinikov K, Boselli S, Tamayo D, Bagnardi V, Laffi A, Rubino M, Spada F. COVID-19 in patients with neuroendocrine neoplasms: Preliminary results of a worldwide survey (The INTENSIVE study). European Journal of Cancer. Published: June 29, 2021. doi: https://doi.org/10.1016/j.ejca.2021.06.029. **IF 7.275 Q1.**

3. **La Salvia A**, Portigliatti Pomeri A, Persano I, Trevisi E, Parlagreco E, Colombi N, Brizzi MP, Picci RL, Oliva F. Serotoninergic brain dysfunction in neuroendocrine tumor patients: A scoping review. Compr Psychiatry. 2021 May 19;109:152244. doi: 10.1016/j.comppsych.2021. **IF 2.567 Q2.**

4. Soldevilla B, López-López A, Lens-Pardo A, Carretero-Puche C, Lopez-Gonzalvez A, **La Salvia A**, Gil-Calderon B, Riesco-Martinez MC, Espinosa-Olarte P, Sarmentero J, Rubio-Cuesta B, Rincón R, Barbas C, Garcia-Carbonero R. Comprehensive Plasma Metabolomic Profile of Patients with Advanced Neuroendocrine Tumors (NETs). Diagnostic and Biological Relevance. Cancers (Basel). 2021 May 27;13(11):2634. doi: 10.3390/cancers13112634. **IF 6.126 Q1.**

5. Espinosa-Olarte P, **La Salvia A**, Riesco-Martinez MDC, Anton-Pascual B, Garcia-Carbonero R. Chemotherapy in NEN: still has a role? Rev Endocr Metab Disord. 2021 Apr 11. doi: 10.1007/s11154-021-09638-0. **IF 6.192 Q1.**

6. Trevisi E, **La Salvia A**, Daniele L, Brizzi MP,De Rosa G,Scagliotti GV, Di Maio M. Neuroendocrine breast carcinoma: a rare but challenging entity. Med Oncol. 2020 Jul 25;37(8):70. doi: 10.1007/s12032-020-01396-4. **IF 3,25 Q1.**

7. López-López A, Godzien J, Soldevilla B, Gradillas A, López-Gonzálvez A, Lens-Pardo A, **La Salvia A**, Riesco-Martínez MC, García-Carbonero R, Barbas C. Oxidized lipids in the metabolic profiling of neuroendocrine tumors - Analytical challenges and biological implications. J Chromatogr A. 2020 Aug 16;1625:461233. doi: 10.1016/j.chroma.2020.461233. **IF 3,716 Q1.**

8. **La Salvia A**, Persano I, Trevisi E, Parlagreco E, Muratori L, Scagliotti GV, Brizzi MP. Ocular metastases from neuroendocrine tumors: A literature review. Semin

Oncol. 2020; 2020 Apr-Jun;47(2-3):144-147. doi: 10.1053/j.seminoncol.2020.04.003. **IF 4,942 Q1.**

9. **La Salvia A**, Brizzi MP, Trevisi E, Parisi F, Muratori L, Atzeni F, Di Maio M, Scagliotti GV. Carcinoid heart failure in a duodenal neuroendocrine tumor: role of cardiac surgery in a challenging patient and brief review of the literature. Acta Oncol. 2020 Mar;59(3):315-319. doi: 10.1080/0284186X.2019.1672891. Epub 2019 Oct 4. PMID: 31583924. **IF 3.473 Q2.**

10. Lamberti G, Faggiano A, Brighi N, Tafuto S, Ibrahim T, Brizzi MP, Pusceddu S, Albertelli M, Massironi S, Panzuto F, Badalamenti G, Riccardi F, Butturini G, Gelsomino F, De Divitiis C, Modica R, Bongiovanni A, **La Salvia A**, Torchio M, Colao A, Ferone D, Campana D; ItaNet. Non-conventional doses of somatostatin analogs in patients with progressing well differentiated neuroendocrine tumor. J Clin Endocrinol Metab. 2019 Sep 23. pii: dgz035. doi: 10.1210/clinem/dgz035. PubMed PMID: 31545377. **IF 5.789 Q1.**

11. **La Salvia A**, Brizzi MP, Muratori L, Trevisi E, Di Maio M, Scagliotti GV. Capecitabine plus temozolomide in well or moderately differentiated primary atypical neuroendocrine tumors: a single centre experience of two cases. Endokrynol Pol. 2018 Oct 25. doi: 10.5603/EP.a2018.0076. PubMed PMID: 30359462. **IF 1,341. Q4**

12. Marandino L, **La Salvia A,** Sonetto C, De Luca E, Pignataro D, Zichi C, Di Stefano RF, Ghisoni E, Lombardi P, Mariniello A, Reale ML, Trevisi E, Leone G, Muratori L, Marcato M, Bironzo P, Novello S, Aglietta M, Scagliotti GV, Perrone F, Di Maio M. Deficiencies in health-related quality of life assessment and reporting: a systematic review of oncology randomized phase III trials published between 2012 and 2016. Ann Oncol. 2018 Oct 10. doi: 10.1093/annonc/mdy449. PubMed PMID: 30304498. **IF 11,855. D1**

13. Pusceddu S, Vernieri C, Di Maio M, Marconcini R, Spada F, Massironi S, Ibrahim T, Brizzi MP, Campana D, Faggiano A, Giuffrida D, Rinzivillo M, Cingarlini S, Aroldi F, Antonuzzo L, Berardi R, Catena L, De Divitiis C, Ermacora P, Perfetti V, Fontana A, Razzore P, Carnaghi C, Davì MV, Cauchi C, Duro M, Ricci S, Fazio N, Cavalcoli F, Bongiovanni A, **La Salvia A**, Brighi N, Colao A, Puliafito I, Panzuto F, Ortolani S, Zaniboni A, Di Costanzo F, Torniai M, Bajetta E, Tafuto S, Garattini SK, Femia D, Prinzi N, Concas L, Lo Russo G, Milione M, Giacomelli L, Buzzoni R, Delle Fave G, Mazzaferro V, de Braud F. Metformin Use Associates With Longer Progression-free Survival of Patients With Diabetes and Pancreatic Neuroendocrine Tumors Receiving Everolimus and/or Somatostatin Analogues. Gastroenterology. 2018 Apr 12. pii: S0016-5085(18)30443-8. doi: 10.1053/j.gastro.2018.04.010**. IF 18,392. D1**

14. Pusceddu S, Barretta F, Trama A, Botta L, Milione M, Buzzoni R, De Braud F, Mazzaferro V, Pastorino U, Seregni E, Mariani L, Gatta G, Di Bartolomeo M, Femia D, Prinzi N, Coppa J, Panzuto F, Antonuzzo L, Bajetta E, Brizzi MP, Campana D, Catena L, Comber H, Dwane F, Fazio N, Faggiano A, Giuffrida D, Henau K, Ibrahim T, Marconcini R, Massironi S, Žakelj MP, Spada F, Tafuto S, Van Eycken E, Van der Zwan JM, Žagar T, Giacomelli L, Miceli R; NEPscore

Working Group. Aroldi F, Bongiovanni A, Berardi R, Brighi N, Cingarlini S, Cauchi C, Cavalcoli F, Carnaghi C, Corti F, Duro M, Davì MV, De Divitiis C, Ermacora P, **La Salvia A**, Luppi G, Lo Russo G, Nichetti F, Raimondi A, Perfetti V, Razzore P, Rinzivillo M, Siesling S, Torchio M, Van Dijk B, Visser O, Vernieri C**.** A classification prognostic score to predict OS in stage IV well-differentiated neuroendocrine tumors. Endocr Relat Cancer. 2018 Jun;25(6):607-618. doi: 10.1530/ERC-17-0489. Epub 2018 Mar 20. **IF 5,267. Q1**

15. Brizzi MP, **La Salvia A**, Tampellini M, Sonetto C, Volante M, Scagliotti GV. Efficacy and safety of everolimus treatment in a hemodialysis patient with metastatic atypical bronchial carcinoid: case report and literature review. BMC Cancer. 2018 Mar 20; 18(1):311. doi: 10.1186/s12885-018-4205-0. **IF 3,288. Q2**

16. Kasajima A, Papotti M, Ito W, Brizzi MP, **La Salvia A**, Rapa I, Tachibana T, Yazdani S, Sasano H, Volante M. High interlaboratory and interobserver agreement of somatostatin receptor immunohistochemical determination and correlation with response to somatostatin analogs. Hum Pathol. 2018 Feb;72: 144-152. 72, pp. 144 - 152. doi: 10.1016/j.humpath.2017.11.008 **IF 3,014. Q1**

17. **La Salvia A,** Partelli S, Tampellini M, Tamburrino D, Falconi M,Scagliotti GV, Brizzi MP. Management of hepatic metastases of well/moderately differentiated neuroendocrine tumors of the digestive tract. J Cancer Metasta Treat 2016;2:294-303.2, pp. 294 – 303. doi: 10.20517/2394-4722.2016.37.

18. Parlagreco E, Persano I, **La Salvia A**, Pia A, Scagliotti GV, Brizzi MP. Glucagonoma: how the misdiagnosis of a paraneoplastic cutaneous manifestation affects the clinical outcome: a case report. European Journal of Medical Case Reports. 2021;5(3):01–05. doi:10.24911/ejmcr/173-1606402831.